STUDIES ON LACTOFERRIN,
A METAL BINDING PROTEIN IN HUMAN MILK

A Thesis presented in partial fulfilment
of the requirements for the degree of
Doctor of Philosophy
in Chemistry
at Massey University

Jeffrey Ernest Plowman

1979

"Its a bit late in the day to introduce the idea now, but almost any mammal's milk would be easier to modify than cow's milk. Pig's milk is actually nearest to human milk. Camel milk and mare's milk have a better balance for humans. Sheep's milk is OK and so is goat's. Reindeer milk would be a bit fat, dog's milk a bit thin. Now, otter's milk could be just right. Perhaps we should look into it."

M. Bateman ("Sunday Times" - London, 16 March 1975)

ABSTRACT

Lactoferrin (Lf), isolated from human colostrum, has been complexed with a variety of transition metal ions. In addition to binding two iron(III) or copper(II) ions it strongly and specifically binds two cobalt(III), chromium(III) and manganese(III) ions, in the presence of bicarbonate. Such strong, specific binding of copper(II) to lactoferrin will not occur in the absence of bicarbonate, instead only a weak interaction is observed. Lactoferrin has also been shown to weakly bind manganese(II), cobalt(II), nickel(II), zinc(II), cadmium(II), lead(II) and mercury(II), though manganese(II) will undergo aerial oxidation in the presence of the protein and bind as manganese(III). These metal ion protein complexes have been examined using the techniques of fluorescence, electronic, e.s.r. and Resonance Raman spectroscopy. The close similarity between the spectra of the complexes Fe_2Lf, Cu_2Lf, Co_2Lf, Mn_2Lf and Cr_2Lf with those of transferrin and ovotransferrin reinforce the postulate that the metal binding sites in all three proteins are similar. The sites in all three proteins are essentially rhombic in character and contain 2-3 tyrosyl residues and at least one histidyl residue. A distinct heterogeneity is evident from the e.s.r. spectrum of Cr_2Lf and metal ion replacement studies indicate that chromium in one site is more labile than the other. In addition to the specific sites lactoferrin appears to have a number of non-specific sites on the outside of the protein capable of weakly coordinating metal ions such as chromium(III) and copper(II). Differences evident in the non-specific sites available to copper when manganese(III) is bound to lactoferrin, to those available when iron(III), cobalt(III) and chromium(III) are bound, suggest that the stronger binding of manganese(III) results from it inducing a different conformational change in the protein to those other metals and one that favours the higher stability of its metal-protein complex.

A series of small molecular weight complexes of iron(III) with bi-, tri-, tetra- and hexadentate ligands, containing phenolate groups were prepared and examined by electronic,

e.s.r. and Mössbauer spectroscopy. Complexes of copper(II) with nitrogen bases and chloro- and bromo-substituted phenolates were prepared and examined by electronic and e.s.r. spectroscopy. Results from these studies would favour the involvement of three tyrosyl residues and two cis histidyl residues in the metal-binding sites of lactoferrin and from studies on the copper complexes it seems likely that one histidyl and one tyrosyl are axially coordinated to the metal. Evidence from a single crystal x-ray structure is presented which would favour the interaction of bicarbonate ion with iron(III) via a solvent (water) molecule.

ACKNOWLEDGEMENTS

I am most grateful to:

Dr E. W. Ainscough and Dr A. M. Brodie for their invaluable assistance, advice and encouragement through all stages of this project.

Dr W. C. Tennant, Dr D. G. McGavin and Dr A. R. Gainsford of Chemistry Division, D.S.I.R., Petone, for their assistance in running and analysing e.s.r. and Mössbauer spectra and for the use of their Mössbauer spectrometer.

Dr K. L. Brown of Chemistry Division, D.S.I.R., Petone, for the single crystal x-ray structural analysis of one of my compounds.

Professor N. F. Curtis of the Chemistry Department, Victoria University, Wellington, for the use of his Faraday Balance.

Professor A. D. Campbell of the Chemistry Department, Otago University, Dunedin, for microanalyses.
Professor T. M. Loehr of Oregon Graduate Centre, Beaverton, Oregon, for running and analysing spectra of some metal-lactoferrin solutions.

Dr A. W. Addison of the Chemistry Department, Drexel University, Philadelphia for supplying two of the ligands used in Chapter 2.

Dr S. V. Rumball, Dr E. N. Baker, Dr G. G. Midwinter, Mr A. Trow, Mr S. J. Bloor and others of the Chemistry/Biochemistry/Biophysics Department, Massey University, for their assistance and advice.

Mrs L. Reid for typing this thesis and Mrs J. Trow for preparation of some of the diagrams.

TABLE OF CONTENTS

LIST OF FIGURES

LIST OF TABLES

INTRODUCTION

In 1951, an iron containing protein now commonly known as lactoferrin was isolated from human milk (1), which along with another iron containing protein, found in cow's milk in 1939 (2), was shown to be similar to proteins isolated from human serum (transferrin) (3,4,5) and egg white (ovotransferrin) (6). Subsequent studies have shown that lactoferrin is also present in milk of other mammalian species, although it occurs in highest concentration in human milk (Table 1). Human lactoferrin shows a greater affinity for iron than other proteins in this class. The first iron association constant (k_1) is 260 times greater than human serum transferrin and 10 times greater than bovine lactoferrin (7). Recent investigations into the role of milk and milk proteins in infant nutrition have indicated that lactoferrin (usually no more than 15 - 20% saturated with iron) plays an important role in preventing development of such illnesses as gastroenteritis. The bacteriostatic effect of human milk on intestinal bacteria such as Escherichia Coli (responsible for gastroenteritis) can be attributed to lactoferrin's strong affinity for iron acting in conjunction with a specific antibody (8). There is good reason to suppose that lactoferrin and antibodies reach the intestine intact, since there is no evidence for hydrolysis of milk proteins in the infant stomach for up to 90 minutes after feeding, and it is believed that large amounts of milk pass directly to the small intestine(9). Lactoferrin is also present in other bodily secretions and intracellular fluids, in smaller concentrations than milk (Table 2) where it is felt to act as an antimicrobial agent in these fluids (10,11,12). Transferrin, in addition to exhibiting a similar antimicrobial function (13,14) is also known to transport iron from the intestine to the bone marrow and to iron stores in the liver. While no similar transport function is proven for lactoferrin it has been suggested that it may act as a source of iron for the infant (15).

Like the related proteins, human serum transferrin and ovotransferrin, lactoferrin is a glycoprotein with two carbohydrate groups attached and a molecular weight of

Table 1 Concentration of Lactoferrin in Various Mammalian Milks [a]

2mg/cm^3	0.2-2mg/cm^3	20-200μg/cm^3	>50μg/cm^3
Human	Guinea Pig	Cow	Rat
	Mouse	Goat	Rabbit
	Mare	Sow	Dog

a. Reference(73)

Table 2 Approximate Concentration of Lactoferrin in Various Secretions [a]

Secretion	Concentration (mg/cm^3)
Milk	1.0
Saliva	0.01-0.05
Parotid Saliva	0.002-0.003
Tears	0.01
Nasal Secretions	0.01
Hepatic Bile	0.01-0.04
Pancreatic Juices	
Pseudocyst Fluid	0.05-0.10
Ascites Fluid	0.5
Seminal Fluid	0.5-1.0
Cervical Mucus	0.5-1.0
Urine	0.001

a. Reference(74)

around 80,000 (16,17,18). As well as having an almost identical amino acid composition to transferrin the amino acid sequence of the N-terminal end of lactoferrin when compared with transferrin and ovotransferrin shows some 40% homology (19). Attempts to split lactoferrin and transferrin into subunits by reduction and alkylation or breaking disulphide bonds have proved unsuccessful indicating that it consists of one chain. However, tryptic

digestion of 30% saturated human lactoferrin (20) and human serum transferrin (21) split both proteins into fragments of approximately equal molecular weight, each capable of binding one ferric ion. Furthermore the two carbohydrate units, each having essentially a tuning fork structure (22,23), were distributed equally between the C- and N-terminal fragments in lactoferrin while in transferrin were both bound to the C-terminal fragment. Recent studies suggest that the carbohydrate units may function in the specific interaction of the protein with cellular receptors (24) but the evidence on this question is still conflicting (25). While it was originally felt that the proteins were composed of two identical subunits it is now held that the present protein resulted from the doubling in size of a structural gene for a smaller precursor, leading to some internal homology. While some evidence for this is conflicting (26), recent information from partial sequencing of human serum transferrin has shown that for two sequences separated by at least 22 residues, 23 out of 53 were identical, an extent of homology of 40% (27).

IRON BINDING

The three proteins, transferrin, ovotransferrin and lactoferrin, all combine with iron to produce a salmon pink coloured complex. The reaction has been shown to be stoichiometric; two ions are bound per protein molecule (3,28). The iron in the complex has been shown to be in the high spin ferric state (28,29,30). However, transferrin in solution at neutral pH has been found to react more readily with Fe^{2+} than Fe^{3+} (31) possibly because Fe^{3+} is rapidly hydrolysed to the insoluble ferric hydroxide, whereas Fe^{2+} is only slowly hydrolysed, but can be oxidised to Fe^{3+} and then bound by transferrin.

The pink coloured complex has an absorption maximum at 460-465nm and changes in optical density are used to measure the reaction with iron. Colour formation (and iron-binding) is pH dependent; for lactoferrin the iron does not start to dissociate till the pH is below 4.0 (32) while transferrin starts to dissociate below pH 6.5 and is

complete at pH 4.5 (3,28).

Binding of each iron atom by transferrin or ovotransferrin results in the displacement of three hydrogen ions from the proteins and the simultaneous binding of one bicarbonate ion (14,33). The reaction may be written:

$$H_6Tf + Fe^{3+} + HCO_3^- \overset{k_1}{\rightleftharpoons} (Fe\text{-}H_3Tf\text{-}HCO_3)^- + 3H^+$$

$$(Fe\text{-}H_3Tf\text{-}HCO_3)^- + Fe^{3+} + HCO_3^- \overset{k_2}{\rightleftharpoons} (Fe_2\text{-}Tf\text{-}(HCO_3)_2)^{2-} + 3H^+$$

As a consequence the net positive charge of the protein should decrease one charge for each iron(III) ion bound; this has been confirmed by the measured electrophoretic mobility of the proteins in the presence and absence of iron (30,33).

The binding of iron causes a conformational change in the proteins. Transferrin and ovotransferrin are more stable than their apoproteins to heat, urea, organic solvents, disulphide breaking reagents, iodination and to proteolytic enzymes. It also leads to a change in antigenic reactivity by making certain antigenic sites on the protein inaccessible (26). Transferrin, from sedimentation experiments, is thought to be shaped like a prolate ellipsoid with an axial ratio of 1:3 (34). The loss of iron makes the protein more spherical with an axial ratio of 1:2. It was also evident that the effective hydrodynamic volume of transferrin is lower than apotransferrin. Removal of the carbohydrate residues by treatment of transferrin with neuraminidase seemed to produce no extensive conformational changes. The same type of conformational changes have been observed with lactoferrin (18) and ovotransferrin (35). From spectrophotometric titrations of tyrosine residues it seems that there may be a marked difference in the overall 3-dimensional structures of lactoferrin and transferrin (36). The binding of iron seems to influence the accessibility of tyrosyl residues on the outside of the protein to a greater extent in lactoferrin than transferrin. This could suggest that the greater stability of iron-lactoferrin complexes over transferrin is brought about by the ability of lactoferrin to adopt a configuration favouring the stability of its iron complex. Transferrin not being able to change its

shape to the same extent would be a less efficient binder of iron.

THE IRON-BINDING SITES

The 280nm peak observed in the uv spectra of the proteins and its change upon iron-binding is strongly indicative of the involvement of tyrosine residues in the binding, just as the peak at 465nm in the visible region is characteristic of a phenol-to-iron change transfer transition. Available evidence from spectrophotometric titrations, ultraviolet difference spectra and nitration of tyrosines for lactoferrin, transferrin and ovotransferrin (7,33,36,37,38) suggest that three tyrosines are involved in the binding of each ferric ion, while chemical modification of ovotransferrin by iodination (39) and model complex studies point to only two (40). Binding of each iron(III) ion to transferrin and ovotransferrin has been found to protect two histidines from ethoxyformylation and keep the protein completely active (41). Protein N.M.R. relaxation studies of transferrin have indicated the presence of two water molecules in the binding site, one $2A^{o}$ and the other $5A^{o}$ from the metal (42). It has been suggested that tryptophan may also be bound to the metal or in close proximity to it, as indicated by the fact that in ovotransferrin two tryptophan residues per protein are protected from oxidative modification when iron is bound (39). However fluorescent studies on transferrin, while not ruling out the direct involvement of tryptophan, do suggest that the spectroscopic changes can be explained without the necessity of involving such direct interaction (43).

The precise involvement of bicarbonate, essential for the binding of iron (44), is still uncertain. It appears that in transferrin there is one essential arginine residue for each iron-binding centre which may serve as a binding position for the bicarbonate (45). Bicarbonate can be replaced (in an inert atmosphere) by other anions such as nitrilotriacetate and oxalate, all having optical spectra similar to the bicarbonate complex (46,47) but inorganic anions and citrate are totally ineffective as bicarbonate

substitutes (48). However bicarbonate is bound more strongly than other anions and can displace them from the complexes.

Available evidence suggests that the anion plays a key role in the release of iron from transferrin to immature red blood cells. Replacing carbonate by oxalate reduces the rate at which transferrin donates iron to these cells by some 65%, implying that oxalate is less susceptible to attack than carbonate (49,50,51). It has been proposed that transferrin binds to the receptor site on the membrane surface followed by cleavage of the bond on the metal-protein-anion ternary complex. Presumably the anion is released first, followed by the metal.

From ^{13}C-N.M.R. studies the metal appears to be within 9A^{o} or less of the anion (52) and because the nature of the anion greatly affects the e.s.r. spectrum of the Fe^{3+}-transferrin-anion complex (49) it is felt to be binding to both the metal and the protein, the so called interlocking site. Further support for this comes from studies involving binding of synergistic anions to the metal (48,53). However the involvement of other metal ions such as Cu^{2+}, Cr^{3+}, Co^{3+} and Mn^{3+} with transferrin (54) favour the hypothesis that bicarbonate is bound in proximity, but not directly coordinated, to the metal. This is because so many metal ions, with their differing chemical and physical properties, are each capable of inducing bicarbonate binding. Furthermore Resonance Raman studies have provided evidence that HCO_3^- is not directly bound to iron(III) and has lead to the suggestion that its primary role is to induce a conformational change to bring the binding groups into proximity (40). One proposed arrangement of donor atoms around the ferric ion is given in Figure 1 where Fe^{3+} is shown binding to two tyrosyl groups, two imidazode groups and one water molecule. Other proposed arrangements would involve replacing the water molecule by a third tyrosyl group or the bicarbonate interacting less directly.

When copper is bound to transferrin and lactoferrin the number of tyrosyl residues involved is 1.3 per site (55) and from studies of the Cu-transferrin e.s.r. spectrum at pH 7.6 one nitrogen appears to be involved (56). At pH 9.2,

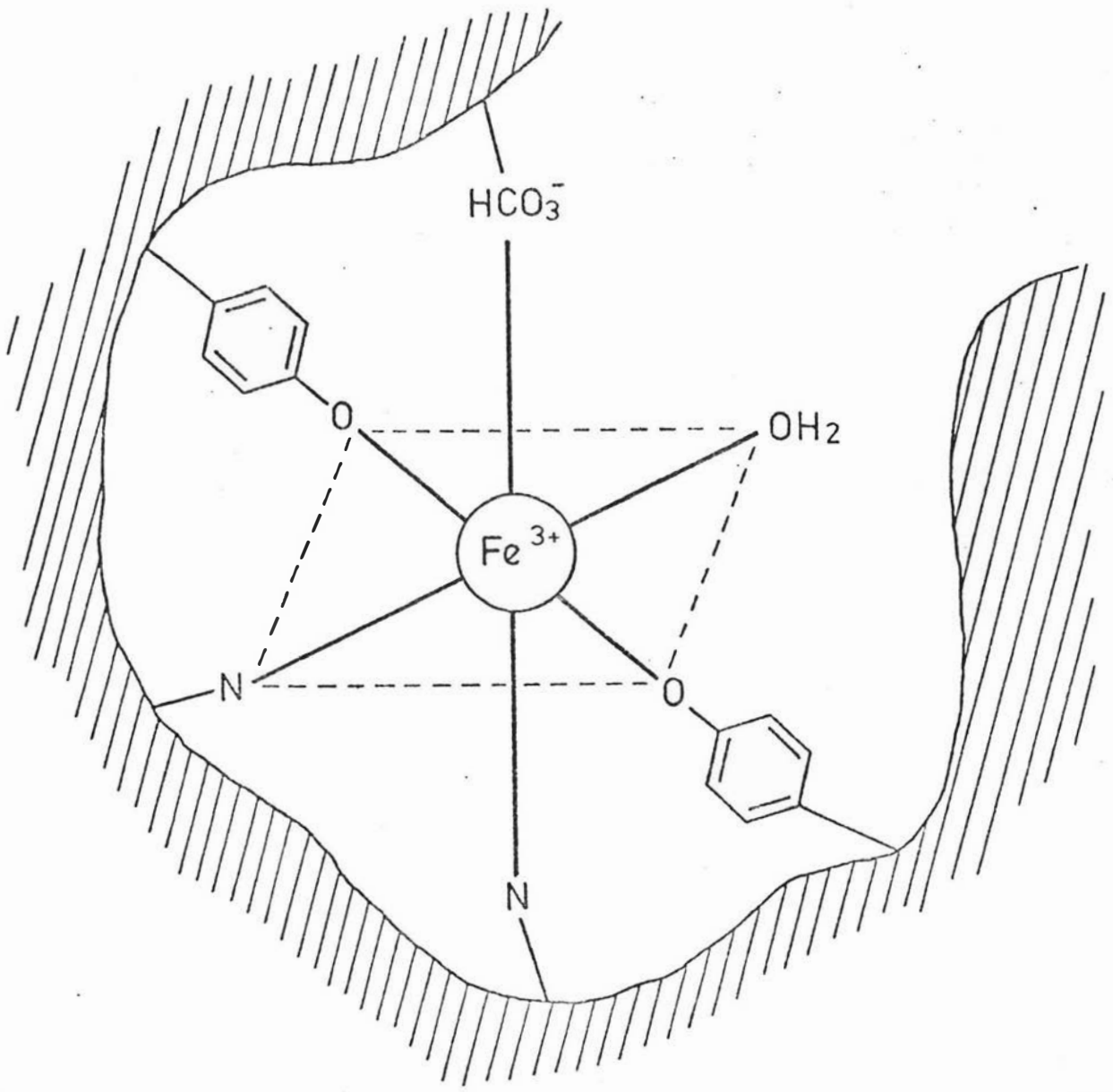

Figure 1 Proposed structure of the iron-binding site of lactoferrin, transferrin and ovotransferrin.

when only one copper is bound, a complex giving rise to an e.s.r. spectrum strongly indicative of 3 or 4 nitrogens bound to copper starts to appear. This has led to the suggestion that there are as many as seven ligands available for the binding of the metal ions in the specific sites.

INTERACTION BETWEEN THE SITES

With two iron binding sites in the protein it is possible that they may be close enough to interact leading to cooperative binding of the iron, as is the case of oxygen binding to haemoglobin. If $k_2 > k_1$ then we would expect to find two species present in solution; apoprotein and Fe_2-protein. But if $k_1 = k_2$ then all three species should exist. The simultaneous existence of all three species in transferrin has been demonstrated by moving boundary (30, 58) and starch gel electrophoresis (59,60) and by isoelectric focussing (61,62), though slight differences between k_1 and k_2 have been demonstrated (52). Furthermore e.s.r. spectra at liquid nitrogen temperature of Cu^{2+} and Fe^{3+} lactoferrin and transferrin give narrower lines than at room temperature meaning that the line width is governed by spin-lattice relaxations and not spin-spin interactions, so the iron atoms must be more than 10A^{o} apart (63). The well resolved zero field Mössbauer spectrum of Fe_2-transferrin indicate long relaxation times and has led to the proposal that the separation is 20A^{o} or more (64). Studies involving the use of trivalent lanthanides as fluorescent probes has demonstrated the lack of fluorescent transfer between Fe^{3+} and Tb^{3+} when both were bound to transferrin suggesting that the separation may be as high as 43A^{o} (65).

HETEROGENEITY OF THE SITES

While no heterogeneity between the sites has yet been demonstrated for lactoferrin there is strong evidence for this in ovotransferrin even though no functional difference is apparent; both sites appear to be equal in their ability to donate iron to chick blood cells (66). The e.s.r. spectrum of ovotransferrin has a broad peak at g = 4.98 down

field of the g = 4.3 signal. This is strong when monoferric ovotransferrin has the second site occupied by gallium , but is much less prominent when the reverse applies (67,68).

Ever since Fletcher and Huehns proposed that transferrin is more than just a passive iron carrier and plays a key role in iron absorption and distribution in the body (69) there have been attempts to demonstrate a heterogeneity between the sites. Studies have shown that transferrin will bind two ions of terbium(III), europium(III), erbium(III) and holmium(III) but only one ion of neodymium(III) and praseodymium(III) (65) and since the size of these ions in descending order is Pr^{3+}, Nd^{3+}, Eu^{3+}, Tb^{3+}, Ho^{3+}, and Er^{3+} it becomes evident that there is a difference in accessibility of the two sites. The e.s.r. spectrum of VO^{2+} and Cr^{3+}-transferrin complexes showed splittings indicative of more than one environment contributing to the spectrum; only one site was occupied by VO^{2+} or Cr^{3+} at pH 6.0 (54,70,71, 72).

LACTOFERRIN

As has become evident from this discussion most studies on the metal binding properties of these proteins have been conducted on transferrin and ovotransferrin, partly because these proteins are more easily obtainable than human lactoferrin and partly because the physiological importance of the latter has only more recently been recognised. To date studies have indicated that although the proteins are all clearly different, their ligating groups in the binding sites are essentially similar and yet lactoferrin is able to retain its iron more tightly than the others. A solution to this apparent paradox is not immediately evident from the limited studies conducted on lactoferrin. Furthermore there is still some uncertainty about the number and nature of the ligating groups in the sites of these proteins. Hence an investigation was conducted on the metal binding properties of lactoferrin and small molecular weight phenolate complexes of iron and copper.

Chapter 1 LACTOFERRIN

1.1 INTRODUCTION

Very few studies have been made on human lactoferrin since its discovery in 1951. Only recently has research on human milk revealed the important part played by lactoferrin in regulating the level of microbial populations in the infant intestine by limiting the amount of iron available. Like the related proteins, transferrin and ovotransferrin, lactoferrin is known to strongly bind two iron(III) ions, in sites which appear to be essentially similar. However, there is still some uncertainty as to whether two or three tyrosyl groups are involved when iron(III) is bound and whether bicarbonate is directly bound to the metal. When copper(II) is bound some studies indicate that only one nitrogen is involved while others suggest that in one site one nitrogen is bound and three or four in the other. Lactoferrin binds iron much more tightly than transferrin and ovotransferrin and over a much wider pH range than transferrin. Yet there is no apparent explanation for this fact except for the suggestion that lactoferrin may undergo a greater conformational change on metal binding thus favouring the stability of metal-lactoferrin complexes.

To obtain more information about the binding sites of lactoferrin the metal ions of the first transition series including iron(III), copper(II), cobalt(III), chromium(III) and manganese(III), were reacted with the apoprotein. Preliminary investigations were conducted into determining the optimum conditions under which these metal ions bound to the specific sites. The resulting metal lactoferrin complexes were studied by the techniques of fluorescence, electronic, e.s.r. and Resonance Raman spectroscopy.

1.2 EXPERIMENTAL

1.2.1 PREPARATION OF GLASSWARE AND DIALYSIS TUBING

All glassware was treated with Triton X100 and A. R. concentrated nitric acid and then thoroughly rinsed with distilled deionised water to minimise metal ion contamin-

ation.

To remove heavy metal contaminates dialysis tubing was allowed to simmer for one hour in two changes of 50% ethanol, then washed with two changes of 10mM $NaHCO_3$/1mM EDTA, then two changes of distilled deionised water and stored in water at 4°C prior to use.

1.2.2 PREPARATION OF BUFFERS

(a) Phosphate Buffer, 0.01M, pH 7.6

This buffer was prepared by mixing 0.01M $Na_2HPO_4.2H_2O$ and 0.01M $NaH_2PO_4.2H_2O$ in the ratio 87:13.

(b) Tris-HCl Buffer, 0.05M, pH 7.41 (4°C)

This buffer was prepared by dissolving 6.057g of tris (hydroxymethyl)-aminomethane in one litre of distilled deionised water and titrating to pH 7.1 at 25°C with A. R. concentrated hydrochloric acid.

1.2.3 ISOLATION OF LACTOFERRIN

The method is a modified version of the one reported by Querinjean et.al. (18). To 100-200cm^3 of fresh human colostrum at 4°C was added 1 - 2 drops of β-mercaptoethanol and then sufficient ammonium sulphate until the concentration was 2M. The pH was adjusted to 7.0. The solution was centrifuged twice at 12000 r.p.m. at 4°C for 20 minutes, to remove the fat and the casein. The supernatant was dialysed against one change of deionised water (containing two drops of β-mercaptoethanol per 5 litres) for four hours and two changes of phosphate buffer (with β-mercaptoethanol) overnight. The supernatant was loaded onto a previously prepared and packed column of CM-Sephadex C-50 and the column washed with buffer until the eluent is clear. The column was washed with a 0-0.5M salt gradient and the elution curve showed two peaks (Figure 1.1). The second proved to contain lactoferrin while the first (generally referred to as pre-lactoferrin), from SDS gel electrophoresis (Figure 1.2(a)), proved to contain a mixture of proteins which included some lactoferrin. The fractions from the second peak were concentrated in a Chemlab Ultrafiltration cell fitted with

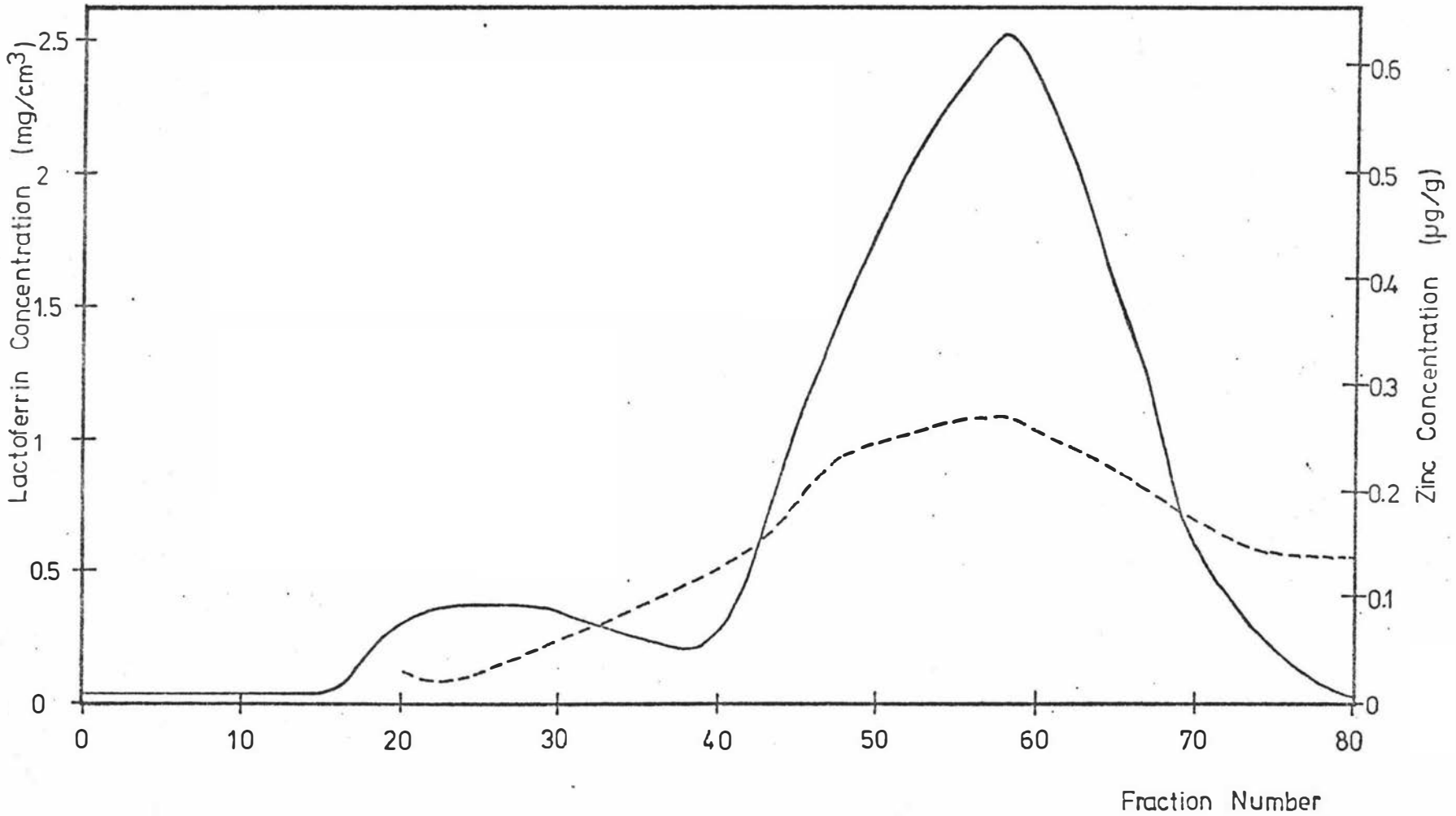

Figure 1.1 CM-Sephadex C-50 chromatography of the supernatant prepared from human milk; concentration of prelactoferrin and lactoferrin (——) in the fractions determined from the absorbance of the solution at 280nm, zinc concentration (- -) in the fractions measured by atomic absorbance.

an Amicon Diaflo XM50 membrane. In some preparations the fractions were analysed for their zinc content before concentration.

The CM-Sephadex C-50 gel was regenerated by washing, first with one change of 0.1M NaOH, then quickly by several changes of distilled deionised water. This was followed by successive changes of 0.1M, 0.05M and 0.01M, pH 7.6 phosphate buffer to constant pH and conductivity at each stage.

The yield of apolactoferrin averaged 1-2mg per cm^3 of colostrum and the percentage iron saturation, estimated from the absorbances at 280nm and 465nm (Table 1.6), was around 15%, though on a number of occasions was as low as 6% (where 100% saturation is equivalent to two iron(III) ions binding). Apolactoferrin, as isolated, was used since metal ion uptake and e.s.r. experiments (see section 1.3.2 and section 1.3.5) indicated that dialysis against 0.1M citric acid, pH 2.0, adversely affected the protein.

1.2.4 GEL ELECTROPHORESIS

(a) SDS Gel Electrophoresis

SDS gel electrophoresis was performed on the denatured protein using a gel containing 7% acrylamide, 0.24% bis-acrylamide, 0.1% tetramethylethylenediamine in gel buffer, polymerised by ammonium persulphate. The protein sample containing 10% of a solution of 6M urea/1% SDS/1% β-mercaptoethanol/0.1M Tris-glycine, was denatured by heating to 100°C for two minutes after which 10μl of the boundary marker, 0.05% Bromophenol Blue, was added. After pre-electrophoresing the gels in the gel buffer, 0.1M Tris-glycine/0.1% SDS (pH 8.3), for 30 - 40 minutes the upper reservoir buffer is changed, the protein samples loaded and the gels run for two to three hours using a current of 4mA per gel. The gels were stained by Coomassie Brilliant Blue R250 and excess stain removed by washing with 7% acetic acid/7% methanol.

The purity of the preparations was estimated by running gels containing 5,20,50 and 100μg of protein (Figure 1.2b) and measuring the intensity of the protein bands at 600nm on

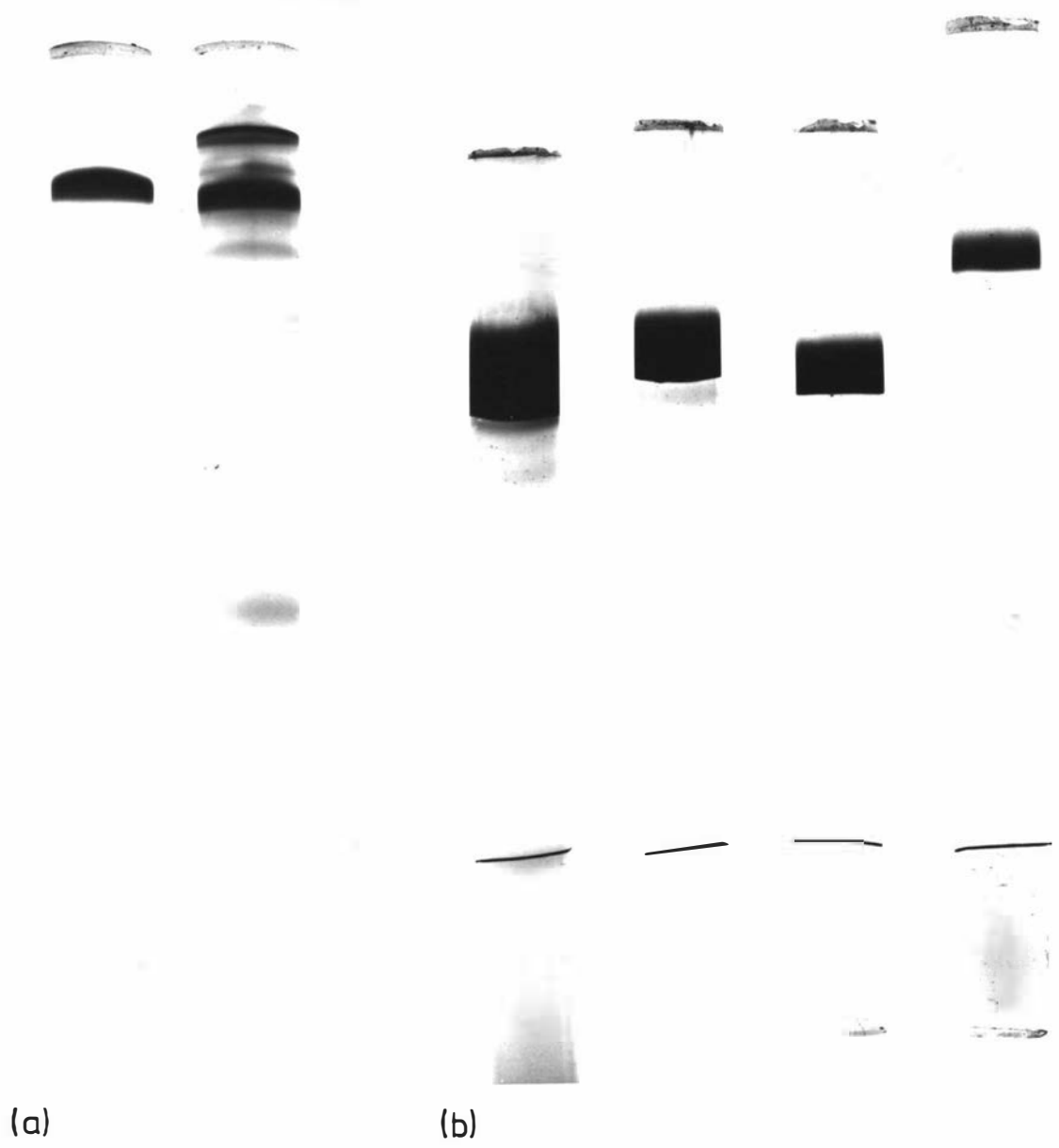

Figure 1.2 (a) SDS polyacrylamide gel electrophoresis of the two bands eluted from a CM-Sephadex C-50 column; left, lactoferrin, right prelactoferrin (the band preceeding lactoferrin).
(b) SDS polyacrylamide gel electrophoresis of lactoferrin; left to right, gels containing 100, 50, 20 and 5 μg of lactoferrin.

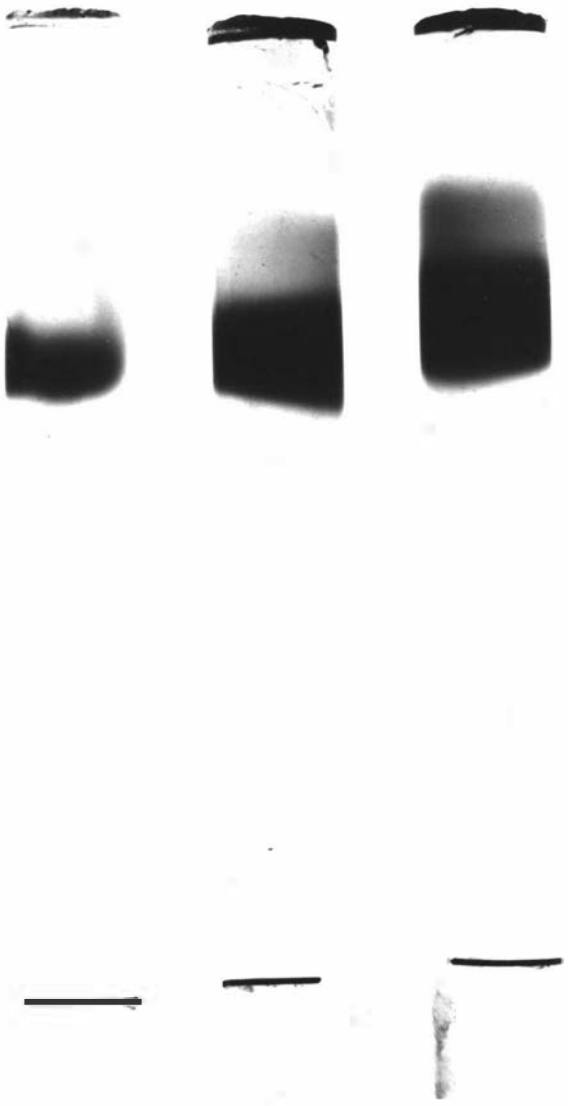

Figure 1.3 Polyacrylamide gel electrophoresis of lactoferrin at pH 2.9; left to right, gels containing 10, 50 and 100 μg of lactoferrin.

a Beckman Acta III fitted with a gel scanning accessory. Comparison of the intensity of the bands due to impurities with the band containing 5μg of lactoferrin enabled estimates of the amount of impurity to be made. From this it was shown that lactoferrin in all preparations was 99% pure.

(b) Gel Electrophoresis at pH 2.9

Polyacrylamide gel electrophoresis was successfully performed on the undenatured protein to determine whether proteins of similar molecular weight to lactoferrin (i.e. transferrin) were present. A gel containing 12% acrylamide, 0.32% bis-acrylamide in Tris-Citric acid buffer (pH 2.9) and polymerised by $FeSO_4$ was used. The gels were run in a solution of 0.37M glycine, adjusted to pH 4.0 with citric acid, at a current of 4mA per gel, the boundary marker being 0.1% Fuschin Basic. The gels were stained with Coomassie Brilliant Blue R250 and excess stain removed by washing with 7% acetic acid/ 7% methanol. From this technique lactoferrin was found to be 99% pure (Figure 1.3). No other proteins of similar molecular weight were observed to be present in significant amounts in the preparations.

1.2.5 PREPARATION OF METAL-LACTOFERRIN COMPLEXES

The manganese(III) and cobalt(III) complexes of lactoferrin (Mn_2Lf and Co_2Lf, where Lf = lactoferrin) were prepared by a modification of the procedure described for transferrin (54). A five-fold excess of the appropriate metal(II) ion citrate complex was added to a 2×10^{-4}M solution of apolactoferrin in 0.05M Tris buffer, pH 7.4. After the addition of excess $NaHCO_3$ the solutions were allowed to stand at 4°C for one week. Increments of 5μl 1.0% H_2O_2 were added to the protein solution during this period until the intensities of the visible absorption bands maximised. Uncombined metal ions were removed by Sephadex G-25 filtration followed by chromatography on Chelex 100. The solutions were concentrated to about 1×10^{-4}M by ultra-filtration. When preparing Cr_2Lf the initial pH had to be below 7.0 to avoid precipitation of $Cr(OH)_3$. The metal was added as $CrCl_3$ and after binding to lactoferrin had been observed to occur (usually after one week) the pH was increased to 7.6. Cr_2Lf was best prepared

by adding no more than two moles of $CrCl_3$ per mole of lactoferrin.

1.2.6 METAL ION UPTAKE EXPERIMENTS

The kinetics of the reaction of the metal chelate with lactoferrin was followed by the absorbance change at 465nm. Measurements were conducted on a Shimadzu MPS 5000 spectrophotometer, solutions were thermostated and maintained at 25°C with a circulating water bath. The metal chelates were prepared by dissolving $Fe(NO_3)_3.9H_2O$ or $CuCl_2.2H_2O$ in solutions containing equimolar amounts of citrate, ethylenediaminetetraacetate (EDTA) or nitrilotriacetate (NTA). Solutions were all freshly prepared before use. Studies were conducted in both phosphate buffer 0.01M, pH 7.6 that was 0.33M in NaCl and Tris buffer 0.05M, pH 7.4 that was 0.5M in NaCl. Runs were made in duplicate and in all cases two molar equivalents of the appropriate metal ion were added to the protein.

1.2.7 FLUORESCENCE SPECTROSCOPY

Measurements were made on a Turner Model 430 spectrofluorimeter using buffer to set zero fluorescence and apolactoferrin to set 100% fluorescence. The metal chelates were prepared as 0.01M solutions, then diluted to 10^{-4}M, before adding to a $\sim 10^{-6}$M solution of apolactoferrin; iron(III) and lead(II) as NTA complexes, manganese(II) and cobalt(II) as citrate complexes and copper(II), nickel(II), zinc(II) and mercury(II) as their chloride salts. Solutions containing 1, 2, 3 and 4 moles of metal ion per protein were prepared in duplicate and allowed to stand overnight before measurements were made. Solutions were normally kept for no more than two days as an increase in the relative fluorescence after this provided evidence for a steady protein degradation (Table 1.4).

1.2.8 ELECTRONIC AND ATOMIC ABSORBANCE SPECTROSCOPY

Electronic absorption spectra were recorded on a Shimadzu MPS 5000 spectrophotometer and metal ion concentrations were measured on a Varian Techtron AA5 atomic absorbance

spectrophotometer. Protein concentrations were determined from the absorbances at 280nm (Table 1.6).

1.2.9 ELECTRON SPIN RESONANCE SPECTROSCOPY

Lactoferrin was concentrated to around 4×10^{-4}M by ultrafiltration. Fe_2Lf and Cr_2Lf were prepared by adding iron(III) and chromium(III) as NTA complexes. Isotopically pure ^{65}Cu was obtained as its oxide from Oak Ridge National Laboratory and dissolved in 1M HCl before use. Bicarbonate-free ^{65}Cu-Lf was prepared by a modification of the method of Aisen et.al.(46). Apolactoferrin in 0.01M phosphate buffer is carefully titrated to pH 4.0 with 1M phosphoric acid and to this is added 2 molar equivalents of $^{65}CuCl_2$. The solution is placed at one end of a Thunberg tube joined to an e.s.r. tube by a graded seal and the system is successively evacuated and flushed with nitrogen for 1½ hours. Sufficient $Na_2HPO_4.2H_2O$, added as a solid, gave on mixing a final pH in the range 7 to 8.

E.S.R. spectra were recorded at -160°C on a Varian E104A spectrometer with a Varian E-257 Variable Temperature accessory. Spectral g values were calibrated with a 1,1-diphenyl-2-picryl-hydrazyl (DPPH) standard.

1.2.10 RESONANCE RAMAN SPECTROSCOPY

Resonance Raman spectra were collected on a computer-controlled Jarrell-Ash 25-300 Raman spectrometer by Professor T. M. Loehr on samples of Fe_2Lf, Cu_2Lf, Co_2Lf, Mn_2Lf and Cr_2Lf suspended in a variable temperature nitrogen flow accessory maintained at -40°C. Light from a Coherent Radiation Laboratory CR-04 Argon ion laser was used, while the detector employed in these studies was an ITT FW-130 (S-20) photomultiplier.

1.2.11 ISOELECTRIC FOCUSSING

Isoelectric focussing was conducted in a column based on the LKB 8100-1 (110cm^3 capacity) electrofocussing model. Initial studies were performed in a pH 3-10 ampholyte then later in LKB and Biolyte pH 7-10 and 8-10 ampholyte

solutions. The ampholytes were supported in a sucrose density gradient with electrode solutions of 1% sulphuric acid and 10% NaOH. The current was passed through the column for periods of up to 50 hours at a constant voltage of 500V. After this the column was drained at a rate of $1cm^3$/minute and samples of $2cm^3$ were collected. The pH was measured with a combination glass/calomel pH electrode and the protein concentration determined from the absorbance at 280nm (Table 1.6).

1.3 RESULTS AND DISCUSSION

1.3.1 METAL ION BINDING BY LACTOFERRIN

(a) Zinc

Zinc is present in human milk in higher concentrations than iron. The total concentration of zinc in milk on the first day of lactation is 10 ± 5μg/g (of milk) declining to 3.14 ± 1.35μg/g after 14 days and 1.31 ± 0.5μg/g after 10 weeks. In contrast iron has a concentration on the first day of lactation of 1.9 ± 5.6μg/g which drops thereafter to around 0.8μg/g (75).

Fractions from several preparations of lactoferrin were analysed by atomic absorbance for their zinc content. The results from one preparation are illustrated in Figure 1.1. In this preparation the concentration of protein was found to be $1.21mg/cm^3$ of milk while the concentration of zinc associated with lactoferrin was $0.323\mu g/cm^3$ of milk; a zinc/protein ratio of 0.327. Similar ratios were observed in other preparations (76). However there is a wide variation in the zinc/protein ratio in the fractions from the column (Figure 1.1); in fraction 40 it is 0.575, fraction 50 it is 0.168, fraction 60 it is 0.136 and fraction 70 it is 0.353, good evidence for a weak association between zinc and lactoferrin. Furthermore the zinc/protein ratio drops to ~0.1 when lactoferrin is concentrated by ultrafiltration (76) suggesting that the zinc is easily removed. Thus the low zinc protein ratio may be a consequence of this weak association.

(b) Manganese(III), Chromium(III) and Cobalt(III)

Previously human lactoferrin has been shown to form the complexes Fe_2Lf and Cu_2Lf (7,77) and results from this study have shown that the average number of metal ions per molecule of lactoferrin, when the metal is manganese or cobalt is 2.0 ± 0.2. However, unlike iron(III) and copper(II), manganese(III), cobalt(III) and chromium(III) do not bind to lactoferrin in phosphate buffer necessitating the use of the more weakly coordinating Tris buffer. Both manganese and cobalt appear to be in the trivalent state (i.e. high spin Mn(III) and low spin Co(III)) as hydrogen peroxide is essential in the formation of Co_2Lf and while Mn_2Lf will form slowly in air addition of hydrogen peroxide accelerates the process. The absence of signals in the e.s.r. spectra of both complexes provides further support for this idea as low spin cobalt(III) is diamagnetic while high spin manganese(III) is e.s.r. inactive. When the metal is chromium(III) studies indicated that excess chromium was not readily removed by chromatography on Sephadex or Chelex, like transferrin (54), thus the Cr_2Lf (Lf = lactoferrin) was best prepared by adding two moles of chromium(III) per mole of lactoferrin. The ability of lactoferrin to retain excess chromium(III) (e.g. reported saturation values of lactoferrin as high as 240% instead of the expected 100%) when added as $CrCl_3$ is very similar to a phenomenon reported for transferrin (78). Sephadex and Chelex columns normally firmly bind $FeCl_3$, in the presence of transferrin, however, most $FeCl_3$ is eluted bound non-specifically to the protein.

1.3.2 METAL ION UPTAKE

Table 1.1 and Figure 1.4 show the times required to half saturate lactoferrin and transferrin with various iron(III) and copper(II) chelates. With Fe-NTA the $t_{\frac{1}{2}}$ values for all the proteins in phosphate buffer or Tris buffer were short (e.g. $t_{\frac{1}{2}} < 10$ seconds) indicating a rapid initial phase. For the citrate-treated protein the reaction was complete in $1\frac{1}{2}$ minutes, while with apolactoferrin it was 90 minutes. With the 1:1 complex of iron(III) with citrate $t_{\frac{1}{2}}$ ($2\frac{1}{2}$ - 4 minutes) for the apo-

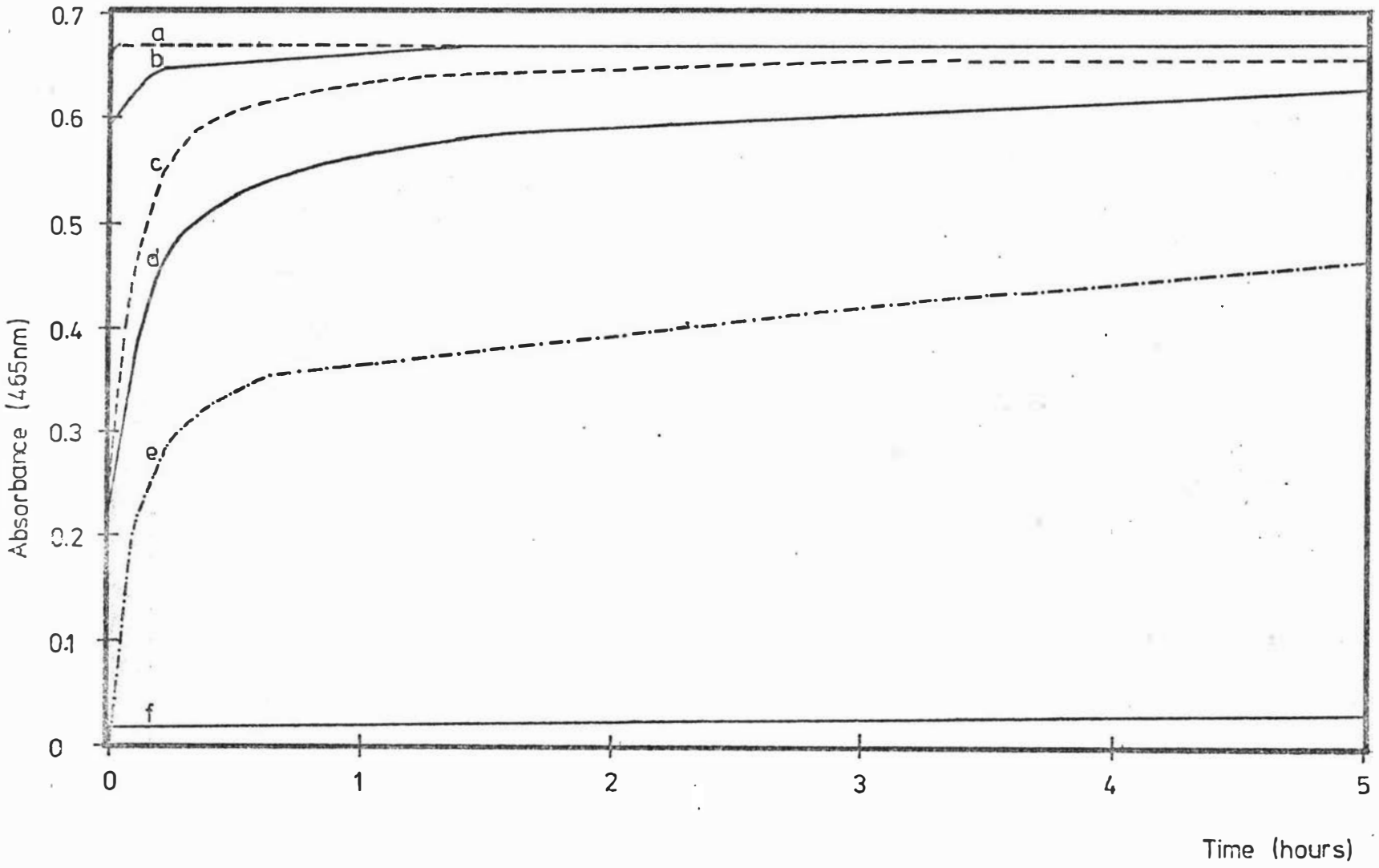

Figure 1.4 Uptake of (a) 1:1 iron-NTA and (c) 1:1 iron-citrate by citrate-treated apolactoferrin. Uptake of (b) 1:1 iron-NTA, (d) 1:1 iron-citrate, (e) 1:10 iron-citrate and (f) 1:1 iron-EDTA by apolactoferrin. All solutions contained 1.6×10^{-4} moles of apolactoferrin (in phosphate buffer 0.01M, pH 7.6, which is 0.33M in NaCl) and 3.2×10^{-4} moles of metal-chelate.

Table 1.1 Times required to half saturate Apolactoferrin and Apotransferrin with Iron(III) and Copper(II). ($t_{\frac{1}{2}}$)

	Apolacto-ferrin[a]	Citrate-Treated Apolactoferrin[a]	Apotrans-ferrin[b]
Fe-NTA (1:1)[c]	<10 seconds	<10 seconds	3 seconds
Fe-Citrate (1:1)	4 minutes	2½ minutes	8 hours
Fe-Citrate (1:10)	28 minutes	-	~4 minutes
Fe-EDTA (1:1)[d]	3 days	-	~4 days
$Cu-Cl_2$	<10 seconds	-	-
Cu-Citrate (1:1)	<10 seconds	-	-
Cu-EDTA (1:1)	No binding	-	-

a. Apolactoferrin (iron-free lactoferrin)in phosphate buffer
b. Apotransferrin (iron-free transferrin) in Tris buffer (79)
c. NTA; Nitrilotriacetate
d. EDTA; Ethylenediaminetetraacetate

lactoferrin proteins was longer than when iron was added as a 1:1 complex with NTA, while with 1:1 iron-citrate added to transferrin in Tris buffer $t_{\frac{1}{2}}$ was as long as eight hours (79). Slowest binding occurs with Fe-EDTA, $t_{\frac{1}{2}}$ for apolactoferrin in phosphate buffer being three days while that for apo-transferrin in Tris buffer being four days. A similar trend is observed for copper(II) chelates. Copper added as $CuCl_2$ binds completely within five minutes, when added as a 1:1 complex with citrate saturation of the protein is complete within 15 minutes, while copper shows no inclination to bind when added as a complex of EDTA. Thus the uptake of iron in order of increasing $t_{\frac{1}{2}}$ is $t_{\frac{1}{2}}$ FeNTA $< t_{\frac{1}{2}}$ FeCitrate $< t_{\frac{1}{2}}$ FeEDTA. Furthermore the faster uptake of iron by apolactoferrin may be reflected in its ability to bind iron(III) more strongly than transferrin. Studies on transferrin have demonstrated that Fe-Citrate exists as a high molecular weight polymer in solution and that it is the rate at which this polymer breaks up into a monomer which determines the rate of uptake of iron(III) by apolactoferrin

(79). Uptake of Fe-NTA by apolactoferrin is quicker because in solution it occurs as a monomer only. EDTA, which is a hexadentate chelating agent, is able to completely surround the ferric ion such that it is well shielded from nucleophilic attack. The partial unwrapping of the chelate exposes the iron, making it much more labile and this determines the rate of uptake of iron(III) by apolactoferrin. From these experiments then the rate at which the EDTA chelate unwraps to expose the iron is much slower than the rate of breakdown of the Fe-Citrate polymer.

When the citrate to iron(III) ratio is increased from 1:1 to 10:1, $t_{\frac{1}{2}}$ for apolactoferrin (in phosphate buffer) increases from four to 28 minutes, the reverse of that observed with apotransferrin when $t_{\frac{1}{2}}$ drops from eight hours to four minutes (79). Considerable amounts of citrate are known to occur in human milk (80); four days after parturition it has been observed to be as high as $0.9mg/cm^3$, a citrate to lactoferrin ratio of 174:1 (assuming the lactoferrin concentration to be $2mg/cm^3$). In spite of its central role in the metabolism of all cells, the significance of the presence of citrate in milk and its mode of secretion are not known. Citrate is known to be very closely associated with transferrin (44) and is not readily removed by dialysis against water. However it is effectively removed by dialysis against 0.1M $NaClO_4$ or passage down a Sephadex G-25 column. It seems likely that with such high citrate:lactoferrin ratios existing in milk that some citrate must still be closely associated with lactoferrin after isolation. This is supported by the fact that dialysis of apolactoferrin against 0.1M $NaClO_4$ causes precipitation of the protein which is only reversed by dialysis against citric acid, indicating that citrate plays an important role in stabilising lactoferrin in solution. It also appears that there is an indeterminate amount of citrate closely associated with apolactoferrin which should be taken into consideration when dealing with uptake of Fe-Citrate complexes by the apoprotein.

In tris buffer $t_{\frac{1}{2}}$ for iron(III) uptake from Fe-Citrate by apolactoferrin is now 12 minutes, the different buffer

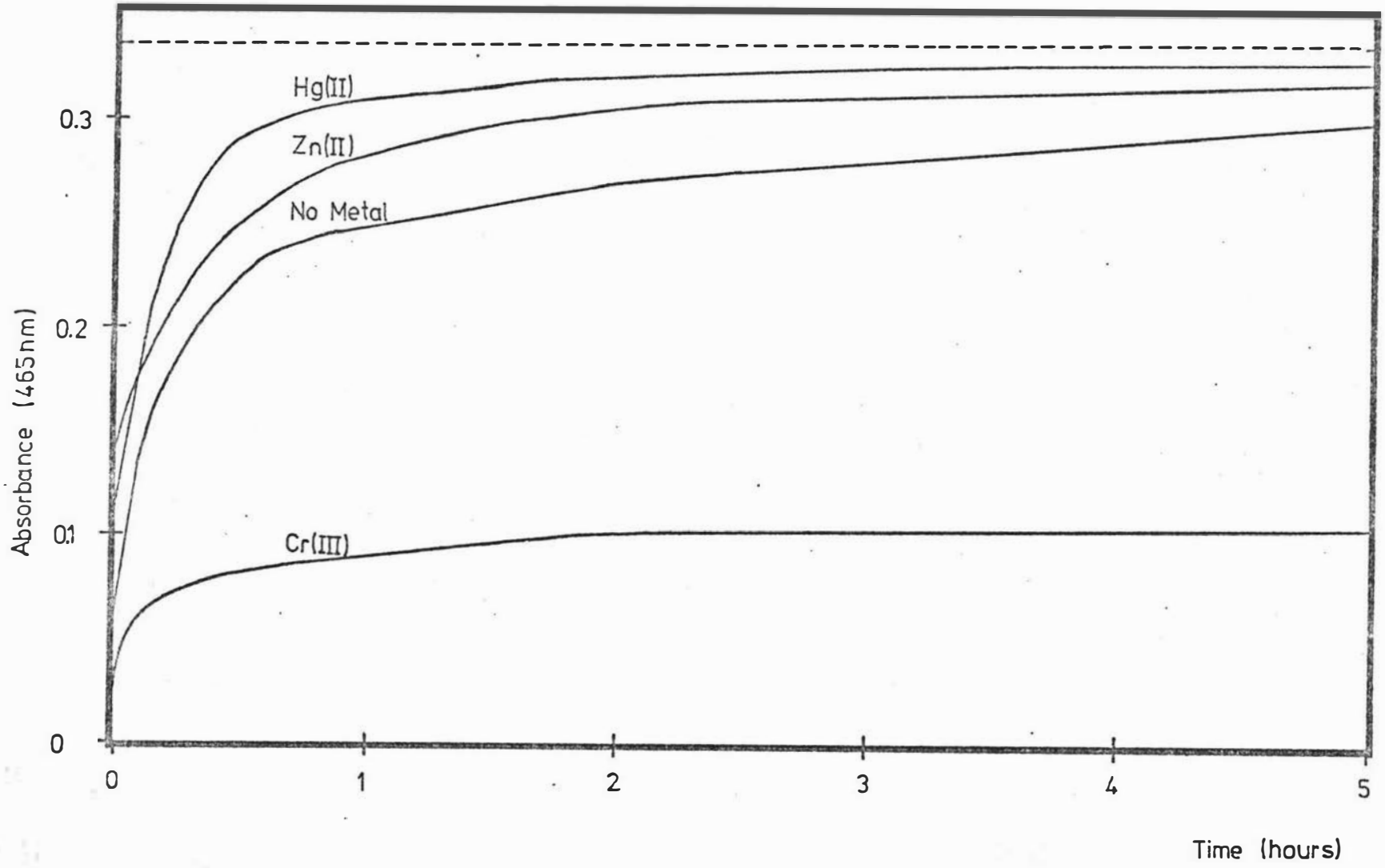

Figure 1.5 The influence on the uptake of a 1:1 complex of iron-citrate by apolactoferrin (in 0.05M, pH 7.4 Tris buffer, 0.05M in NaCl) of other metal ions. All solutions contained 0.89×10^{-4} moles of apolactoferrin and 1.78×10^{-4} moles of Cr(III), Zn(II), Hg(II) and iron-citrate.

having a pronounced effect on $t_{\frac{1}{2}}$ (Figure 1.5). In the presence of two molar equivalents of zinc(II) or mercury(II) $t_{\frac{1}{2}}$ is about five minutes, providing evidence that these ions are weakly bound and suggesting that the decreased $t_{\frac{1}{2}}$ may be due to a faster breakdown of the 1:1 Fe-Citrate polymer in solution or a more favoured conformation of the protein for iron(III) binding. In contrast two chromium(III) ions bound to the protein strongly inhibit the uptake of Fe-Citrate (76). After four days the saturation of the protein by iron(III) is no more than 44%, good evidence for the specific binding of chromium(III).

1.3.3 FLUORESCENCE SPECTROSCOPY STUDIES

The absorption of light is followed by its emission at a longer wavelength - this emission is fluorescence. Fluorescence is quantified by determining the Quantum yield, Q;

$$Q = \frac{\text{photons emitted}}{\text{photons absorbed}}$$

Interaction with molecules in the environment can reduce the quantum yield through external conversion (i.e. processes that can cause the molecules to drop to the ground state without light emission) hence this process is known as quenching. There are only three intrinsic fluors in a protein tryptophan, tyrosine and phenylalanine, listed in order of decreasing Q. In practice only tryptophon can be detected; phenylalanine has a very low Q and tyrosine fluorescence is weak due to quenching, usually when it is ionised or near an amino or carboxyl group or tryptophan.

For apolactoferrin in phosphate buffer the wavelength of maximum excitation is 292nm and maximum emission is 348nm, whereas in Tris buffer the corresponding values are 290nm and 334nm. Comparative values for apotransferrin in Hepes buffer are 280nm and 328nm (43). Since tryptophan fluorescence maxima can be expected to vary from 370-315nm as the solvent polarity is decreased then it would appear that the important tryptophan residues are in very non polar environments.

Table 1.2 Fluorescence Quenching of Apolactoferrin by Divalent and Trivalent Metal Ions (in Tris Buffer)

	% Fluorescence as a Function of Metal: Protein Ratio			
Metal Ion	1:1	2:1	3:1	4:1
Fe(III)	46.8	22.3	22.8	22.5
Cu(II)	70.5	58.5	59.5	59.5
Cr(III)	78.5	74.0	73.3	72.0
Cr(III)[a]	-	62.5	-	-
Mn(II)	79.5	77.5	77.5	76.5
Mn(III)[a]	-	35.5	-	-
Co(II)	80.0	77.3	77.5	76.5
Co(III)[a]	-	47.0	-	-
Ni(II)	83.0	81.0	81.0	81.0
Zn(II)	81.5	82.0	80.8	79.5
Cd(II)	79.5	77.0	75.5	76.0
Hg(II)	83.5	80.5	76.5	78.0
Pb(II)	77.5	73.5	75.5	76.5

a. These measurements were made one week after the addition of the metal ion.

The addition of iron(III) and copper(II) to apolactoferrin causes a quenching of the fluorescence which reaches a maximum after the addition of two metal ions per protein molecule (Table 1.2). As for serum transferrin and ovotransferrin (43) it appears that tryptophan residues are not directly bound to the metal ions, but their fluorescence may be quenched by a long range energy transfer to an absorption band produced by the metal protein interaction. Moreover the fluorescence titration curve for iron(III) and copper(II) binding is not linear (76) and as for serum transferrin may be analysed assuming a random binding model giving a result of $k_1 = 0.8k_2$ (where k_1 and k_2 represent the fraction of the original fluorescence quenched by the

binding to one and two sites on the same molecule). For serum transferrin an almost identical result has been obtained, i.e. $k_1 = 0.75k_2$ (43), and in both cases the non linear dependence of the fluorescence on metal binding suggests that it is not an all or none process.

Fluorescence quenching is also exhibited by the trivalent ion-lactoferrin complexes (Table 1.2) which is most significant for manganese(III) and cobalt(III), in line with the strong specific site interaction of these ions. While these complexes are prepared by oxidising manganese(II) and cobalt(II) in the presence of apolactoferrin, cobalt(II) shows much more resistance to oxidation by H_2O_2 than manganese(II) and only appears to bind at the specific sites once the metal:protein ratio is greater than 2 (Table 1.3). Furthermore only manganese(II) will undergo aerial oxidation in the presence of the protein, followed by binding to the specific sites as indicated by the increase in fluorescence quenching of such solutions with time (Table 1.4).

In contrast to manganese(III) and cobalt(III) the divalent metal ions manganese(II), cobalt(II), nickel(II), zinc(II), cadmium(II), mercury(II) and lead(II) with apolactoferrin in a 1:1 mole ratio exhibit a lesser quenching (Table 1.2). Increasing the metal:protein ratio does not alter the quenching significantly while addition of iron(III) as its NTA complex causes an immediate increase in fluorescence quenching (to a relative fluorescence of around 30%) indicating that almost all of the added iron(III) has bound at the specific sites (a fluorescence quenching of 23% would be expected for complete saturation by iron) (Table 1.5). This is in marked contrast to ovotransferrin where fluorescence quenching is observed on binding iron(III), chromium(III) and copper(II) but not with other metal ions (81). However, ultraviolet difference spectral studies have demonstrated that manganese(II), cobalt(II), cadmium(II), zinc(II) and nickel(II) combine with the tyrosyl residues of the specific sites of ovotransferrin, though they do not bind as strongly as iron(III), chromium(III) and copper(II) which can displace them

Table 1.3 Binding of Manganese(II) and Cobalt(II) by Apolactoferrin After the Addition of Hydrogen Peroxide.

Metal Ion	Time After Addition of H_2O_2 (Hours)	% Fluorescence as a Function of Metal:Protein Ratio			
		1:1	2:1	3:1	4:1
Mn(II)	0	73	68.5	67	68.5
	24	66	51	45	41
	48	66	52	44	39
Co(II)	0	82	82	81	77
	24	77	77	75	72
	48	80	75	70	69

Table 1.4 Binding of Manganese(II) and Cobalt(II) to Apolactoferrin in the Absence of Hydrogen Peroxide.

Metal	Metal:Protein Ratio	% Fluorescence as a Function of Time After the Addition of the Metal (Days).			
		1	5	6	7
Mn(II)	2:1	74	56.5	40	38
Co(II)	2:1	78.5	78	80	89.5

from the specific sites relatively easily (82). Like ovotransferrin the absence of colour on interaction of the divalent metal ions in Table 1.2 with lactoferrin does not necessarily mean that no complex is formed, hence by analogy with ovotransferrin we would expect them to be interacting with the tyrosyl residues of the specific sites of lactoferrin.

Only weak fluorescence quenching was observed one to two days after the addition of chromium(III) to apolactoferrin, though stronger quenching was exhibited after one week (Table 1.2). Chromium(III), one to two days after

Table 1.5 Binding of Two Iron(III) Equivalents by Metal-Lactoferrin Complexes

Metal	% Fluorescence as a Function of Metal:Protein Ratio			
	1:1	2:1	3:1	4:1
Cr(III)	37.5	31	37.5	33.5
Ni(II)	35.5	34	35.5	33
Zn(II)	32	34	35	32.5
Cd(II)	34	30	32	33
Hg(II)	33	30.5	31	32
Pb(II)	27	28.5	26	29.5

addition to apolactoferrin, is still only partially bound as it can be almost totally displaced by iron(III) at this stage (Table 1.5). One week after the addition of chromium-(III) to apolactoferrin it is only possible to displace 50% of specifically bound chromium by iron(III) (Section 1.3.2).

1.3.4 ELECTRONIC SPECTROSCOPY

All the complexes show an increased absorbance in the ultraviolet near 295nm, when compared with the apoprotein, pointing to deprotonated tyrosyl residues coordinated to metal ions (7,54). The visible spectra (Figures 1.6 - 1.9, Table 1.6) resemble those reported for the human serum transferrin and ovotransferrin complexes (40,54,83), thus reinforcing the postulate that the metal binding sites in all these proteins are very similar and involve the same ligating donor atoms. Both Mn_2Lf and Co_2Lf show intense bands in the 400nm region (Figure 1.7) which are tentatively assigned, as for Fe_2Lf, to a phenolate-to-metal charge transfer type transition. However data for suitable small molecule manganese and cobalt complexes are not available for comparison. In the case of Mn_2Lf, at least two shoulders are discernible (Figure 1.7) on the longer wavelength side of the 435nm band which, although of high intensity, are presumably a result of d-d absorptions "stealing intensity"

Table 1.6 Electronic Spectral Data for Human Lactoferrin Complexes.

Complex [a]	Colour	λ_{max}(nm)	$E^{1\%}_{1cm}$ [b]	$\varepsilon_{(l\ mole^{-1}\ cm^{-1})}$ [d]
ApoLf [c]	Colourless	283	10.9	-
Fe_2Lf [c]	Salmon pink	283	14.3	-
		465	0.51	4140
Cu_2Lf	Lemon	283	12.5	-
		438	0.60	4800
		677	0.08	620
Co_2Lf	Yellow	283	13.6	-
		405	1.28	10340
Mn_2Lf	Brown	283	14.7	-
		340(sh)	1.23	9950
		435	1.19	9620
		520(sh)	0.60	4850
		640(sh)	0.28	2310
Cr_2Lf	Grey green	283	12.2	-
		442	0.064	520
		612	0.035	280

a. Lf = Human lactoferrin.

b. $E^{1\%}_{1cm}$ is absorbance of 1% protein solution in a 1cm cell.

c. Data from ref. 7.

d. Assuming MW of 81000.

from the nearby charge transfer band. Certainly for a range of high spin manganese(III) complexes (which like copper(II)) complexes are expected to be subject to Jahn Teller distortions (84)) up to three d-d bands are generally observed in the 500-1000nm range (85,86).

In agreement with previous reports (77,87) the copper-(II) complex, Cu_2Lf, exhibits a band at 438nm (Figure 1.6) which from studies of small molecular weight complexes (Chapter 3) can be assigned to a copper-to-phenolate charge transfer transition. The wavelength of this absorption when

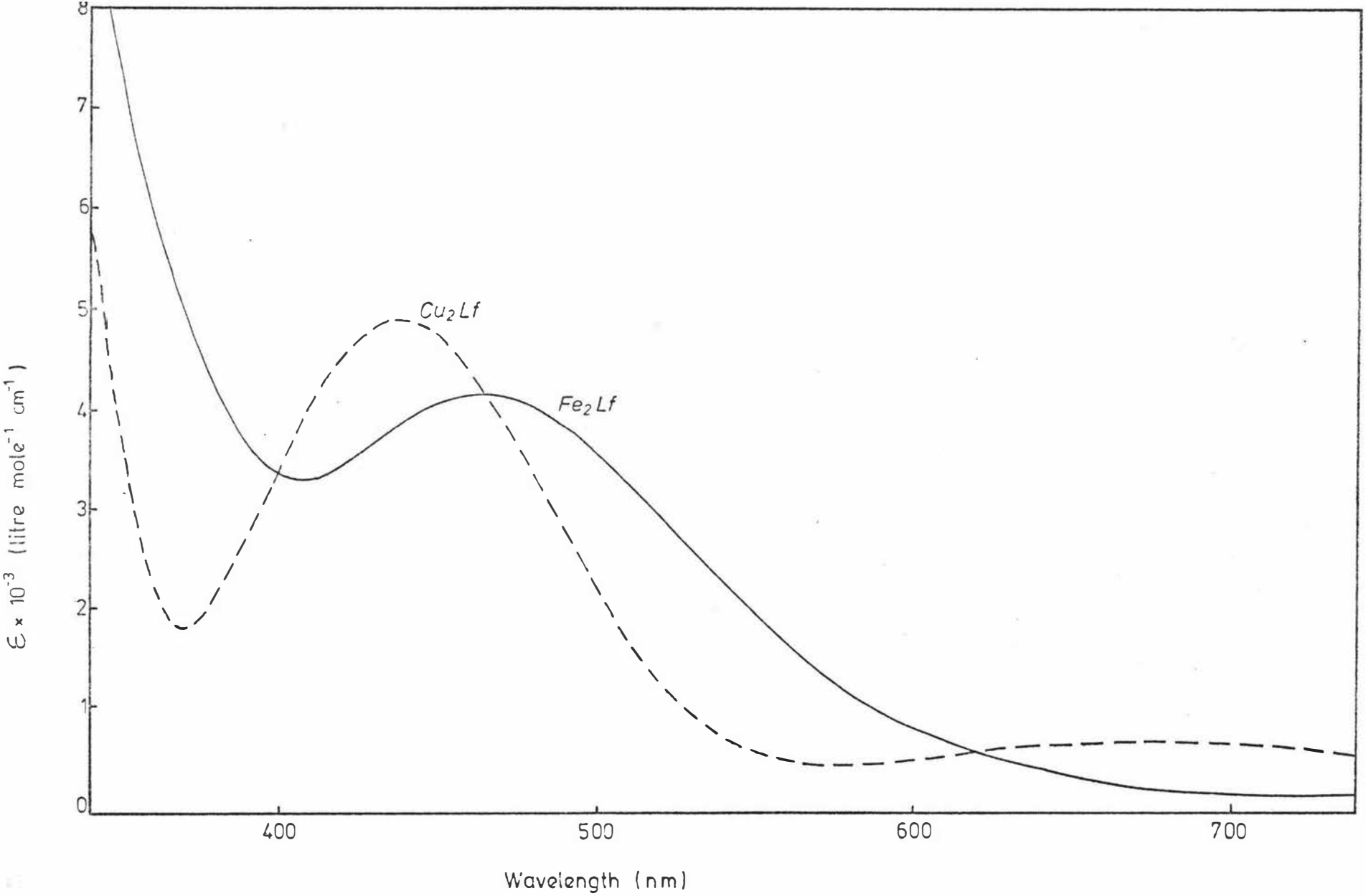

Figure 1.6 Visible absorption spectra of Fe_2Lf (——) and Cu_2Lf (- -), phosphate buffer pH 7.6, 0.01M.

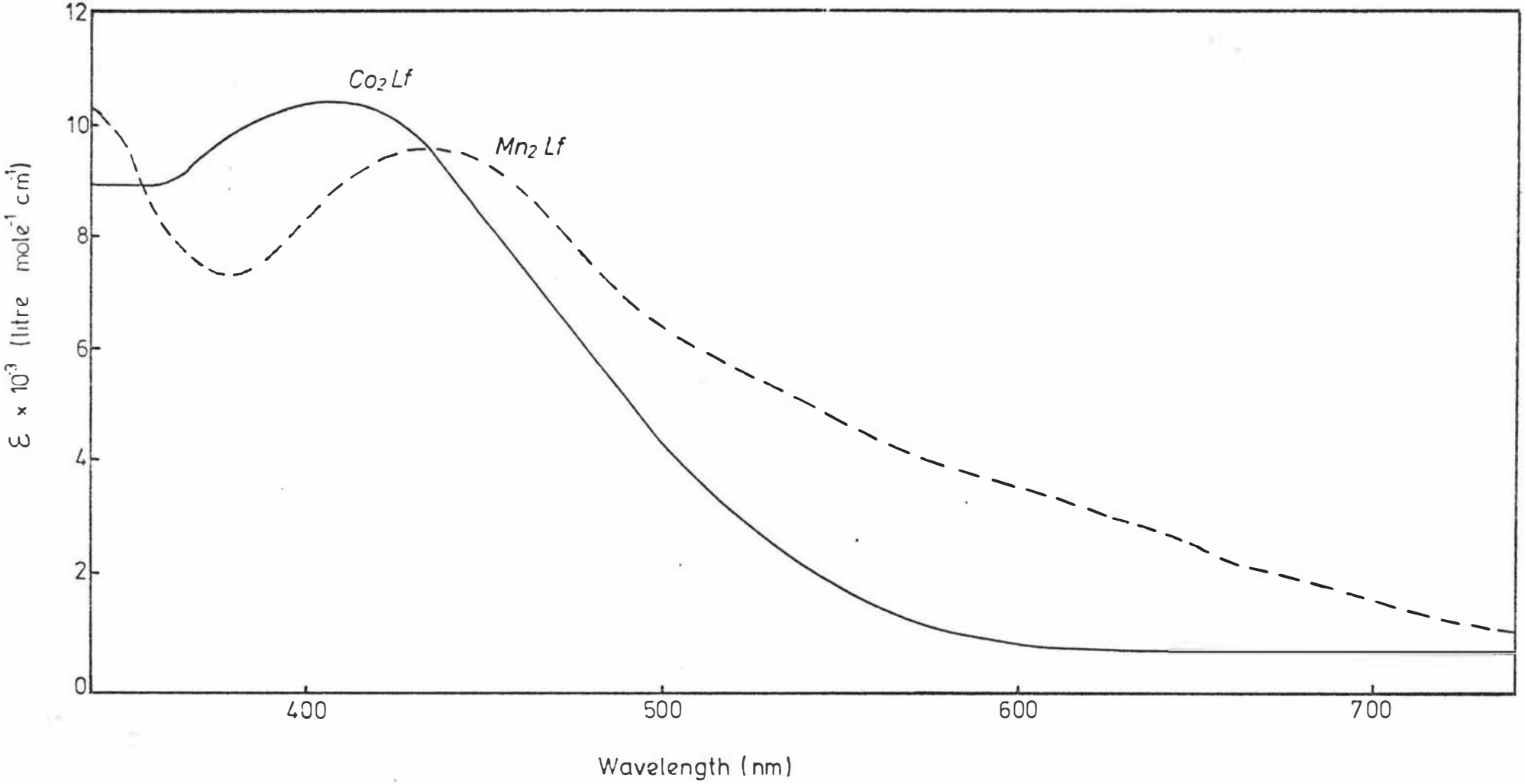

Figure 1.7 Visible absorption spectra of Co_2Lf (——) and Mn_2Lf (- -), Tris buffer pH 7.4, 0.05M.

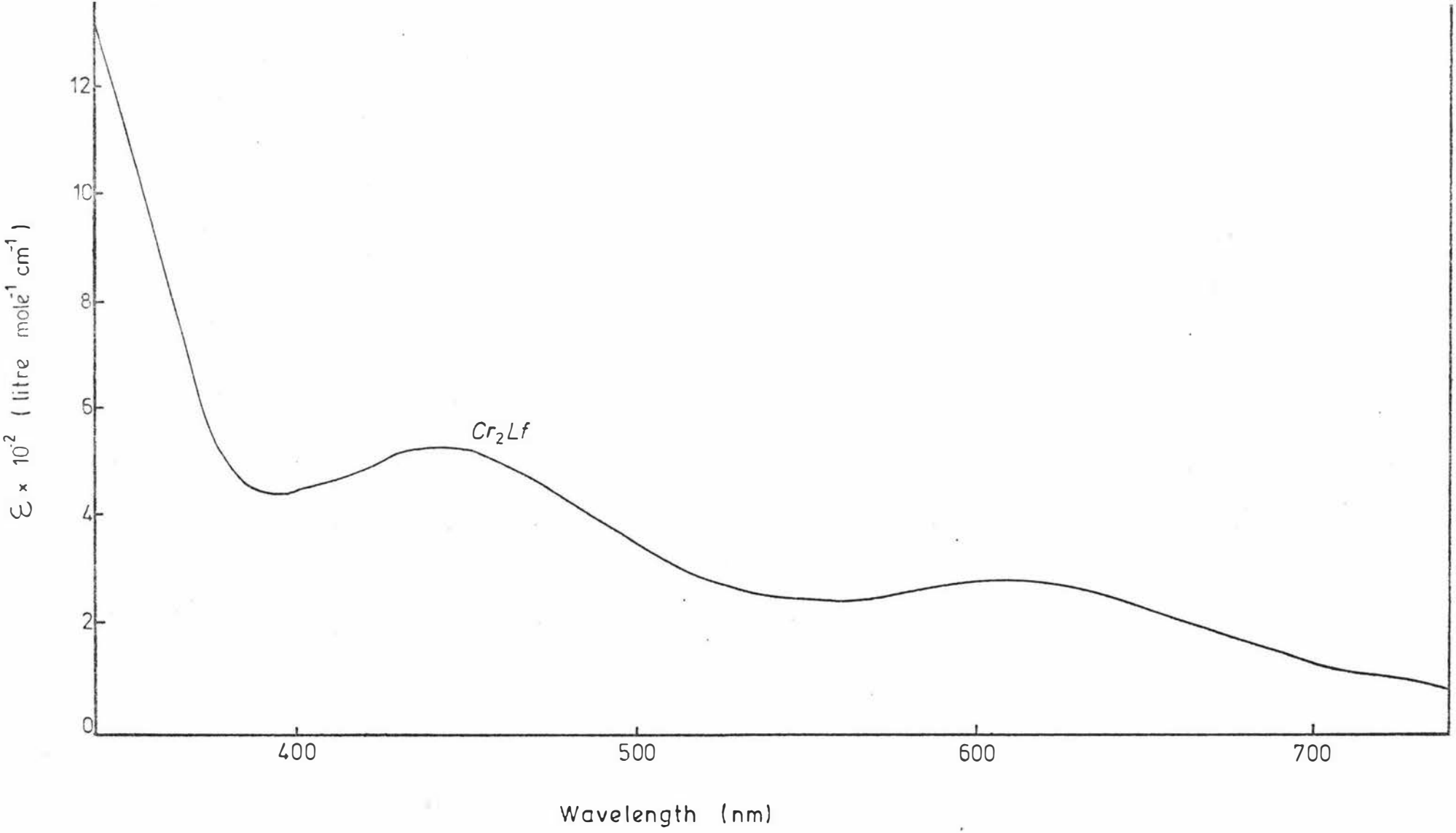

Figure 1.8 Visible absorption spectrum of Cr_2Lf, Tris buffer pH 7.4, 0.05M.

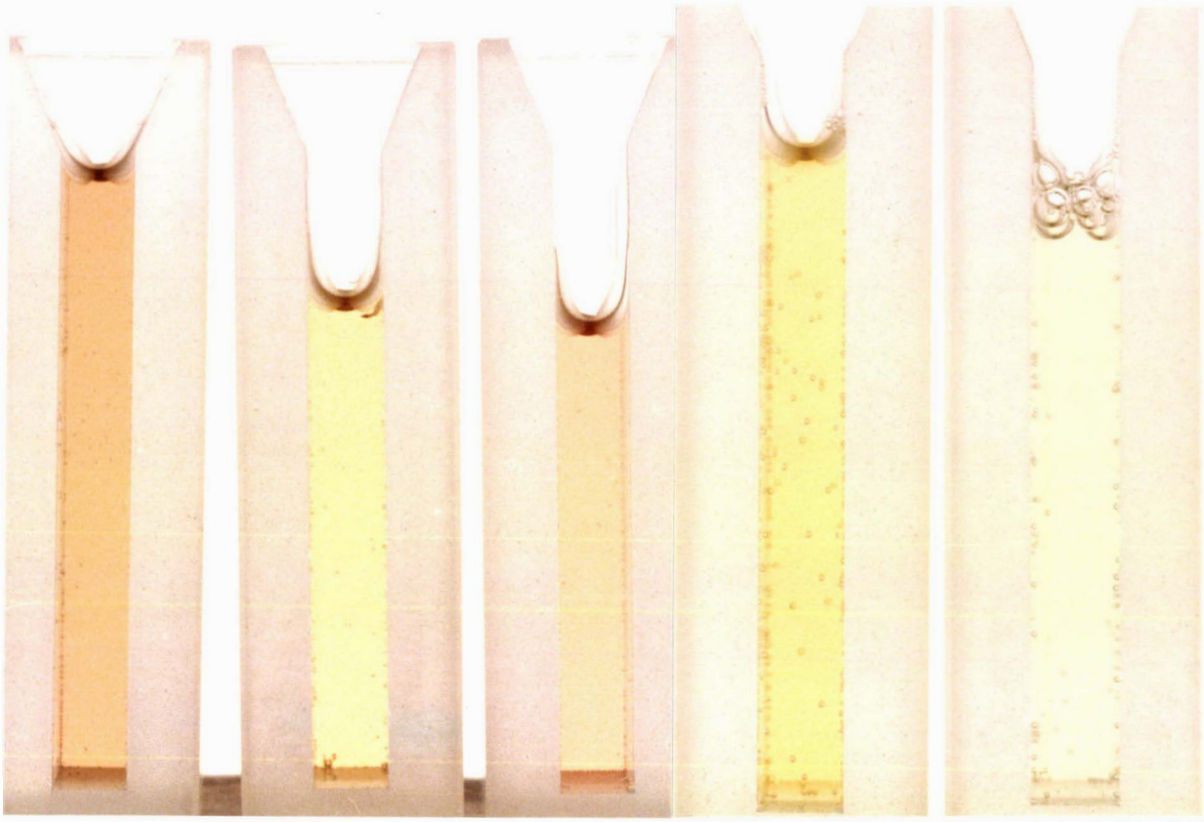

Figure 1.9 Transition metal complexes of lactoferrin; left to right, Mn_2Lf, Co_2Lf, Fe_2Lf, Cu_2Lf and Cr_2Lf.

compared with the data for small molecule complexes (Chapter 3) is indicative of tyrosyl residues equatorially bound to copper(II) in a tetragonal environment. However, not previously reported for Cu_2Lf is a weaker band at 677nm (Figure 1.6), assignable to a d-d transition (88). Assuming the rule of average environment (89) the position of the absorption points to the coordination of one, or at the most two nitrogen donor atoms bound to a copper(II) ion in a distorted tetragonal or rhombic site, a fact also demonstrated by e.s.r. studies (Section 1.3.5).

Finally, the Cr_2Lf complex, which does not exhibit a charge transfer band in the visible region, allows the observation (Figure 1.8) of the two spin allowed d-d transitions $^4A_{2g} \rightarrow {}^4T_{1g}$ and $^4A_{2g} \rightarrow {}^4T_{2g}$ (at 442nm and 612nm respectively) expected for an octahedral chromium(III) complex (90). That chromium is binding in the specific site is evident from the fact that the binding of the metal to apolactoferrin is more rapid in the presence of excess bicarbonate and the resulting spectrum is very similar to the analogous chromium transferrin complex, for which evidence has been presented to support specific binding (54). Furthermore the chromium once bound is not readily displaced from the specific binding site by iron(III) (Sections 1.3.2 and 1.3.5).

The electronic spectrum of Cr_2Lf is similar to those of chromium(III) ions known to have a CrO_6 coordination (Table 1.7) and does not seem consistent with the involvement of both nitrogen and oxygen ligands only as suggested by studies on other lactoferrin complexes. However, the absorption maxima do in fact resemble those of chromium(III) complexes containing chloride ions, as well as nitrogen and oxygen donors (Table 1.7), which may indicate that because of the chemical inertness of the chromium(III) ion, at least one chloride ion has been retained in the coordination sphere rather than a water molecule (since the metal ion is added as commercial chromium(III) chloride which contains $[Cr(H_2O)_4Cl_2]^+$ ions (96)). However, similar spectra are obtained when chromium(III) is added as its nitrate salt or as a complex with NTA suggesting that the Tris buffer may be

Table 1.7 Electronic Spectral Data for Cr(III) Complexes

Complex[a]	λ_{max}(nm)		Donor Set	Ref
Cr_2Lf	442	612	?	b
Cr_2Tf	440	615	?	54
$[Cr(H_3edta)Cl_2(H_2O)_2]$	450	620	CrO_3NCl_2	91
$[Cr(H_2O)_5Cl]^{2+}$	428	608	CrO_5Cl	92
$[Cr(cat)_3]^{3-}$	475	592	CrO_6	93
$[Cr(H_2O)_6]^{3+}$	407	573	CrO_6	94
$[Cr(H_2O)_5(NH_3)]^{3+}$	397	545	CrO_5N	94
$[Cr(H_2O)_4(en)]^{3+}$	385	512	CrO_4N_2	95
$[Cr(edta)(H_2O)]^{-}$	395	545	CrO_4N_2	95

[a]Abbreviations: Lf = human lactoferrin, Tf = human serum transferrin, edta = ethylenediaminetetraacetato, cat = catecholato, en = ethylenediamine. [b]This work.

a source of the chloride ion in these cases.

1.3.5 ELECTRON SPIN RESONANCE SPECTROSCOPY

(a) The Spectrum of Fe_2Lf

In general, the phenomenological spin Hamiltonian describing the e.s.r. spectra of iron(III) ions in sites of less than cubic symmetry may be characterised by two zero-field splitting parameters, D and E, or frequently by D and λ (= D/E). An axial distortion from cubic symmetry is represented by the D term, while a planar or rhombic distortion is expressed in the E term. The spin Hamiltonian is then written as the sum of the Zeeman energy and terms for the axial and rhombic distortions;

$$\mathcal{H} = \beta H.g.\hat{S} + D\left[\hat{S}_z^2 - \tfrac{1}{3}S(S+1)\right] + E(\hat{S}_x^2 - \hat{S}_y^2)$$

Zeeman Axial Rhombic

The relative magnitudes of these terms will determine the fields at which e.s.r. transitions are observed for a given microwave frequency. When the term in D dominates the

Hamiltonian, as in the high spin ferriheme proteins, λ has a value near zero. Resonances in frozen solutions of proteins will then be observed near $g^1 = 6$ (arising from those molecules oriented so that the symmetry axis of the ferriheme group is perpendicular to the external magnetic field) and $g^1 = 2$ (from molecules oriented with the symmetry axis parallel to the field). When the E term is large compared to other terms, all orientations of the iron(III) ion will give resonances near $g^1 = 4.3$. In this case it has become customary to speak of λ being equal to 1/3, since it is always possible to find a coordinate system (or equivalently to choose an axis of quantization) where $|E|/|D| \leq 1/3$, and $D = 0$ in one reference (a pure rhombic distortion) corresponds to $\lambda = 1/3$ in another. Should terms in D and E be small compared to the Zeeman term, then the symmetry is cubic and all orientations will give rise to $g^1 = 2$. This is the situation found in the hexaquo complex of manganese-(II). Quartic terms due to the cubic field are usually very much smaller than the quadratic terms and are customarily neglected because of the number of parameters they introduce (49).

The e.s.r. spectrum of Fe_2Lf (Table 1.9, Figure 1.10), is identical to a previously reported spectrum (49) and is characteristic of the class of iron(III) compounds in which the iron is in a site of rhombic symmetry. Fe_2Lf and Fe_2OvoTf (OvoTf = ovotransferrin) exhibit a broad shallow peak around $g = 4.98$ not observed in Fe_2Tf. Addition of perchlorate to Fe_2OvoTf causes this broad signal to decrease in intensity, while in Fe_2Tf the signal increases in intensity when perchlorate is added (97). For ovotransferrin the broad signal is much more prominent when monoferric ovotransferrin (prepared by isoelectric focussing) has the second site occupied by gallium and much less prominent when monogallium ovotransferrin has its second site occupied by iron (67). The sum of the latter two spectra gives a spectrum the same as that of native Fe_2OvoTf indicating that each bound iron makes an independent contribution to the spectrum. Recent studies have shown that lactoferrin and transferrin consist of two independent halves each containing one

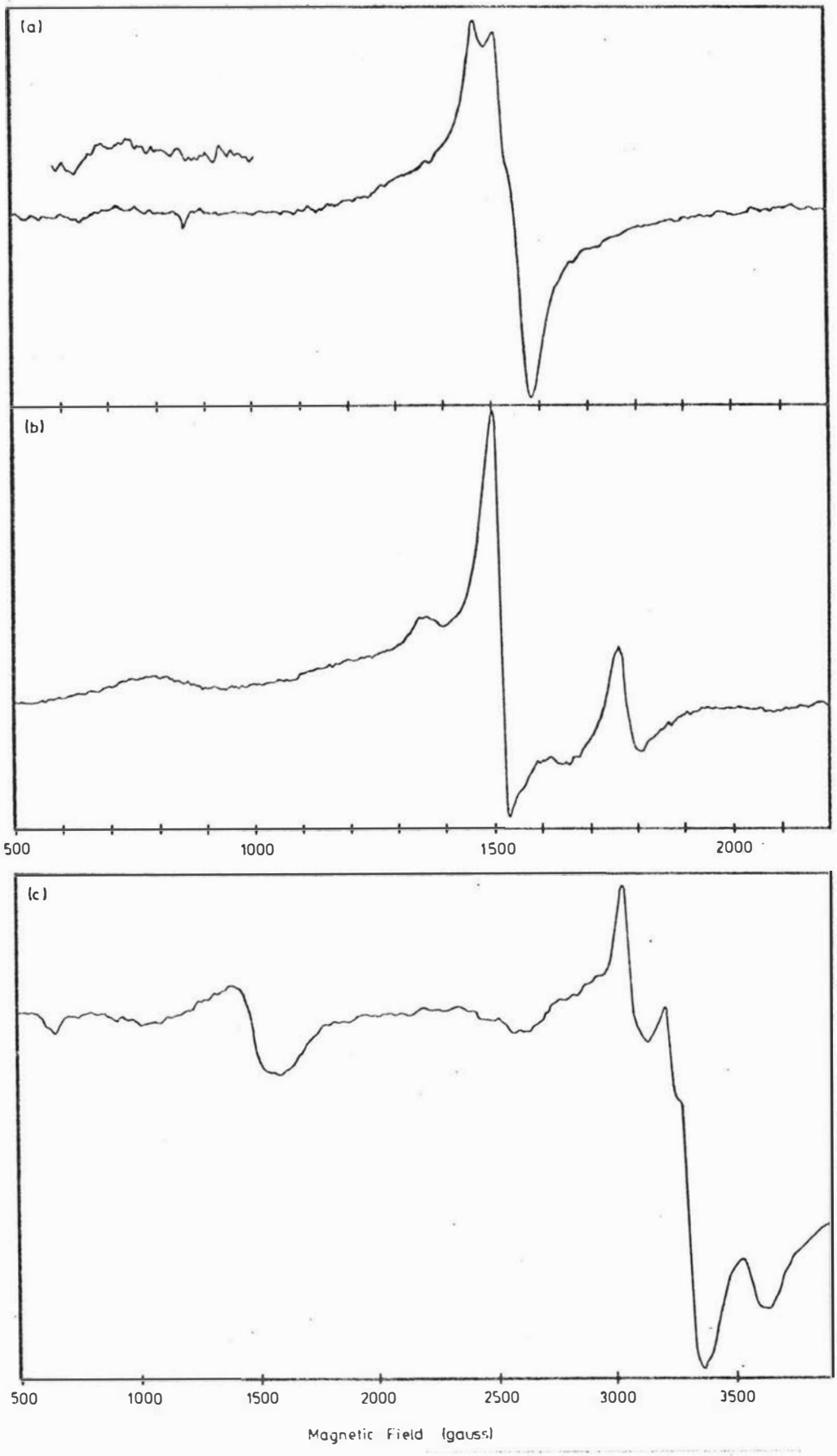

Figure 1.10 E.S.R. spectra at ~160°C of (a) Fe_2Lf in phosphate buffer, pH 7.6, 0.01M and Fe_2Lf in phosphate buffer titrated to pH 2.0 with (b) citric acid and (c) phosphoric acid.

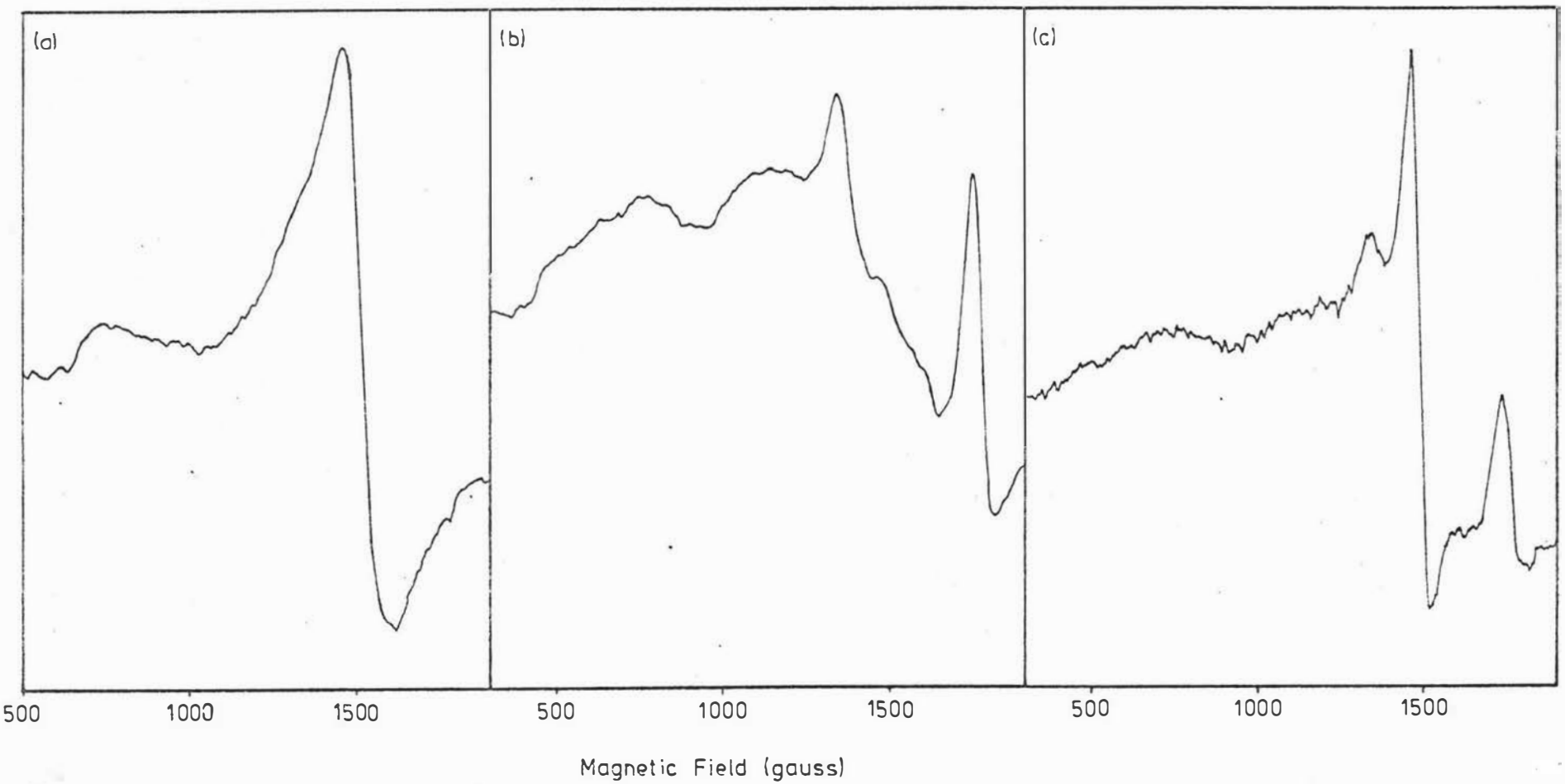

Figure 1.11 E.S.R. spectra at -160°C of a solution containing 1 mole of ferric perchlorate and 3 moles of citric acid at (a) pH 2.0, (b) pH 4.1 and (c) pH 4.7.

Table 1.8 Characterisation of Iron(III) High Spin E.S.R. Spectra

g^1 value[a]	Symmetry	Axial Relationship
2	Cubic	x=y=z
6 and 2	Tetragonal/axial	x=y≠z
9 and 4.3[b]	Rhombic	x≠y≠z

a. $g^1 = h\nu/\beta H$ b. The g = 9 signal is very weak

specific binding site and linked by the polypeptide chain (20,21). The broad signal at g = 4.98 has been attributed to a protein conformation of one of these halves in which the iron is strongly bound at the specific site (97). The conformation adopted by Fe_2OvoTf in solution lies more in the direction of strong binding occurring in both sites. Addition of perchlorate, a chaotropic agent (one which alters the hydrogen bonding properties of aqueous solutions), is felt to change the protein conformation of both halves of Fe_2OvoTf to one in which iron(III) is less strongly held. The reverse is felt to occur in Fe_2Tf. Similar investigations have not been carried out on Fe_2Lf; it has proved impossible to prepare monoferric lactoferrin by isoelectric focussing (section 1.3.7), while the effect of perchlorate and other anions on Fe_2Lf and Cu_2Lf has yet to be investigated.

(b) The Spectrum of Cu_2Lf

Copper has a relatively simple electron configuration. With 9 d-electrons the copper(II) ion can be considered as having a single d-hole, as opposed to a single d-electron, with a spin of $\frac{1}{2}$ and the same wave functions. The t_{2g} and e_g sets of orbitals in copper(II) when subject to a tetragonal distortion, a consequence of the Jahn Teller effect, are split further and the $d_{x^2-y^2}$ orbital is left with the lowest energy. In this case the orbital angular momentum of the copper(II) ion is said to be quenched, because the

electron hole resides solely in this orbital configuration and cannot interchange with the others. Under these circumstances the copper(II) hole has only angular momentum (and hence magnetic moment) associated with the electron spin, $s = \frac{1}{2}$, and the g value of the copper(II) ion approaches close to the free electron g value of $g_e = 2.0023$. Nevertheless the copper(II) hole may spend a very small amount of its time in the higher energy orbitals, giving rise to the perturbations of the g value, which depend on the energy level splittings, Δ, and thus on the nature of the copper ligands. For octahedral symmetry the g-value will be isotropic, but in tetragonal symmetry the g-value is anisotropic; g_{11} and $g_{\perp}$ arise depending on whether the magnetic field is directed along the tetragonal (Z) axis or perpendicular to it. In copper(II) interaction of the electron hole with the nucleus of copper (spin = $\frac{3}{2}$) gives rise to hyperfine splitting, which appears as four equally spaced lines in the low field region. Smaller "superhyperfine structure" may come from interactions with the ligands, the most common being nitrogen (spin = 1) (98).

The e.s.r. spectrum of Cu_2Lf (Table 1.11, Figure 1.12) is identical to that obtained previously (7). Hyperfine structure in the g_{11} and $g_{\perp}$ regions provide strong evidence for the presence of nitrogen in the specific sites. Computer simulations of the structure of the low field peak in the g_{11} region support the involvement of only one nitrogen in coordinating copper(II) (99) as has been demonstrated with Cu_2Tf, (Tf = Transferrin) (56).

(c) Interactions Between Lactoferrin and Citrate

E.S.R. experiments indicate that iron(III) is retained by the protein in the specific sites at pHs above 4, though complete removal does not occur until the pH is below 3, thus confirming titration studies where the red colour of the complex is not lost until the pH drops below 4 (32). When Fe_2Lf is titrated to pH 2.0 with citric acid the pink colour disappears and the solution exhibits a spectrum identical to that observed for a 1:3 iron(III)-citrate complex at pH 4.7 (Figures 1.10, 1.11 and Table 1.9), clear evidence for the formation of a ferric-citrate complex

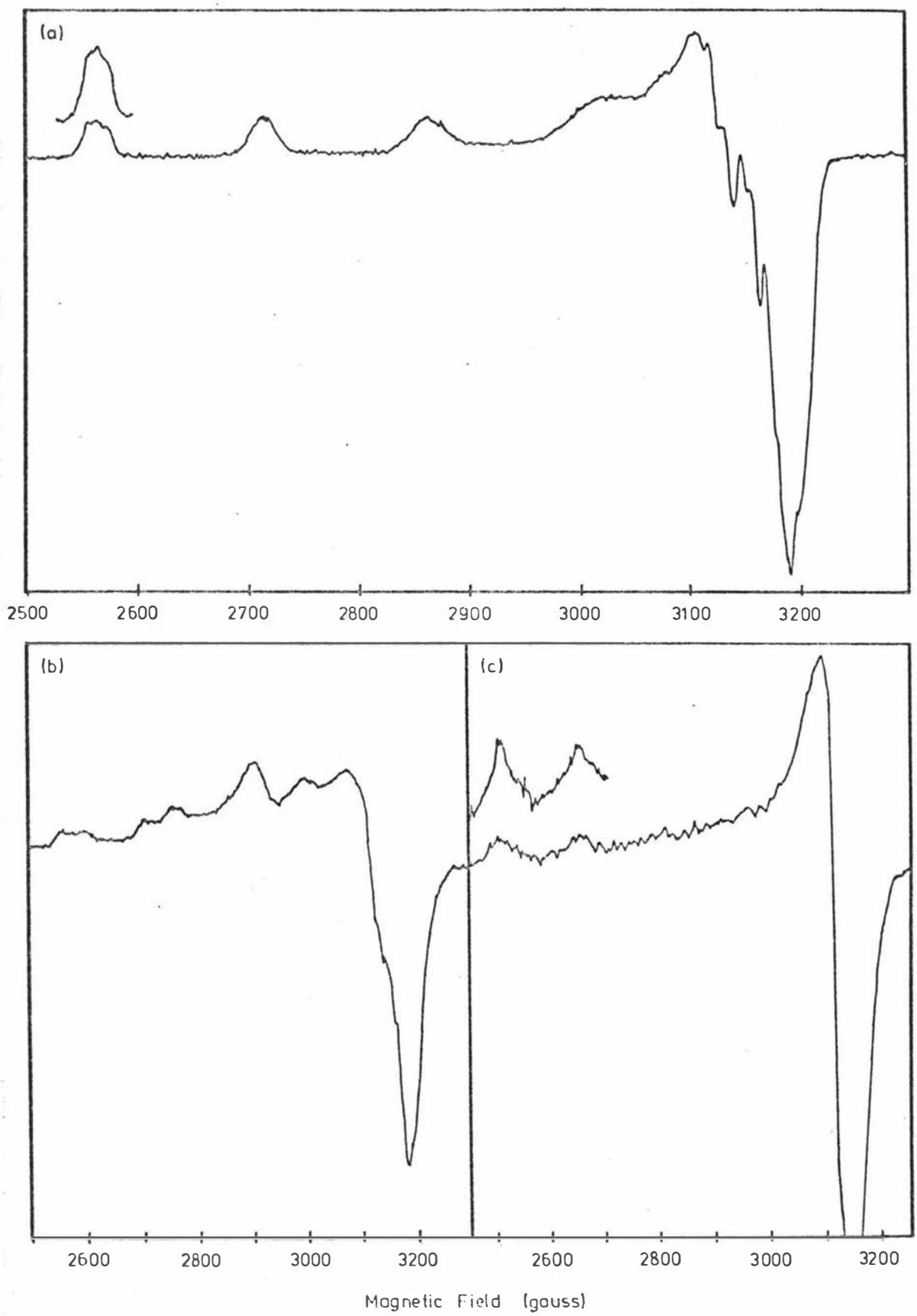

Figure 1.12 E.S.R. spectra at -160°C in phosphate buffer 0.01M, pH 7.6 of (a) Cu_2Lf, (b) 2 molar equivalents of copper(II) added to Fe_2Lf and (c) bicarbonate-free copper-lactoferrin.

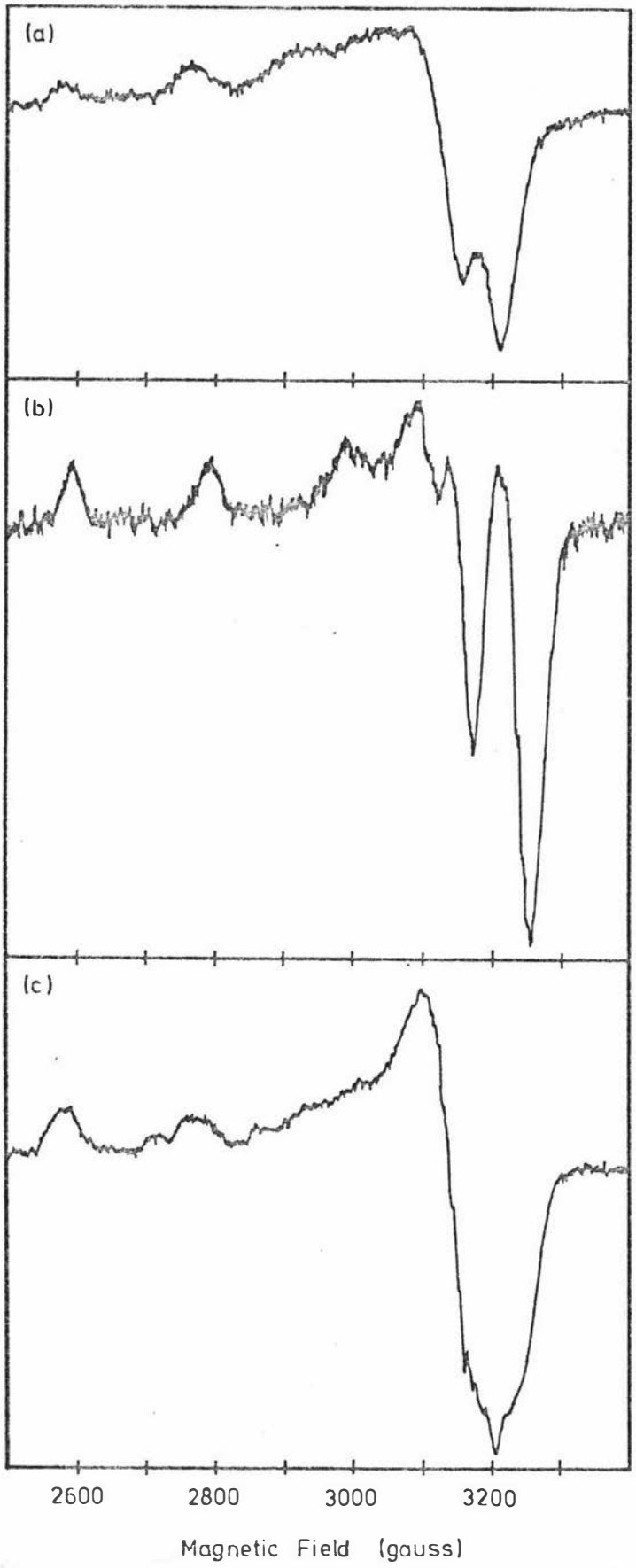

Figure 1.13 E.S.R. spectra at -160°C of (a) copper(II) in Tris buffer, pH 7.4, 0.05M and 2 molar equivalents of copper(II) added to (b) Mn_2Lf and (c) Cr_2Lf in Tris buffer.

Table 1.9 E.S.R. Spectra of Complexes of Iron(III) with Lactoferrin

Species	pH	g Values
Fe_2Lf	7.6	8.72, 4.378, 4.240, 4.139
Fe-Lf-Citrate	2.0	8.069, 4.783, 4.264, 3.633
Fe-Lf-Phosphate	2.0	9.547, 4.317, 2.112, 1.956, 1.827
Fe-Phosphate	1.0	
Fe-Citrate (1:3)	2.0	9.355, 4.218, 1.967
Fe-Citrate (1:3)	4.1	8.683, 5.587, 4.656, 3.648
Fe-Citrate (1:3)	4.7	8.567, 4.795, 4.312, 3.648

rather than that of a ferric-citrate-lactoferrin complex, involving the specific sites of the protein. The sharper spectrum observed at pH 2.0 in the presence of lactoferrin is probably a result of a decrease in the ordering of the solvent water molecules, the protein is probably disrupting intermolecular hydrogen bonds. A similar effect has been observed with an iron(III)-transferrin-citrate solution at pH 4.1 (44). Titration of Fe_2Lf to pH 2.0 with phosphoric acid gives a strong e.s.r. signal at g = 2 (Figure 1.10, Table 1.9) indistinguishable from that obtained with iron-(III) nitrate in phosphoric acid at a similar pH, and consistent with a near octahedral FeO_6 coordination.

It has been reported that apolactoferrin can be prepared by dialysis against citric acid (0.1M, pH 2.0) followed by several changes of deionised water (18). Returning the pH to 7.6 by the addition of Na_2HPO_4 usually results in some precipitation of the protein. Apolactoferrin prepared in this manner showed a more rapid binding of iron(III) as a complex of both NTA and citrate (Figure 1.4, Section 1.3.2). Furthermore Cu_2Lf prepared from this protein shows a weak signal at g = 1.98 not observed for Cu_2Lf prepared from apolactoferrin which had not been treated with citric acid or for non specifically bound copper(II) (Table 1.11, Figure 1.12). It appears that the second species in the e.s.r. spectrum of

Table 1.10 E.S.R. Spectra of Complexes of Chromium(III) with Lactoferrin and NTA

Species	g Values			
	Type 1	Type 2	Non-Specific	Unbound
Cr_2Lf	5.43	5.62, 5.15, 2.42	2.05	-
Cr-NTA(1:1)	-	-	-	1.98

Cu_2Lf, stated as being due to 3-4 nitrogens coordinating to copper(II) (87), corresponds to this g = 1.98 signal and in fact is evidence for disruption of the protein's conformation as a result of the extreme conditions needed to remove iron(III).

(d) Interactions Between Chromium(III) and Lactoferrin

The e.s.r. spectrum of Cr_2Lf (Table 1.10, Figure 1.14) is characterised by three sharp signals at g = 5.62, 5.43 and 5.15 and two broader signals at g = 2.42 and 2.05 similar to those reported for the analogous Cr_2Tf complex (54). These signals would appear to be consistent with the presence of three species of chromium(III) in the complex. Metal ion uptake studies (Section 1.3.2) have shown that iron(III) can displace up to 50% of the specifically bound chromium(III) in Cr_2Lf and as the addition of iron(III) or copper(II) causes the immediate appearance of a pink or yellow colouration of the protein and disappearance of the line at g = 5.43, then this signal may be due to a site that is more accessible to attack by other metals. The broad signal at g = 2.05 may be due to non specific chromium(III)-lactoferrin. It is very difficult to remove excess chromium(III) from Cr_2Lf (Section 1.3.1) while the addition of excess iron(III) to Cr_2Lf causes this signal to increase slightly in intensity over that at g = 2.42. The signals at g = 5.62, 5.15 and 2.42 may then be assignable to the second specific chromium(III) site which appears to be less accessible to metal ion attack. When one iron(III) ion

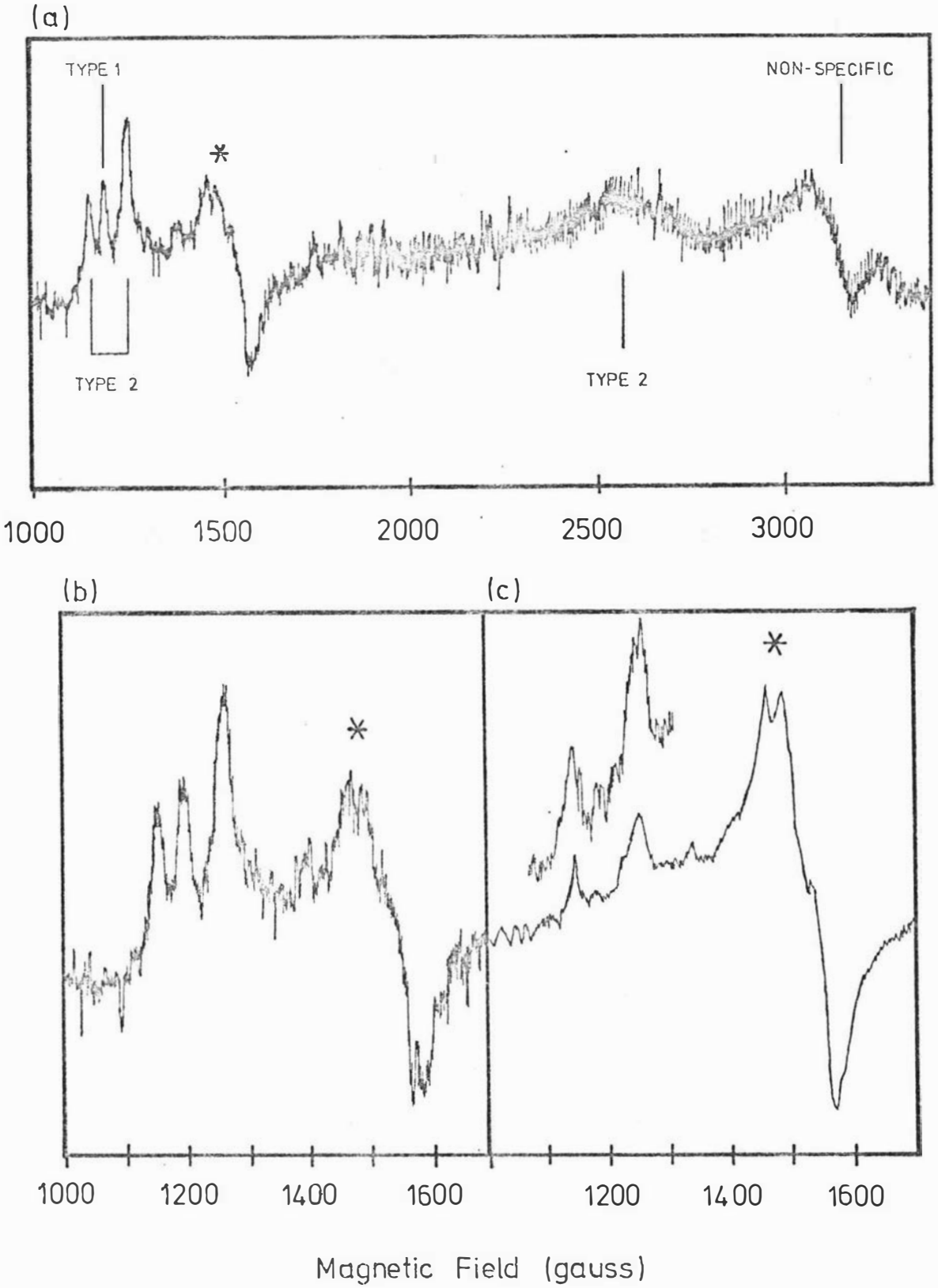

Figure 1.14 E.S.R. spectra at −160°C of (a) and (b) Cr_2Lf in Tris buffer and (c) Cr_2Lf after the addition of one molar equivalent of iron(III). (* The signal around 1500 gauss is due to iron(III) which in (a) and (b) is present when the protein is isolated.)

is added to Cr_2Lf (Figure 1.14) the slight increase in the intensity of the lines at g = 4.240 and 4.139 due to specifically bound iron relative to that at g= 4.578 (as opposed to the relative intensities in Fe_2Lf (Figure 1.10) may indicate that some inhomogeneity in the sites exists when iron(III) is bound, and that they are distinguishable by e.s.r., though this may be a consequence of the lower signal to noise ratio in the spectrum.

(e) Interactions Between Copper(II) and Lactoferrin

(i) Bicarbonate-Free Copper-Lactoferrin

In the absence of bicarbonate the colourless copper-lactoferrin complex (Table 1.11, Figure 1.12) has an e.s.r. signal indicative of no more than one nitrogen coordinated to the metal. Lowering the pH of Cu_2Lf to pH 4.0 results in the immediate loss of the yellow colour and the appearance of a signal identical to the bicarbonate-free copper-lactoferrin signal (76).

(ii) Addition of Copper(II) to Fe_2Lf, Co_2Lf and Cr_2Lf

When copper(II) is added to Fe_2Lf, Co_2Lf and Cr_2Lf some of the specifically bound metal is displaced. When it is added to Fe_2Lf λ_{max} for the complex shifts from 465nm to 458nm, or when added to Co_2Lf λ_{max} shifts from 405nm to 415nm, while in the case of Cr_2Lf the characteristic yellow colour associated with specifically bound copper(II) appears almost immediately. Furthermore the e.s.r. spectra of these complexes are characterised by at least two major species one of which can be attributed to specifically bound copper(II) (Table 1.12, Figure 1.12 and 1.13). In Fe_2Lf the second species in the spectrum has been assigned to a non specific copper-protein interaction which, from the broadness of the signals in the g_{11} region suggests at least two nitrogens coordinating to copper. Furthermore there is a difference between this signal and that of bicarbonate-free copper-lactoferrin indicating that the binding of iron(III) in the specific sites makes available a different site on the protein for binding copper(II) from what is available when no metal is specifically bound.

When copper is added to Cr_2Lf one of the major species

Table 1.11 E.S.R. Spectra of Complexes of Copper(II) with Lactoferrin and Copper(II) in Buffer Solutions

Species	Buffer	g_{11}	A_{11}(a)	g_1	A_1(a)	½ Width(a)
Cu_2Lf (Specific)	Phosphate	2.315	151	2.057	11.2	28
CuLf (Nonspecific)	"	2.276	150	2.072	-	~40
CuLf-HCO_3 Free	"	2.372	145	2.076	-	~42
Cu(II)-Phosphate	"	-	-	2.078	-	-
Cu(II)-Tris	Tris	2.260	185	2.072	-	~45
Biuret-Cu[a]	"	2.206	210	2.05	-	-

a. Reference (56)

Table 1.12 E.S.R. Spectra of Copper(II) added to Fe_2Lf, Cr_2Lf and Mn_2Lf

Reaction	Buffer	g_{11}	A_{11}(a)	g_1	A_1(a)	Species
Cr_2Lf+2Cu	Tris	2.31	150			Specific
		2.26	185	2.035	-	Cu-Tris
		~2.24	~190			-
Fe_2Lf+2Cu	Phosphate	2.32	150	2.07	-	Specific
		2.27	150			Non Specific
Co_2Lf+2Cu	Tris	2.32	150	2.063	11	Specific
		a -	-			-
Mn_2Lf+2Cu	Tris	2.230	202	2.05	-	Biuret Cu
Mn_2Lf+5Cu	"	2.234	200	2.061	-	Biuret Cu
		2.269	177			CuTris
Cu-Lf HCO_3-Free	Phosphate	2.372	145	2.076		-
		a -	-			-

a. Second species present in spectrum as shoulders to the peaks of the major species.

present in the spectrum can be assigned to an interaction between copper and the buffer, most probably involving the nitrogen of tris(hydroxymethyl)-methylamine (Figure 1.13).

(iii) Addition of Copper(II) to Mn_2Lf

Manganese(III) would appear to be more strongly bound than iron(III), cobalt(III) and chromium(III) as addition of copper(II) is insufficient to displace it from the specific sites; no change is observed in the visible spectrum on the addition of copper and there are no signals due to specific copper-lactoferrin in the e.s.r. spectrum. The e.s.r. spectrum is remarkably similar to that produced by a Biuret type copper(II) complex (Table 1.11 and 1.12, Figure 1.13) found to occur with transferrin at pHs greater than 9.2 (56), providing evidence that copper is coordinating at a site containing at least three nitrogens. There is also a distinct similarity between this spectrum and that previously reported for bicarbonate-free copper-lactoferrin where the parameters of the major species in that spectrum are g_{11} = 2.25, A_{11} = 200 gauss and $g_{\perp}$ = 2.06 (7). Thus the binding of manganese(III) to lactoferrin would appear to induce a different conformational change of the protein to that found with other metal ions, making available a different external site on the protein for the binding of copper. There would appear to be only a limited number of such sites available for copper. Addition of more than two equivalents of copper(II) to Mn_2Lf gives rise to a second species in the e.s.r. spectrum which may be due to an interaction between copper and the buffer (Table 1.12).

In general small molecular weight complexes of manganese(III) are close in stability to those of iron(III), and in some instances are more stable, while they are more stable than those of other metals in the first transition series. For instance log k_1 for a manganese(III) complex with the ligand hydroxyethylethylenediaminetriacetic acid (HEDTA) is 22.7 while that of iron(III) with HEDTA is 19.06 and copper(II) 18.8 (100). The ionic radii of chromium(III) and iron(III) are very similar (101) and that of manganese(III) would be expected to be the same. However, the latter with the d^4 configuration (one electron short of a half filled

shell) is likely to be subject to Jahn Teller distortions, like copper(II), which increase the axial bond lengths and decrease the equatorial bond lengths. For instance a single crystal x-ray structural analysis of tris-(8-quinolinato)chromium(III) shows the chromium to be binding in an essentially distorted octahedral configuration with Cr-O (phenolate) bond lengths of 1.949(10)A^{o} and Cr-N bond lengths of 2.063(8)A^{o} (102). Replacing chromium by manganese in this complex results in a lengthening of the axial metal-nitrogen bonds by 0.2A^{o} to 2.254(13)A^{o} and a small shortening of the equatorial metal-oxygen bonds to 1.915(8)A^{o} while the equatorial metal-nitrogen bonds remain essentially unchanged (Table 1.13). The equatorial Mn-O (phenolic) and Mn-N bond lengths are not too dissimilar to their equivalents in high spin iron(III) complexes, for instance in the complex $[Fe(IIIa)_2(MeOH)_2](NO_3).2H_2O$ the Fe-N bond length is 2.068(3)A^{o} and the Fe-O(phenolic) bond length in $Mg[Fe(Va)]4H_2O$ is 1.907(&)A^{o} (103 ,107). A similar length for the axial M-N bond has also been reported for the complexes mer-tris-(N-benzylsalicylaldiminato) manganese-(III) and tris-(pyridine-2-carboxylato) manganese(III) (Table 1.13). However the Mn-O-(carboxylate) bond lengths appear to be shorter than Fe-O-(carboxylate) bond lengths, which in $Mg[Fe(Va)]4H_2O$ (see Chapter 2 for compound numbering system) are 2.041(7)A^{o} (103).

Thus it would appear that manganese(III) would favour an environment with a tetragonal distortion from octahedral symmetry and these steric requirements induce a different conformational change of the protein to that observed with iron(III), chromium(III) and cobalt(III). This may account for the increased stability of the Mn_2Lf complex over that of Cr_2Lf and Fe_2Lf and may be further evidence for the idea that lactoferrin is able to change its conformation to a greater extent than transferrin to adopt a configuration favouring the stability of its iron(III) complex (36).

1.3.6 RESONANCE RAMAN SPECTROSCOPY

Resonance Raman Spectra of lactoferrin (Table 1.14, Figure 1.15) (108) are dominated by four strong resonance-

Table 1.13 Bond Lengths of Manganese(III) Complexes

Complex	Axial Mn-N(A^o)	Equatorial Mn-N(A^o)	Mn-O(A^o)
[a] Mer-tris-(N-benzylsalicylaldiminato) Mn(III)	2.261(10)	2.082(6)	1.898(15)
[b] Tris-(8-quinolinolato) Mn(III)	2.254(13)	2.058(6)	1.915(8)
[c] Tris-(pyridine-2-carboxylato) Mn(III)	2.236(35)	2.059(5)	1.914(21)

a. Reference (104)
N-benzylsalicylaldiminato

b. Reference (105)
8-quinolinolato

c. Reference (106)
pyridine-2-carboxylato

enhanced vibrational modes of metal ion coordinated tyrosinates at 1600, 1500, 1250-1270 and 1170cm^{-1} as have been observed in transferrin and ovotransferrin (40,83). From comparison with a small molecular weight copper(II) complex (83) the two highest bands can be assigned to C-C stretching, the 1260cm^{-1} band to C-O stretching and the lowest frequency to C-O bending of the phenolate ligand. The other bands in the region 1900-900cm^{-1} are non-resonant features which arise from protein motions; ~1450cm^{-1} (CH_2 deformation), 1005cm^{-1} (phenylalanine ring breathing mode) and ~940cm^{-1} (backbone C-C stretching) while the broad feature at ~1660cm^{-1} arises from solvent (H_2O deformation). Spectral lines in the region below 900cm^{-1} were largely obscured by contributions from the frozen solvent.

The Resonance Raman spectra of Fe_2Lf and Cu_2Lf are nearly identical as are the spectra of Co_2Lf and Mn_2Lf. However the two sets differ in that the ~1253cm^{-1} band is approximately 20cm^{-1} lower in frequency in the case of the latter two metal-protein complexes, while the other three tyrosinate modes are nearly coincident. These results are nearly identical to those of the metal substituted transferrins and ovotransferrins (83). It was difficult to determine the position of Cr_2Lf in the above classification because its low absorptivity led to weak resonance enhancement. Only the 1604cm^{-1} frequency was clearly evident among the four tyrosinate modes and the spectrum was dominated by the non-resonant peaks.

Relative Raman intensities were calculated using the CH_2-deformation at ~1450cm^{-1} as an internal intensity standard, since the large contribution from solvent at ~1050cm^{-1} in some of the spectra precluded the use of the phenylalanine peak at ~1004cm^{-1}. In Co_2Lf and Cu_2Lf the excitation profiles of the four resonance-enhanced vibrational modes parallel the optical absorption spectrum in the region between 514.5 and 457.9nm (Figure 1.16) as would be expected for resonance enhancement by single electronic states (109) whose respective optical transitions are given in Table 1.6 (Figures 1.6 - 1.8). However, for Fe_2Lf the tyrosinate frequencies appear to decrease in intensity as λ_{max} is approached. Such behaviour is probably due to excitation profile fine structure similar to that observed

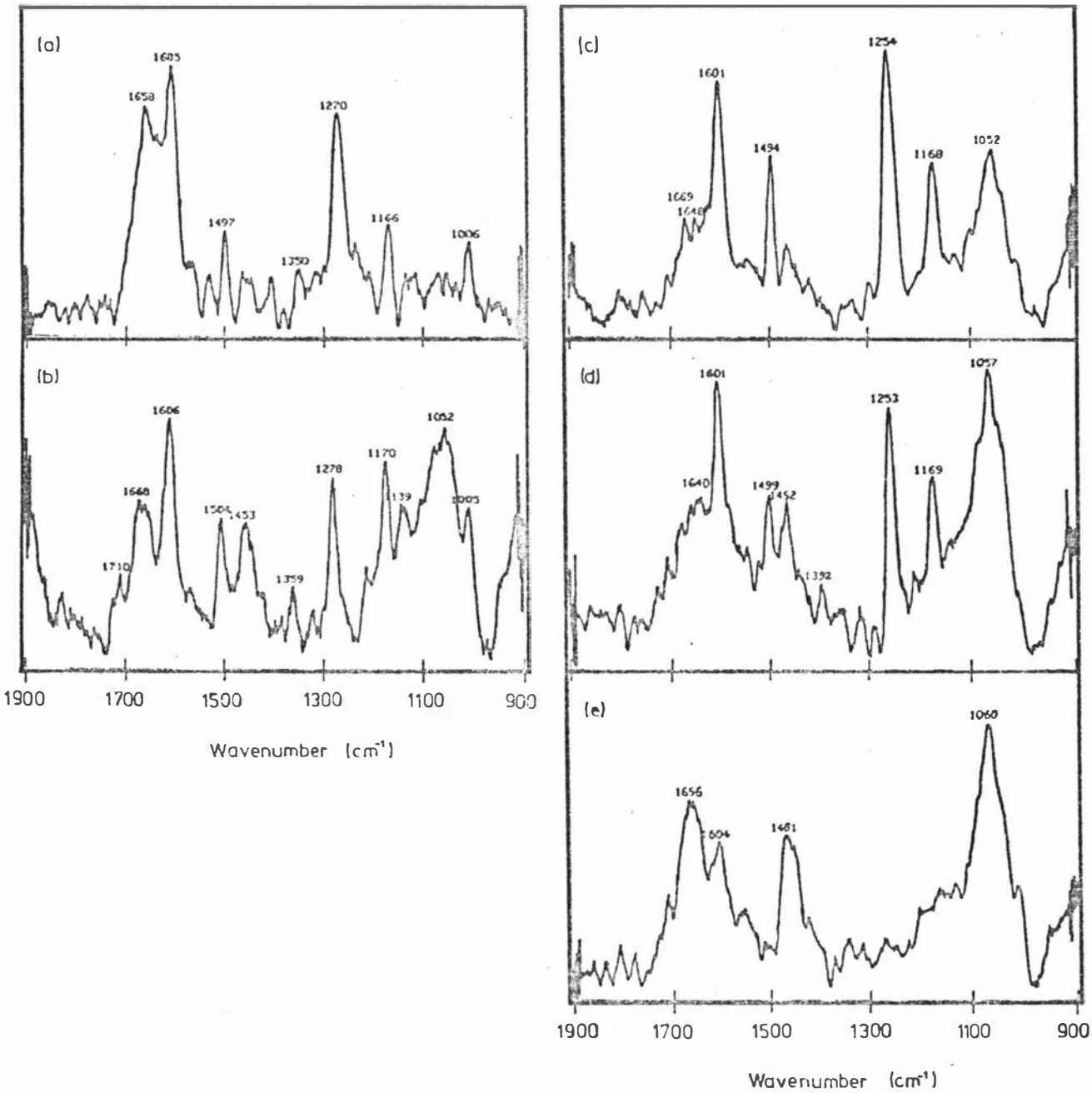

Figure 1.15 Resonance Raman spectra of (a) Fe_2Lf, (b) Cu_2Lf, (c) Co_2Lf, (d) Mn_2Lf and (e) Cr_2Lf recorded using 457.9nm radiation at -40°C.

Table 1.14 Raman Spectral Data for Native and Metal-Substituted Human Lactoferrins[a]

$Fe(III)_2Lf$	$Cu(II)_2Lf$	$Mn(III)_2Lf$	$Co(III)_2Lf$	$Cr(III)_2Lf$	Assignments[b]
~1657	~1660	~1660	~1650	~1656	H_2O
1604	1603	1601	1601	1604	tyr ligand
1500	1501	1499	1494	1505?	
1447	1450	1462	1462	1461	$\delta(CH_2)$
1272	1275	1253	1254	1267?	tyr ligand
1170	1169	1169	1168	-	
1004	1002	-	~1010	-	ν(phe)
939	936	-	933	943	ν(c-c)

a. Spectra were obtained using 457.9 to 514.5 mm excitation.

b. Based on Reference 40 and 116.

for Fe_2Tf (40). Since fewer excitation wavelengths were used in this study, it was not possible to resolve fine structure in the excitation profiles.

The similarity between these spectra and those of transferrin and ovotransferrin (83) strengthens the idea that the metal binding sites in all these proteins are similar. The appearance of the resonance-enhanced tyrosinate vibrational modes in the Raman spectra of all the metal substituted lactoferrins and transferrins upon excitation close to the visible absorption maxima means that these absorption bands are primarily due to charge transfer transitions between tyrosinate and metal. The fact that the lactoferrin tyrosinate vibrations (particularly the peak at $\sim 1270 cm^{-1}$) are similarly affected by changing the metal ion indicates that the tyrosinate coordinate of the metals is the same in lactoferrin as in ovo- and serum-transferrin.

Two non-heme-iron dioxygenases, protocatechuate-3,4-dioxygenase and pyrocatechase, have been recently found to exhibit a similar set of four resonance-enhanced tyrosinate ring modes at about 1605, 1505, 1275 and $1175 cm^{-1}$ (110, 111, 112). This has led to the proposal for the existence of an entire class of iron-tyrosinate proteins in which tyrosinate coordination dominates the visible absorption and Resonance Raman spectra (111). The lack of contribution of histidine, bicarbonate or other iron ligands to the $\sim 465 nm$ absorption band of lactoferrin has prevented these ligands from being identified in the Resonance Raman spectra.

Of the four characteristic tyrosinate vibrational frequencies, the one at $\sim 1275 cm^{-1}$ appears to be the most sensitive to metal substitution and active site structure. In the iron proteins it varies from $1293 cm^{-1}$ in pyrocatechase (112) and 1285 - $1270 cm^{-1}$ in the transferrins to $1265 cm^{-1}$ in protocatechuate-3,4-dioxygenase (110) while substitution of cobalt(III) or manganese(III) and iron(III) or copper(II) in the transferrins results in a $\sim 20 cm^{-1}$ decrease. It is reasonable that this frequency be more responsive to changes in the metal ion environment since it contains a substantial contribution from C-O stretching motion, whereas the other tyrosinate vibrational modes involve primarily phenyl ring

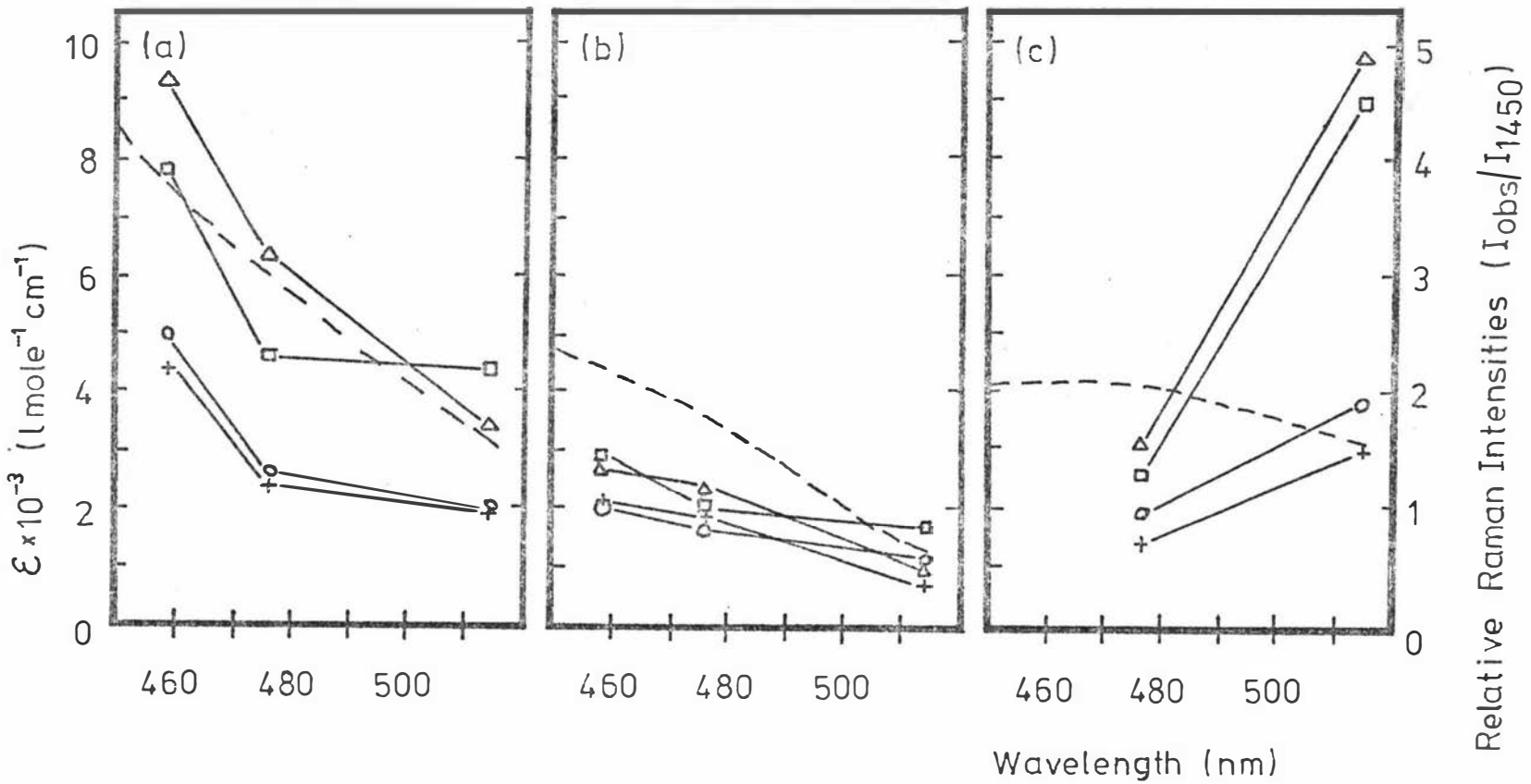

Figure 1.16 Resonance Raman excitation profiles of (a) Co_2Lf, (b) Cu_2Lf and (c) Fe_2Lf. The dashed lines are the optical absorption spectra for each sample (left ordinate axis). The wavelength dependence of the Raman intensities relative to the CH_2-deformation mode at ~1450cm^{-1} are indicated for the tyrosinate ligand frequencies of ca. 1600cm^{-1}(□), 1500cm^{-1}(○), ~1260cm^{-1}(△) and 1170cm^{-1} (+) (right ordinate axis).

deformations (83). However the observed decrease in the C-O stretching frequency cannot be explained merely on the basis of increased metal-oxygen bond strengths. In the case of the metal substituted transferrins there is no correlation between C-O stretching frequency and the electronegativity of the metal (83) and in the case of the iron(III)-transferrins there is no correlation between the C-O stretching frequencies and the stability constants for iron binding. Human lactoferrin has been shown to bind iron 60 times stronger than ovotransferrin (7, 113) yet its C-O vibration at 1272cm^{-1} is actually higher in energy than the corresponding 1270cm^{-1} peak in ovotransferrin (83). Thus, the variability in the frequency of the ~1270cm^{-1} vibration is likely due to small changes in the geometry of the iron-tyrosinate moiety. A similar conclusion was drawn from the observed spectral changes in the iron-tyrosinate chromophore of protocatechuate-3,4-dioxygenase following its reaction with substrate and oxygen (110).

1.3.7 ISOELECTRIC FOCUSSING

Isoelectric focussing is a technique by which it is possible to concentrate proteins at their isoelectric point (I.E.P.), the pH at which they are electrically neutral. Diferric-, monoferric- and apolactoferrin differ from each other in the electric charge each possess, hence it should be possible to separate them on the basis of their isoelectric points. It was hoped that by this technique it would be possible to isolate monoferric lactoferrin in sufficient quantity for further studies as has been done with ovotransferrin (67).

Inital experiments were performed to determine the I.E.P. of the three species concerned; Fe_2Lf, FeLf and Lf. A value of pH 9.0 $\pm$ 0.2 was obtained for Fe_2Lf, but attempts to determine the I.E.P. of FeLf and Lf were less successful. In all cases recovery of the protein was only 20% and optical density measurements indicated that a considerable amount of material, possibly denatured protein, was present at lower pH. This may explain the results of other groups in which the isoelectric point was found initially to be

pH 9 but then overnight drop to pH 5.5 and 5.8 (114, 115).

The ability of lactoferrin to displace sodium from a cation exchange resin (CM-Sephadex C-50) at pH 7.6 suggests that at this pH it is below its isoelectric point. Furthermore the fact that Fe_2Lf would not run in an acrylamide gel at pH 8.9 is further confirmation of its high isoelectric point. However, because of the difficulties outlined above this line of study was abandoned.

1.4 CONCLUSION

Lactoferrin in addition to binding two iron(III) or copper(II) ions has been demonstrated in this study to strongly and specifically bind two cobalt(III), chromium(III) and manganese(III) ions. In addition it appears to be able to weakly bind manganese(II), cobalt(II), nickel(II), zinc(II), cadmium(II), lead(II) and mercury(II). In the presence of apolactoferrin manganese(II) has been shown to readily undergo aerial oxidation and bind to the protein as manganese(III) where it appears to be held in the specific sites more tightly than iron(III). While the latter can be partially displaced by copper(II) manganese(III) cannot. It would appear that the greater stability of Mn_2Lf over Fe_2Lf may be a consequence of manganese(III) inducing a different conformational change on apolactoferrin.

The close similarity between, the electronic, e.s.r. and Resonance Raman spectra of the complexes Fe_2Lf, Cu_2Lf, Co_2Lf, Mn_2Lf and Cr_2Lf with those of transferrin and ovotransferrin reinforce the postulate that the metal binding sites in all of these proteins are similar and contain 2 - 3 tyrosyl residues and at least one histidyl residue. The site appears to be flexible enough to accommodate the different stereochemical requirements of the metals employed. Iron(III), chromium(III), manganese(III) and copper(II) all appear to occupy a site of essentially distorted octahedral symmetry; rhombic in the case of the former two and distorted tetragonal in the case of the latter two. A distinct heterogeneity between the two specific binding sites is evident from the e.s.r. spectrum of Cr_2Lf and metal ion replacement studies indicate that chromium in one site is

more labile than the other. In addition to the two specific sites lactoferrin appears to have a number of non specific sites on the outside of the protein capable of weakly co-ordinating metal ions such as copper(II) and chromium(III).

Chapter 2 SMALL MOLECULE COMPLEXES OF IRON

2.1 Introduction

Studies on the iron-binding sites of lactoferrin and transferrin have indicated that there are two imidazole and two to three tyrosyl residues coordinated to the ferric ion (7,33,36-41) though the precise coordination sphere is still unknown. One bicarbonate ion is also known to be essential for the binding of the ferric ion, though whether or not it is directly coordinated to the metal is still questionable (40,44-53). In a recent study Gaber et.al. (40) reported the Resonance Raman and electronic spectra of the complex $Na[Fe(Va)]4H_2O$ (Figure 2.1) along with that of Fe_2Tf. The similarities between these spectra reinforced the postulate that the characteristic red colour of the iron-protein is a result of a phenolate-to-iron charge transfer transition. Furthermore these spectral similarities have been cited as evidence for the involvement of only two tyrosine residues in the specific binding of the ferric ion.

With the view to investigating the iron-tyrosinate interaction further and the effect that nitrogen bases such as imidazole may have on that interaction, a more comprehensive range of small molecule ferric ion complexes have been prepared using the ligands illustrated in Figure 2.1. This has allowed a spectroscopic study to be made on a series of complexes embracing the chromophores FeO_6, FeO_4N_2, FeO_3N_3, FeO_2N_4, and $FeO_2N_2O^1_2$ (where O represents the phenolate oxygen and O^1 the carboxylate oxygen). To clarify the electronic spectra in particular, ligands which are essentially colourless in the anionic form were selected. To mimic the tyrosine moiety substituted hydroxyphenyl derivatives were used whereever possible. However, for the FeO_6 type, data obtained for catecholate complexes was used as similar phenolate complexes are not known. Ideally, isolated (non-conjugated) tyrosine and histidyl systems should be considered but these systems are not always easy to work with or are unknown. So systems ranging from

Figure 2.1 Nomenclature and structures of the ligands complexed with iron(III) (the number and structure refer to the deprotonated ligand, the name refers to the corresponding acid form).

Nicotinylhydroxamic Acid

Ia.

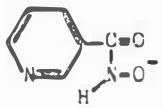

Salicylhydroxamic Acid

Ib.

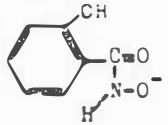

Benzohydroxamic Acid

Ic.

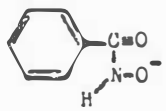

Tropolone

II.

3-(2-Hydroxyphenyl)-5-methylpyrazole

IIIa.

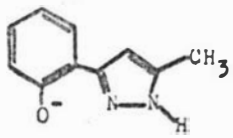

3-(2-Hydroxyphenyl)-5-phenylpyrazole

IIIb.

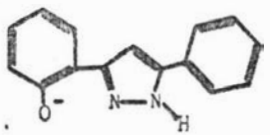

2-(2-Hydroxyphenyl)-benzoxazole

IV.

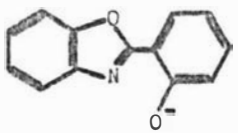

N,N'-Ethylenediamine-bis-(2-hydroxyphenylglycine)

Va.

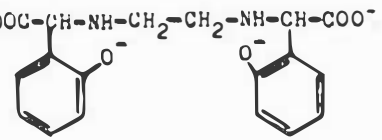

N,N-di-(2-Hydroxybenzyl)-ethylenediamine-N,N'-diacetic Acid

Vb.

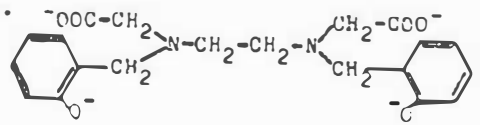

2-Hydroxy-N-(2-hydroxybenzylidine)-aniline

VIa.

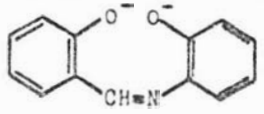

VIb.

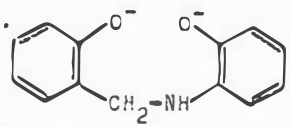

2-Hydroxy-N-(2-azobenzylidene)-aniline

VIc.

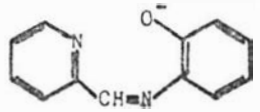

VId.

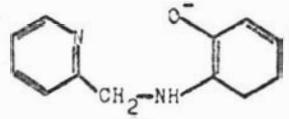

1,10-(2-Hydroxybenzylidene)-1,4,7,10-tetraazaoctane

VIIa.

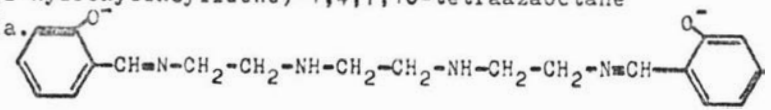

VIIb.

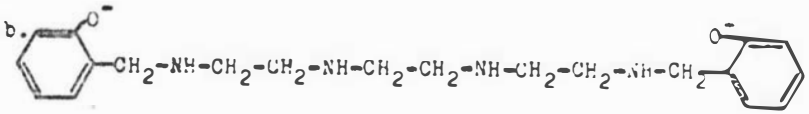

1,12-(2-Hydroxybenzylidene)-1,5,8,12-tetraazadecane

VIIc.

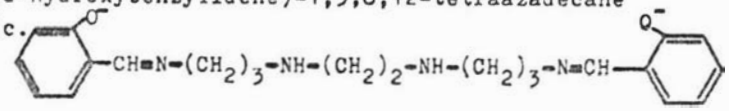

VIId.

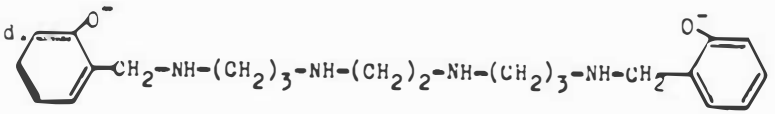

bis-Salicylaldehyde-N,N'-ethylenediamine-H_4

VIII.

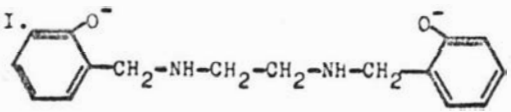

bidentate, tridentate to hexadentate containing aromatic and/or aliphatic nitrogens have to be used and from these factors that influence the peak position and intensity of the charge transfer band in the visible region could be studied. E.S.R. and Mössbauer spectroscopy were also considered to evaluate their sensitivity to changes in the ferric ion environment created by the different ligands. Hence from this, conclusions could be drawn about the nature of iron-binding in the specific site of lactoferrin and transferrin.

2.2 Experimental

2.2.1 SYNTHESIS AND SOURCES OF THE LIGANDS

Ia, Ic, II and IV were obtained from Aldrich Chemical Company, Ia from National Biochemical Corporation, Va from Sigma Chemical Company and imidazole and N-methylimidazole from BDH Laboratories. IIIa and IIIb were prepared by Dr A. W. Addisson (University of British Columbia) and Vb was prepared by Coordination Chemistry Consultants (Texas A and M University). VIa, VIc and SALEN (bis-salicylaldehyde-N,N^1-ethylenediamine) were made by adding 10mmol of the appropriate aldehyde to 10mmol of the appropriate amine and stirring for approximately half an hour. The solutions were taken down to dryness, washed with ether and dried. VIII was prepared by adding two mole equivalents of $NaBH_4$ in ethanol to SALEN, the yellow ligand in suspension turned white and dissolved as the BH_4^- went into solution. It was then filtered, precipitated with water and the white solid recrystallized by dissolving in hot ethanol, upon reduction of the volume and the addition of water the product was precipitated.

2.2.2 SYNTHESIS OF THE COMPLEXES

Preparation of $[Fe(II)_3]$

$[Fe(II)_3]$ was prepared following the method of Cook et.al. (117), 3.66g of tropolone was dissolved in a solution containing 2.52g of $NaHCO_3$ in water to which was added 4.04g of $Fe(NO_3)_3.9H_2O$ in water. The resulting brick red precipitate was filtered off, redissolved in $CHCl_3$ (all except an uncharacterised yellow-brown compound) and

precipitated with CCl_4/diethylether. Analyses were performed on the purple form of the complex.

Preparation of $[Fe(IIIa)_3]1\frac{1}{2}\ H_2O$

IIIa (0.52g, 3mmol) and NaOH (0.12g, 3mmol) were dissolved in approximately $30cm^3$ of hot methanol. To the filtered, cooled solution was added $Fe(NO_3)_3.9H_2O$ (0.404g, 1mmol) in $20cm^3$ of methanol whereupon a fine blood red precipitate formed. This was filtered and washed first with methanol/diethylether, then diethylether and air dried. The molecular weight of this was determined to be 604 daltons (Theoretical value = 575 daltons).

Preparation of $[Fe(IIIa)_2(MeOH)_2]NO_3.2H_2O$

IIIa (0.35g, 2mmol) and NaOH (0.08g, 2mmol) were dissolved in approximately $30cm^3$ of hot methanol and the solution filtered on cooling. To this was added $Fe(NO_3)_3.9H_2O$ (0.404g, 1mmol) in $20cm^3$ of methanol. Initially, the red solution formed with precipitation of the tris complex but on addition of all the ferric nitrate the solution turned purple and the precipitate redissolved. Within five minutes fine needle crystals appeared and these allowed to grow for a period of 2 - 4 hours after which they were filtered off, washed with water and air dried.

Preparation of $[Fe(IIIa)_2(Im)_2]NO_3.\frac{1}{2}H_2O$ (76)

To a hot solution of 0.188g (0.333mmol) of $[Fe(IIIa)_2(MeOH)_2]NO_3.2H_2O$ in ethanol a large ($\sim$10 fold) excess of imidazole was added until the λ_{max} no longer shifted to shorter wavelength. The solution was left to stand at 4^oC for three days after which the resulting dark red crystals were filtered, then washed with ethanol and ether.

Preparation of $[Fe(IIIb)_3]4H_2O$

IIIb (0.708g, 3mmol) and NaOH (0.12g, 3mmol) were dissolved in approximately $30cm^3$ of hot methanol and the solution filtered on cooling. Upon the addition of $Fe(NO_3)_3.9H_2O$ (0.404g, 1mmol) in $20cm^3$ of methanol, a deep red solution formed. A deep red crystalline material was obtained after standing for $1\frac{1}{2}$ hours. It was filtered,

washed with water, ethanol, diethylether and air dried. Further crops were obtained upon standing for two days and, after filtration, by the addition of water.

Preparation of $[Fe(IV)_3]1\frac{1}{2}H_2O$

Sodium metal (0.138g, 6mmol) was added to a slurry of IV in $30cm^3$ of ethanol. As the sodium dissolved and the ligand converted to its anionic form a red coloured solution that fluoresced was produced. To the filtered solution was added $Fe(NO_3)_3.9H_2O$ (0.808g, 2mmol) in $20cm^3$ of ethanol. The resulting red precipitate was filtered, washed with water, then ethanol and air dried.

Preparation of $K[Fe(Vb)]2H_2O$

$K[Fe(Vb)]2H_2O$ was prepared using the method of Gaber et.al. (40) for the analagous Va complex. Equimolar quantities of Vb, freshly precipitated hydrated ferric oxide and $KHCO_3$ were stirred in a 3:1 water:methanol mixture for three days. The solution was filtered, stripped on a rotary evaporator and the resulting precipitate extracted into ethanol. Crystals which appeared when the volume was reduced were filtered and washed with diethylether. A second crop was obtained upon the addition of ether.

Preparation of $[Fe(VIc)_2]PF_6.H_2O$

To VIc (0.39g, 2mmol) and KOH (0.112g, 2mmol) dissolved in warm ethanol or methanol ($30cm^3$) was added $FeCl_3$ (0.162g, 1mmol) dissolved in $10cm^3$ of ethanol or methanol. The mixture was heated for 10 minutes and $5cm^3$ dimethoxypropane added. After cooling (1 hour) the solution was filtered (to remove KCl) and the volume reduced to about $15cm^3$. NH_4PF_6 (2mmol) dissolved in methanol was added and the resulting precipitate was collected and washed with cold methanol and diethylether. The filtrate also produced a second crop.

Preparation of $K[Fe(VIa)_2]2H_2O$

To VIa (0.53g, 2.48mmol) and KOH (0.28g, 5mmol) dissolved in $35cm^3$ of warm ethanol was added $FeCl_3$ (0.20g, 1.25mmol) in $10cm^3$ of ethanol. The mixture was heated for

five minutes and let to stand for an hour. The solution was filtered to remove KCl and then reduced to below half-volume and ether added. The solution was cooled overnight and then black crystals of the product were collected and washed with an ethanol/ether (1:1 V/V)mixture and then diethylether.. The product was recrystallized from a methanol/diethylether mixture.

Preparation of $[Fe(VIIb)]PF_6$

Fe(VIIa) $NO_3.1\frac{1}{2}H_2O$ was prepared according to Tweedle and Wilson (118). One gram of this compound was dissolved in water and 0.55g of $NaBH_4$ slowly added and the solution changed to a wine red colour. It was filtered and KPF_6, dissolved in water, was added and this resulted in the precipitation of the product. It was collected and washed thoroughly with water.

Preparation of $[Fe(VIIc)]PF_6$

This was prepared similarly to the literature preparation of $[Fe(VIIa)]PF_6$ (118), except at the extraction stage where 900cm^3 of water was used. The product was recrystallized from 30cm^3 of an acetone/water mixture (7:3 V/V).

Preparation of $[Fe(VIIc)]I_3$

To 0.29g of $[Fe(VIIc)]PF_6$ dissolved in 50cm^3 of a methanol/acetone mixture (1:1 V/V) was added 0.4g of I_2. After removal of the solvent mixture to below half volume on a rotary evaporator blackish crystals of the product precipitated and these were collected and washed with diethylether.

2.2.3 INSTRUMENTATION

I.R. spectra were recorded on a Beckman IR20 spectrophotometer, electronic spectra on a Shimadzu MPS 5000 spectrophotometer. E.S.R. measurements were made at -196°C on a Varian E104A X-band spectrometer or at -160°C using a Varian E-257 Variable Temperature accessory. Spectral g values were calibrated with a DPPH standard. Conductivity measure-

Table 2.1 ANALYTICAL DATA OF SMALL MOLECULAR WEIGHT FERRIC ION COMPLEXES.

Compound	Found (%)			Calculated (%)		
	C	H	N	C	H	N
$[Fe(II)_3]$	60.7	3.3	-	60.2	3.6	-
$[Fe(IIIa)_3]1\frac{1}{2}H_2O$	59.5	4.7	13.4	59.8	5.0	14.0
$[Fe(IIIa)_2(MeOH)_2]NO_3.2H_2O$	46.7	4.8	12.8	46.8	5.4	12.4
[a] $[Fe(IIIa)_2(Im)_2]NO_3.\frac{1}{2}H_2O$	52.0	4.5	20.7	51.9	4.8	21.0
$[Fe(IIIb)_3]4H_2O$	64.3	4.4	9.8	64.8	5.0	10.1
$[Fe(IV)_3]1\frac{1}{2}H_2O$	65.7	3.7	5.8	65.7	3.8	5.9
$K[Fe(Vb)]2H_2O$	46.2	5.0	5.3	46.6	4.7	5.4
$K[Fe(VIa)_2]2H_2O$	57.0	4.1	5.4	56.4	3.9	5.1
$[Fe(VIc)_2]PF_6.H_2O$	47.0	3.6	9.4	47.0	3.3	9.1
$[Fe(VIIb)]PF_6$	43.3	5.0	10.0	43.1	5.0	10.0
$[Fe(VIIc)]PF_6$	45.8	4.7	9.4	45.6	4.8	9.6
$[Fe(VIIc)]I_3$	32.3	3.4	6.9	32.3	3.4	6.9

a. Reference (76)

Table 2.2 CONDUCTIVITIES AND MAGNETIC SUSCEPTIBILITIES OF SMALL MOLECULAR WEIGHT FERRIC ION COMPLEXES

Compound	Λ_M ($\Omega^{-1}mole^{-1}cm^2$)	Solvent	μ_{eff}(BM)
$[Fe(Ia)_3]6H_2O$	26.1	EtOH	5.88
$[Fe(Ib)_3]4\frac{1}{2}H_2O$	-	-	5.71
$[Fe(Ic)_3]1\frac{1}{2}H_2O$	0.06	EtOH	6.14
$[Fe(II)_3]$	0.54	Acetone	6.17
$[Fe(IIIa)_3]1\frac{1}{2}H_2O$	0	Acetone	5.90
$[Fe(IIIa)_2(MeOH)_2$ $NO_3.2H_2O$	35.8 (0.11	EtOH Nitrobenzene)	5.79
$[Fe(IIIb)_3]4H_2O$	1.35	EtOH	6.13
$[Fe(IV)_3]1\frac{1}{2}H_2O$	-	-	4.25
$K[Fe(Vb)]2H_2O$	76.8	MeOH	5.76
$K[Fe(VIa)_2]2H_2O$	92.54	Acetone	5.98
$[Fe(VIc)_2]PF_6.H_2O$	110	Acetone	4.86
$[Fe(VIIb)]PF_6$	-	-	5.9
$[Fe(VIIc)]PF_6$	87	MeOH	2.02
$[Fe(VIIc)]I_3$	93	MeOH	1.92

ments were made using a Philips PR 9500 and 9510 conductivity meter and cell. All conductivities are consistent with the proposed formulations (Table 2.2). Molecular weights were determined by the vapour pressure method on the Hitachi Perkin-Elmer Molecular Weight Apparatus 115. Magnetic susceptibilities were determined at Victoria University by the Faraday Method using $Hg[Co(CNS)_4]$ as the calibrant. Pascal constants were used to correct for water, ligand and anion diamagnetism. Mössbauer spectra were collected and analysed at Chemistry Division, D.S.I.R. Percentage C, H and N were determined by Professor A. D. Campbell at Otago University and are given in Table 2.1.

2.3 Results and Discussion

2.3.1 PREPARATIONS OF COMPLEXES

FeO_6 Types

Species of the type $[Fe(phenolate)_6]^{3-}$ are not known. The closest systems to this are a number of bidentate ligands, one example of which is $[Fe(catecholate)_3]$ (119). Complexes of hydroxamic acids Ia, Ib and Ic were prepared by the method of Epstein and Straub (120), while the complex of II was prepared by the method of Cook et.al. (117).

FeO_4N_2, FeO_3N_3 and Related Types

The preparation of the tris complexes of IIIa, IIIb and IV are given in the experimental section. The bis complex $[Fe(IIIa)_2(MeOH)_2]NO_3.2H_2O$ crystallized from a 1:2:2 mixture of $Fe(NO_3)_3.9H_2O$:IIIa:NaOH in MeOH over a period of 2 - 3 hours as long purple needles. These appeared to be stable in air for at least 4 - 5 hours, but became pitted over several days indicating the loss of solvent from the crystals. From single crystal x-ray structural analysis the formulation of the complex appeared to be $[Fe(IIIa)_2(MeOH)_2]NO_3.MeOH$ suggesting either some variation in solvation between different batches of compound, or that water may replace the labile methanol molecule in the crystals. The effect of a variety of bases on the electronic spectrum of $[Fe(IIIa)_2(MeOH)_2]NO_3.2H_2O$ was also investigated. No change was evident in λ_{max} when dimethylsulphide and

dimethylphenylphosphine oxide ($(Me)_2Ph\ P{=}O$) were added (Table 2.3), though the latter added in excess caused a steady decrease in the intensity of the charge transfer band suggesting that $(Me)_2PhP{=}O$ was replacing IIIa in the complex. Shifts of λ_{max}, listed in order of shorter wavelength, were observed with dimethylsulphoxide (DMSO), imidazole (Im) and tribenzylamine and it proved possible to isolate crystals of $[Fe(IIIa)_2(Im)_2]NO_3.\frac{1}{2}H_2O$ from solution.

An attempt was made to prepare the complex $[Fe(IIIa)(MeOH)_4]^{2+}$ by preparing a 1:1:1 solution of $Fe(NO_3)_3.9H_2O$: IIIa:NaOH in MeOH. However, no crystals or precipitate appeared from the resulting deep blue solution and as the λ_{max} of the solution decreased on dilution this value was best determined by running a diffuse reflectance spectrum. An attempt was made to prepare $[Fe(IIIb)_2(MeOH)_2]^+$ by preparing a 1:2:2 mixture of $Fe(NO_3)_3.9H_2O$:IIIb:NaOH in methanol. From this was isolated a solid which had an absorbance maximum of 532nm while the resulting filtrate had a λ_{max} of 572nm, indicating a mixture of both tris and bis complexes of IIIb. Attempts to separate these proved unsuccessful.

An attempt was made to prepare the complex $[Fe(VIII)]^+$, however it was not possible to isolate this from solution. Hence studies were performed on 1:1 mixtures of $Fe(ClO_4)_3$: VIII to which one or two molar equivalents of imidazole or N-methylimidazole (N-Me-Im) were added.

$FeO_2N_2O_2^1$ and FeO_2N_4 Types

Complexes of Va and Vb were prepared following the method of Gaber et.al. (40). A complex of the latter has been previously been prepared in solution (127) though it was not isolated as a solid. Preparation of complexes involving the ligands VIa, VIc, VIIa and VIIc are given in the experimental section. In the case of the latter two ligands the method of Tweedle and Wilson was followed (118). The anions of these ligands give rise to orange colours so to clarify the electronic spectra they were reduced by $NaBH_4$ when attached to iron(III). Many of the reduced anions do not have a separate existence. The assignment of

the spectra were simplified because the reduced ligands gave anions that were nearly colourless. However of the complexes involving these reduced ligands only one, $[Fe(VIIb)]PF_6$, was isolated as a solid. That reduction of the ligand had occurred was verified by the i.r. spectrum of the solid, which in comparison with its precursor, shows important differences. The former compound shows two ν(N-H) absorption bands at about 3300cm^{-1} while the latter has one, and the ν(C=N) absorption in the latter at 1620cm^{-1} disappeared upon reduction. $K[Fe(VIa)_2]2H_2O$ and $[Fe(VIc)_2]PF_6.H_2O$ once reduced (in MeOH) were unstable and were oxidised by air back to the parent compounds. However spectral data could be recorded if obtained immediately after reduction. Addition of excess $NaBH_4$ resulted in the reduction of iron(III) to iron(II) and loss of colour.

2.3.2 MOLECULAR STRUCTURE OF $[Fe(IIIa)_2(MeOH)_2]NO_3.MeOH$

In the complex (Figure 2.2) (107) the ferric ion has been shown to be coordinated to two IIIa ions and two methanol molecules. As well there is one occluded methanol molecule and one nitrate group present in the asymmetric unit. The iron is bound to the phenolate oxygen, one of the imine nitrogen atoms and the oxygen atom of methanol in an all-trans arrangement. These six atoms of the inner coordination sphere form a rhombic environment for the iron atom. The Fe-N bond is within the normally expected values for iron-imine interactions and the iron-methanol bond length (2.094(3)A^o) is not significantly different to that found for an Fe^{III}-ethanol interaction (2.113, 2.160A^o) (121). The iron-phenolate bond (1.888(3)A^o) would also appear to be close to normal, it is not significantly different to the iron-phenolate bond in $Mg[Fe(Va)]4H_2O$ of 1.907(7)A^o (103). The occluded methanol molecule is part of a hydrogen bonding scheme involving the methanol molecule bound to the iron atom, the occluded methanol molecule and the nitrate group. The hydrogen atom of the bound methanol is hydrogen bonded to the oxygen of the occluded methanol molecule, the bond length of 1.7A^o is close to values expected for such an interaction (122). The hydrogen atom of the occluded methanol is further

Figure 2.2 The molecular conformation of $[Fe(IIIa)_2(MeOH)_2]NO_3.MeOH$.
Top; the coordination sphere of the ferric ion.
Bottom; the hydrogen-bonding network in the crystal (hydrogen-bonds are indicated by dashed or dotted lines).

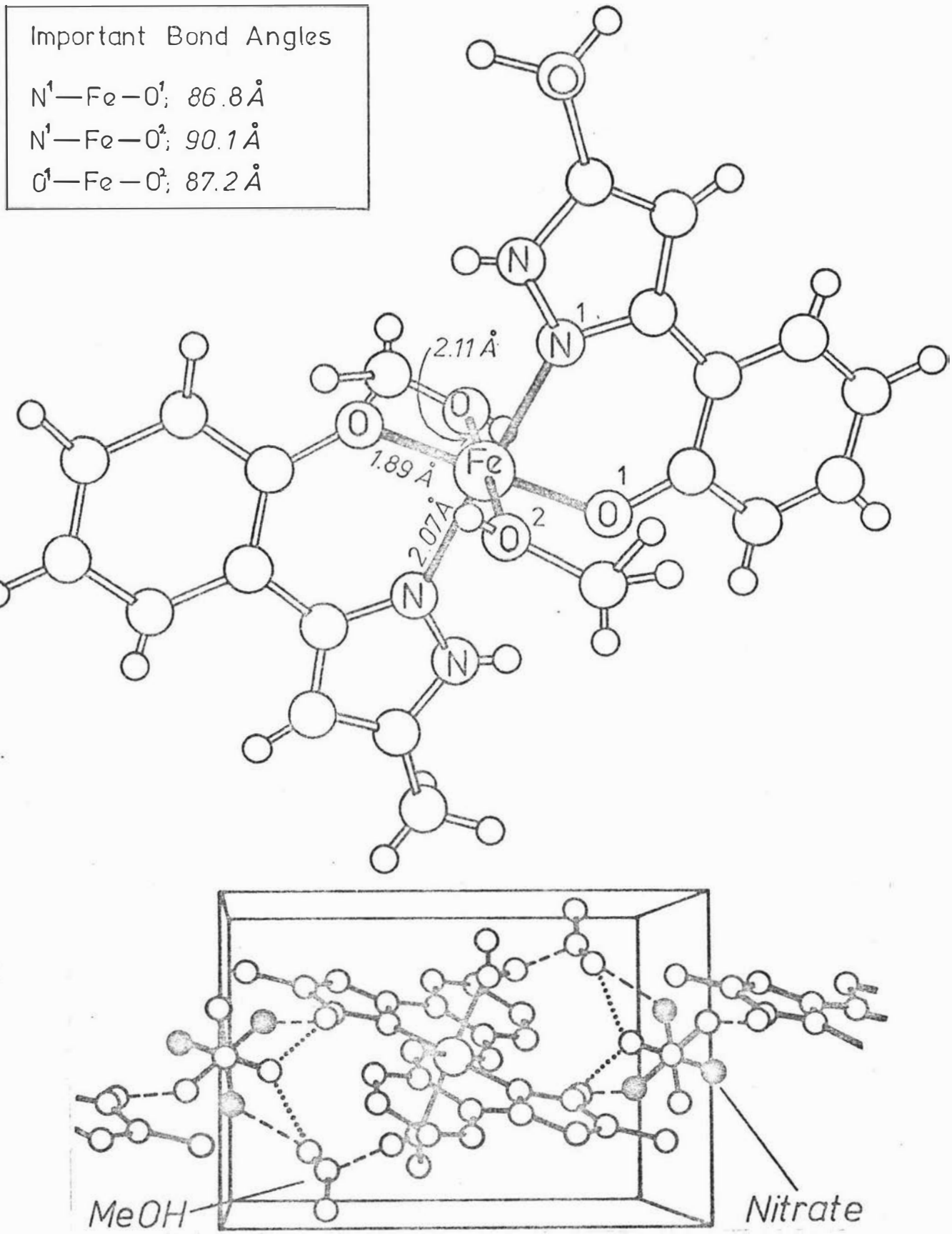

hydrogen bonded to an oxygen of the nitrate, while hydrogen bonding also occurs between the latter and the hydrogen of the imine group in IIIa, thus a lattice of hydrogen bonding is set up. This was also found in two diethyl adducts of porphyrinato iron(III) complexes (121, 123). Furthermore the fact that there was no direct interaction between the nitrate group and the iron atom provided further confirmation for the assignment of the 1360cm^{-1} band in the i.r. spectrum of the complex to ionic nitrate.

2.3.3 ELECTRONIC SPECTRA

The main feature of the electronic spectra of these compounds is the relatively intense charge transfer band that gives rise to the reddish colour (at 420-530nm) and which can be assigned to a transition from the $p\pi$ orbitals on the phenolate oxygen to the half filled $d\pi^*$ orbitals on the ferric ion (40). Such $p\pi \longrightarrow d\pi^*$ transitions are intense where as d-d transitions are very weak and difficult to observe for Fe^{III}. For example a weak shoulder in the spectrum of $Na[Fe(Va)]4H_2O$ has been observed at high concentrations around 900nm, at room temperature and -196°C (Table 2.3). A second band at about 315nm has been reported by Gaber et.al. (40) to be assigned as a $p\pi \longrightarrow d\sigma^*$ type in $[Fe(Va)]^-$ and poorly resolved in Fe_2Tf. A similar band at 315nm can be observed in Fe_2Lf and though discrete bands have been observed in complexes of IIIa, IIIb and IV its identification in other complexes has been difficult. The high intensity of the charge transfer bands is probably due to mixing with low lying phenyl $\pi \longrightarrow \pi^*$ transitions and where these are not present as in $[Fe(EDTA)(OH)]^{2-}$ no charge transfer band is found (124).

However in an attempt to mimic the charge transfer transition of Fe_2Lf (at 465nm) it is important to note that factors such as those listed below will influence the intensity and position of the band.

1. The polydentate nature of some of the ligands as compared with the bidentate and tridentate character of others.
2. The charge on the ligand.

3. The nature of the N-donor atoms (e.g. whether aliphatic or aromatic).
4. The stereochemistry around the ferric ion (e.g. in FeO_3N_3 whether the mer or fac isomer exists and for FeO_2N_4 whether cis or trans arrangement is present), and
5. The actual number of phenolate and nitrogen ligands present.

It is conceivable that particular combinations of the above factors will allow one to "tune in" onto the actual charge transfer energy even though the numbers of phenolates and nitrogen atoms are different in each model. Generally, however, one should be able to at least limit the possible models to one or two types.

Ideally it would be more suitable if one ligand could be used to cover as many types as possible (e.g. cis and trans FeO_2N_4, mer and fac FeO_3N_3). However, this not being the case in the present study ligands have been designed to cover all types of complexes from FeO_6 to $FeO_2N_2O_2^1$ (although the actual geometry is not always known).

FeO_6 Types

Complexes of this type have bands within the range 430-500nm (Table 2.3) making them close in energy to the charge transfer transition observed in Fe_2Lf. Generally they are higher in energy than complexes of the type FeO_3N_3 indicating that the second oxygen in the ligand raises the electron density on iron to a greater extent than nitrogen hence the charge transfer interaction becomes less favourable. However the spectrum of $[Fe(II)_3]$ is more complex than the others in this series. While it has a charge transfer band at 427nm, the intensity of this (at 15,200$lmole^{-1}cm^{-1}$) is much greater than that reported for the other complexes prepared in this study which all have intensities around 4000$lmole^{-1}cm^{-1}$. Additional bands are also observed at lower energy. It may be that these are a consequence of the structure of $[Fe(II)_3]$ which is intermediate between octahedral and trigonal prismatic (125).

Table 2.3 ELECTRONIC SPECTRA OF SMALL MOLECULAR WEIGHT FERRIC ION COMPLEXES

Compound	λ_{max} (nm)[a] Visible Bands	Others	Solvent
[b] Fe_2Lf	465(4140)	283(115,800)	Phosphate Buffer
[c] Fe_2Tf	470(4370)	280(109,700)	Tris Buffer
[d] $[Fe(Catecholate)_3]^{3-}$	496(4700)	-	H_2O
$[Fe(Ia)_3]5H_2O$	433(3430)	260(Sh)	EtOH
$[Fe(Ib)_3]\cdot\frac{1}{2}H_2O$	468	301	EtOH
$[Fe(Ic)_3]1\frac{1}{2}H_2O$	444(4470)	250(sh)	EtOH
$[Fe(II)_3]$	427(15200), 510(sh), 534(sh)	270(sh), 328(31700) 364(17300)	$CHCl_3$
$[Fe(IIIa)_3]1\frac{1}{2}H_2O$	487(3903)	304(24250)	$CHCl_3$
$[Fe(IIIa)_2(MeOH)_2]$ $NO_3.2H_2O$	563(4570)	305(19000)	EtOH
[e] $[Fe(IIIa)_2(Im)_2]NO_3.\frac{1}{2}H_2O$	530	-	EtOH
[e] $[Fe(IIIa)_2(X)_2]^+$			
X=tribenzylamine	527	-	EtOH
DMSO	550	-	EtOH
dimethylsulphide	no change	-	EtOH
$(Me)_2PhP=O$	no change	-	EtOH
$[Fe(IIIa)(MeOH)_4]^{2+}$	640	-	Reflectance
$[Fe(IIIb)_3]4H_2O$	501(3870)	298(39900)	EtOH
$[Fe(IV)_3]1\frac{1}{2}H_2O$	500(sh ~1500)	325(35170), 336(35280), 360(sh)	$CHCl_3$
$[Fe(VIII)]^+$	540	-	MeOH
$[Fe(VIII)(Im)]^+$	480	-	MeOH
$[Fe(VIII)(Im)_2]^+$	490	-	MeOH
$[Fe(VIII)(N\text{-}Me\text{-}Im)_2]^+$	467	-	MeOH
[f] $Na[Fe(Va)]4H_2O$	480(4000), 910	282	H_2O
$K[Fe(Vb)]2H_2O$	492(3830)	277(11380), 318(6300)	H_2O
$K[Fe(VIa)_2]2H_2O$	403(26310), 470(sh)	290(30840), 345(sh)	MeOH
$K[Fe(VIb)_2]$	425	-	MeOH
$[Fe(VIc)_2]PF_6.H_2O$	430(sh)	-	Acetone
$[Fe(VId)_2]PF_6$	465	-	MeOH
$[Fe(VIIa)]PF_6$	430(3000), 490(3600), 620(1900)	340(9000)	Acetone
$[Fe(VIIb)]PF_6$	507	-	MeOH
$[Fe(VIIc)]PF_6$	400(sh), 575(3000)	353(6880)	MeOH
$[Fe(VIId)]PF_6$	509	-	MeOH
$[Fe(VIIe)]I_3$	410(sh), 575(3260)	256(sh), 280(sh), 359(14000)	MeOH

a. Extinction Coefficient in brackets

b. Table 1.6

c. Reference (7)

d. Reference (119)

e. Reference (76)

f. Reference (40)

(sh) = shoulder

FeO_4N_2, FeO_3N_3 and Related Types

In the series of complexes prepared from the ligand IIIa there is an increase in the energy of the charge transfer band from $[Fe(IIIa)(MeOH)_4]^{2+}$ through $[Fe(IIIa)_2(MeOH)_2]^{+}$ to $[Fe(IIIa)_3]$ while the only FeO_4N_2 complex $K[Fe(VIb)_2]2H_2O$ absorbs at the highest energy (Table 2.3). This trend is consistent with the observation that complexation of the ferric ion by successive phenolate groups produces a blue shift in the visible absorption maximum by about $2000cm^{-1}$ per phenolate group (126). Interaction with an increasing number of phenolate oxygens donating charge to the central metal ion can be expected to destabilise the metal orbitals by virtue of a spherical term repulsion between the metal and ligand electron density (143). Hence the ligand-to-metal charge transfer band will decrease in energy as the coordination number decreases.

The charge transfer transition moves from 487nm for $[Fe(IIIa)_3]1\frac{1}{2}H_2O$ to 501nm for $[Fe(IIIb)]_3 4H_2O$ a move consistent with the fact that increasing conjugation of the ligand reduces the $p\pi \longrightarrow p\pi^*$ gap in the complex. Though the charge transfer band of the complex $Fe(IV)_3\ 1\frac{1}{2}H_2O$ is partly obscured by an intense band in the U.V. region centred at 336nm it absorbs around 500 nm making it close in energy to the complex $[Fe(IIIb)_3]4H_2O$.

Addition of bases such as imidazole or tribenzylamine to $[Fe(IIIa)_2(MeOH)_2]NO_3.2H_2O$ shifts the absorbance maximum to higher energy though the shift is not as great as when similar bases are added to $[Fe(VIII)]^{+}$ (Table 2.3). While in the former example a single crystal x-ray structure has shown the phenolate groups to be coordinated *trans* to each other it would appear likely that the phenolates of VIII are *cis* to each other, as the ligand would bind in a planar fashion. This is consistent with data for other pairs of *cis* and *trans* metal complexes where the *trans* isomers have been observed to absorb below the energy of the same band in the *cis* isomers (143). The difference may be due, in part, to interaction of orbitals on neighbouring ligand molecules.

Previous workers have cited a trend in the extinction

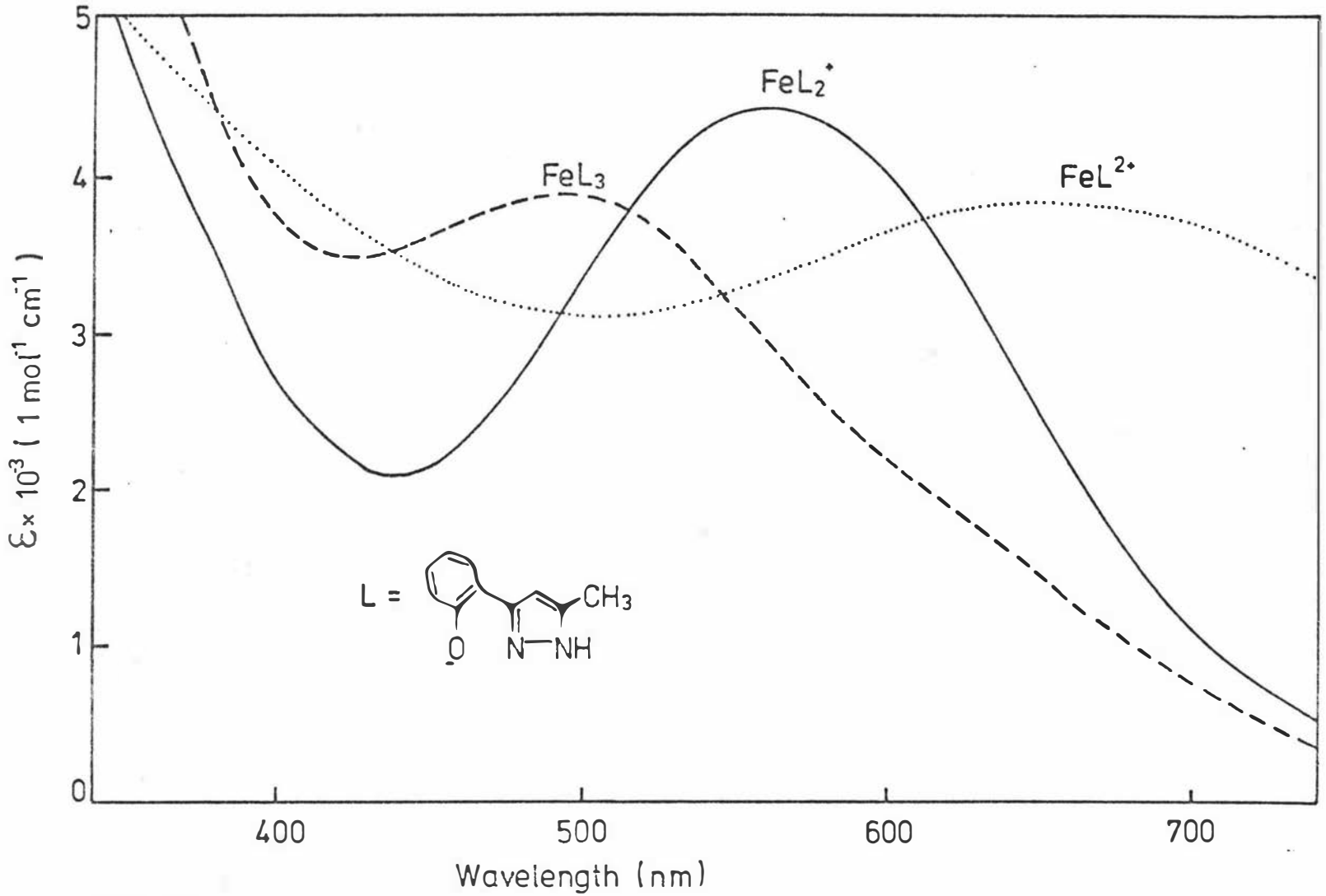

Figure 2.3 Visible absorption spectra of $[Fe(IIIa)_3]1\frac{1}{2}H_2O$ (– –) and $[Fe(IIIa)_2(MeOH)_2]NO_3.2H_2O$ (——) in methanol, and diffuse reflectance spectrum of $[Fe(IIIa)(MeOH)_4]^{2+}$ (••••).

coefficient of 2000lmole^{-1}cm^{-1} per phenolate group (40). While $[Fe(IIIa)_2(MeOH)_2]NO_3.2H_2O$ has an extinction coefficient of 4570lmole^{-1}cm^{-1} $[Fe(IIIa)_3]1\frac{1}{2}H_2O$ has a value of 3903lmole^{-1}cm^{-1} and $[Fe(IIIb)_3]4H_2O$ 3870lmole^{-1}cm^{-1} suggesting that a ceiling is reached after two phenolates are bound.

FeO_2N_4 and $FeO_2N_2O_2^1$ Types

From model building studies a cis arrangement of phenolates in $[Fe(VId)_2]PF_6.H_2O$ seems likely;

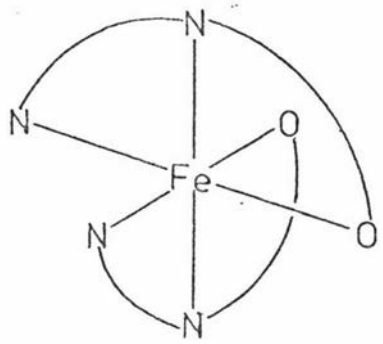

The absorbance maximum of this compound is similar to the other cis FeO_2N_4 system $[Fe(VIII)(N\text{-}MeIm)_2]$. Changing from the tridentate ligand VId to the hexadentate ligands VIIb and VIId, in which cis coordination of phenolates is also felt to occur(118), causes a shift in the charge transfer band to lower energy. This would be in line with the tighter binding expected with the hexadentate system though replacing the two aromatic nitrogens by aliphatic ones may be a contributing factor.

The λ_{max} values of ferric ion complexes of Va and Vb are in line with the stability constants of their respective complexes; $Na[Fe(Va)]4H_2O$ absorbs at 480nm and has a stability constant of 10^{34} while $K[Fe(Vb)]2H_2O$ absorbs at lower energy (496nm) and has a higher stability constant of $10^{39.8}$ (40). The structure of Va is such that steric hindrance may interfere to a certain extent with the participation of all six donor groups, hence the complex involving Vb, with a more favoured arrangement of these same donor groups, is more stable (127). Replacing the two carboxylate groups of Va and Vb by the aliphatic nitrogens of VIIb and VIId may be the cause of the shift of λ_{max} to

lower energy, though the fact that there is likely to be less steric hindrance in these latter ligands may also be important.

2.3.4 ELECTRON SPIN RESONANCE SPECTRA

The e.s.r. spectra of most of the complexes show a strong signal at $g = 4.3$ and a weaker one at $g = 10$ (Figure 2.4, Table 2.4) typical for high spin iron(III) in a rhombic environment as found from the single crystal x-ray structures of $[Fe(IIIa)_2(MeOH)_2]NO_3.MeOH$ (Section 2.32), $Mg[Fe(Va)]4H_2O$ (103) and $[Fe(Ic)_3]1\frac{1}{2}H_2O$ (128). The position of this $g = 4.3$ signal, however bears little relationship to the number of nitrogens (or oxygens) coordinated to the metal, or to the polydentate nature of the ligand as opposed to tridentate or bidentate nature or other factors. In each case there is no evidence of any splitting in the $g = 4.3$ signal as has been observed with Fe_2Tf or Fe_2Lf when HCO_3^- is the anion, the spectra are more like Fe_2Tf when NTA is the anion (49).

The complexes of iron with VIb and VId have signals around $g = 4.3$ while $[Fe(VIc)_2]PF_6.H_2O$ from -196 to -60°C exhibits a signal at $g = 2$ indicative of a low spin complex (Table 2.4). The magnetic susceptibility at 25°C is lower than normal for the high spin ferric ion (Table 2.2) and may be due to the presence of both high spin and low spin species, though this would have to be investigated further. In contrast $K[Fe(VIa)_2]2H_2O$ is high spin at -196°C and 25°C. This would indicate that an increase in the ligand field has occurred in replacing the phenolic OH groups of VIa with aromatic nitrogens in VIc.

The complexes $[Fe(VIIa)]PF_6$ and $[Fe(VIIc)]PF_6$ are both low spin at -196°C as indicated by their $g = 2$ signals (Table 2.4, Figure 2.5). At room temperature the former is high spin (118), while the latter is low spin. In this case the arrangement of 6,5,6-membered chelate rings of VIIc in $[Fe(VIIc)]PF_6$ would give more stability than that of 5,5,5-membered chelate rings of the triethylenediamine backbone in $[Fe(VIIa)]PF_6$ thus accounting for the greater ligand field strength of the former complex. When these

Table 2.4 ELECTRON SPIN RESONANCE SPECTRA OF SMALL MOLECULAR WEIGHT FERRIC ION COMPLEXES

Compound	g Values (at -196°C)	Solvent
[a] Fe_2Lf	8.84, 4.39, 4.29, 4.15	Phosphate Buffer
[b] Fe_2Tf	9.18, 4.42, 4.16, 4.08	0.1M KCl Soln
$[Fe(Ia)_3]6H_2O$	10.01, 4.15	EtOH
$[Fe(Ib)_3]4\frac{1}{2}H_2O$	10.26, 4.42	EtOH
$[Fe(Ic)_3]1\frac{1}{2}H_2O$	9.68, 4.36	EtOH
$[Fe(II)_3]$	8.11, 4.42	$CHCl_3$
$[Fe(IIIa)_3]1\frac{1}{2}H_2O$	8.50, 4.23	Acetone
$[Fe(IIIa)_2(MeOH)_2]NO_3.2H_2O$	7.33, 4.26	Acetone
$[Fe(IIIa)_2(Im)_2]NO_3.\frac{1}{2}H_2O$	8.07, 6.59, 4.28	DMF
$[Fe(IIIb)_3]4H_2O$	8.28, 4.26	Acetone
$[Fe(IV)_3]1\frac{1}{2}H_2O$	7.88, 5.21, 4.18, 2.78	Acetone
$[Fe(VIII)]^+$	9.63, 6.09, 4.25, 2.06	MeOH
$[Fe(VIII)(Im)]^+$	9.49, 4.25, 2.48, 2.01, 1.59	MeOH
$[Fe(VIII)(Im)_2]^+$	9.63, 4.25, 2.02	MeOH
$[Fe(VIII)(N\text{-}Me\text{-}Im)_2]^+$	8.32, 4.24	MeOH
$Na[Fe(Va)]4H_2O$	4.47	H_2O
$K[Fe(Vb)]2H_2O$	4.26	EtOH
$K[Fe(VIa)_2]2H_2O$	8.72, 4.24	MeOH
$K[Fe(VIb)_2]$	8.76, 4.18	MeOH
$[Fe(VIc)_2]PF_6.H_2O$	2.18, 2.05, 1.94	MeOH
$[Fe(VId)_2]PF_6$	8.59, 4.21	MeOH
$[Fe(VIIa)]PF_6$	2.19, 2.13, 1.95	Acetone
$[Fe(VIIb)]PF_6$	6.14, 4.78, 1.94	MeOH
$[Fe(VIIc)]PF_6$	2.34, 2.12, 1.95	Acetone
$[Fe(VIId)]PF_6$	6.72, 4.12, 1.93	MeOH
$[Fe(VIIc)]I_3$	2.33, 2.13, 1.95	Acetone

a. Table 1.9

b. Reference (7)

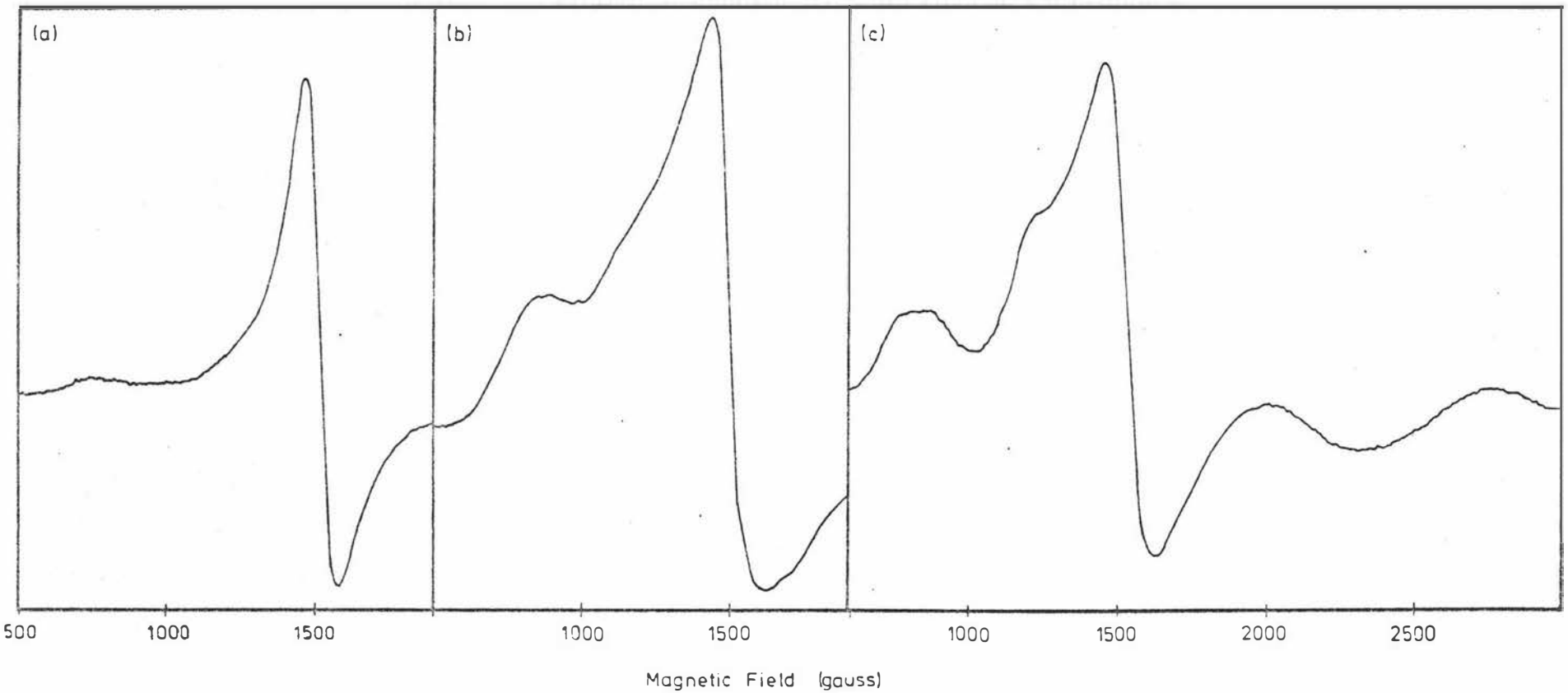

Figure 2.4 E.S.R. spectra at -160°C of (a) $[Fe(IIIa)_3]1\frac{1}{2}H_2O$ and (b) $[Fe(IIIa)_2(MeOH)_2]NO_3.2H_2O$ in acetone, and (c) $[Fe(IV)_3]1\frac{1}{2}H_2O$ in CH_2Cl_2.

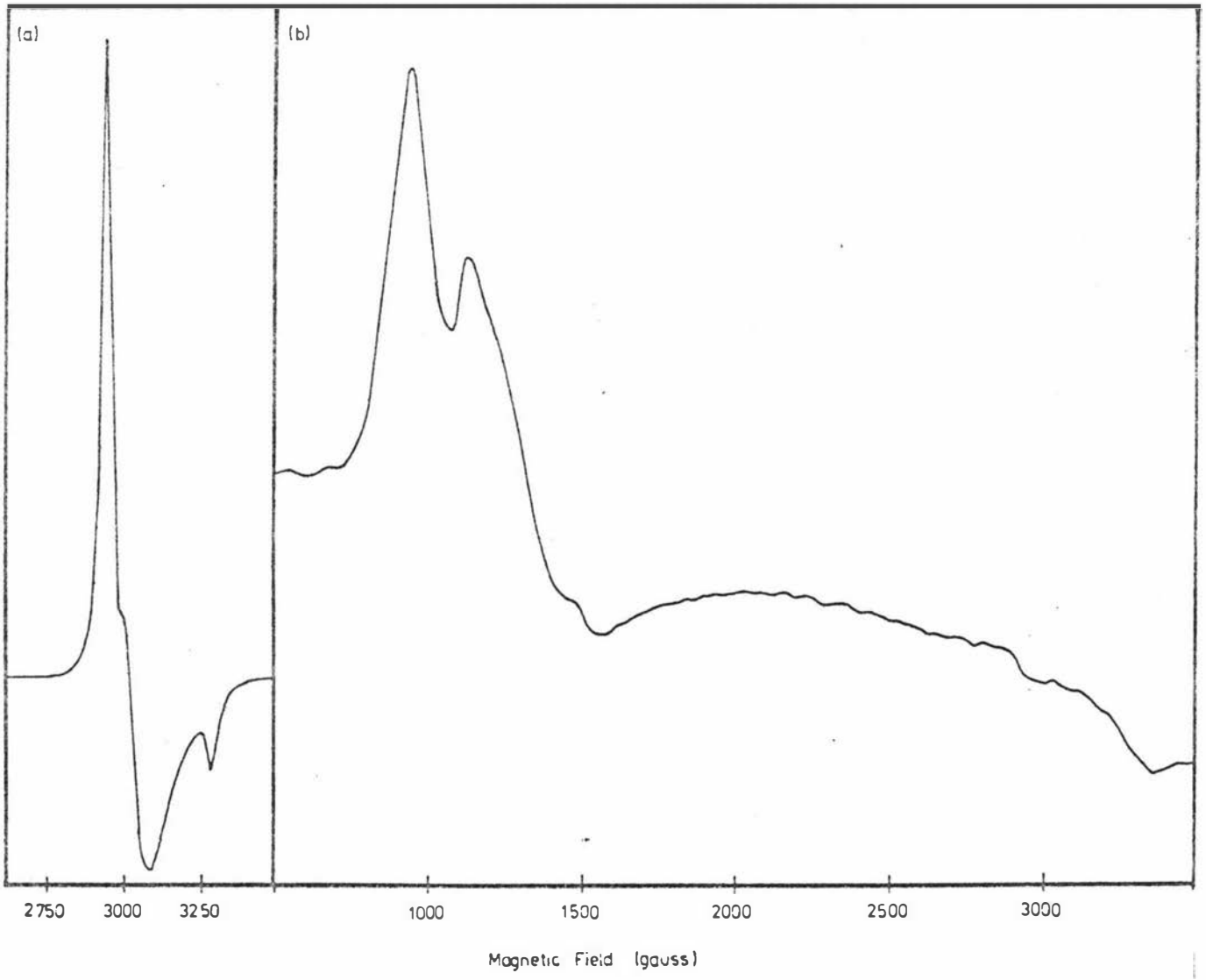

Figure 2.5 E.S.R. spectra at -160°C of (a) $[Fe(VIIa)]PF_6$ in Acetone and (b) $[Fe(VIIb)]PF_6$ in MeOH.

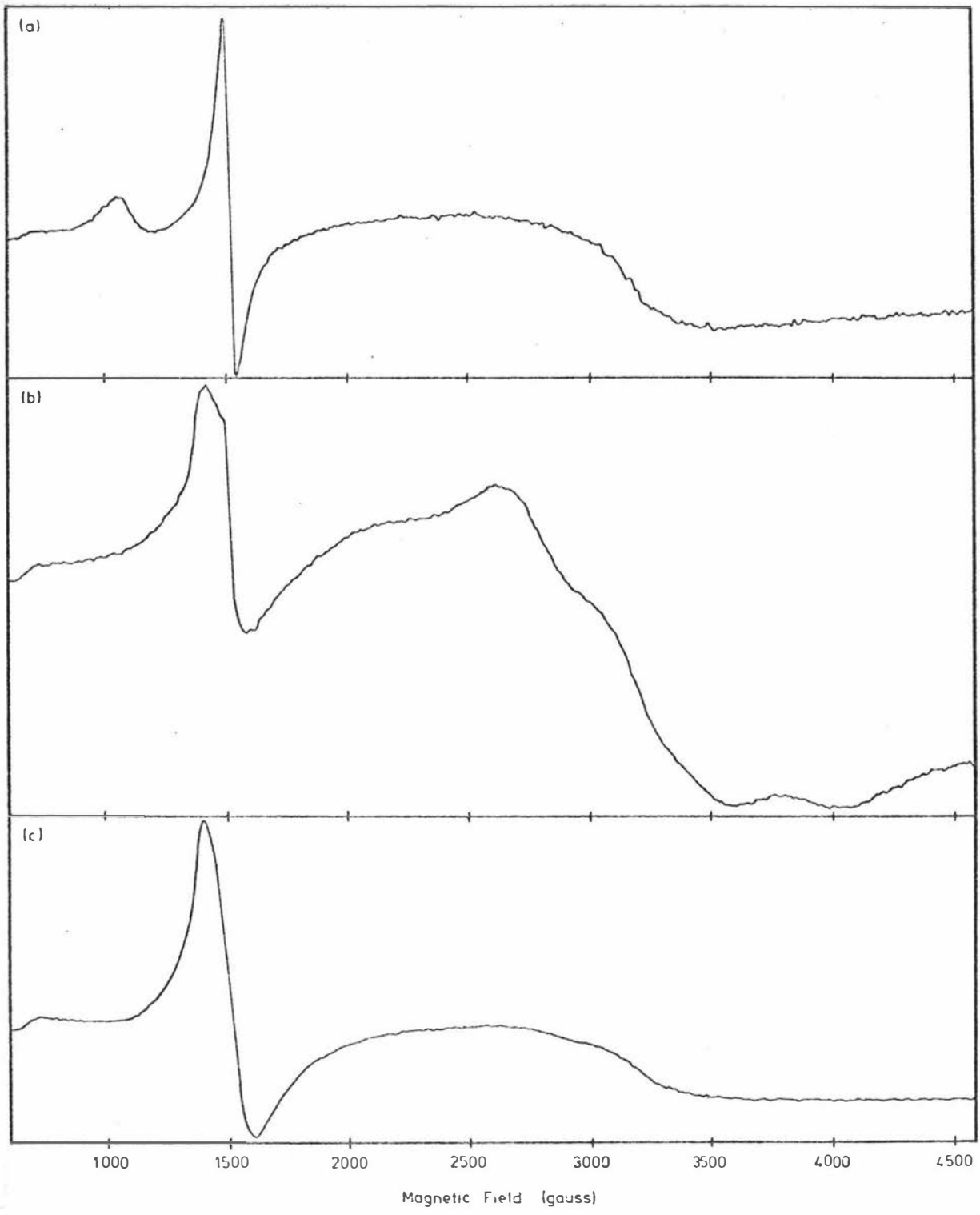

Figure 2.6 E.S.R. spectra at -160°C in MeOH of (a) a 1:1 solution of $Fe(ClO_4)_3$ and VIII, (b) a 1:1:1 solution of $Fe(ClO_4)_3$, VIII and imidazole and (c) excess imidazole added to (b).

ligands are reduced the resulting complexes $[Fe(VIIb)]PF_6$ and $[Fe(VIId)]PF_6$ resemble that of high spin ferric ion in a tetragonal environment, the presence of a $g = 4.3$ signal indicating some rhombic character.

Significant changes are noted in the e.s.r. spectrum of a 1:1 mixture of Fe^{III} and VIII (Table 2.4, Figure 2.6) when a 1 molar equivalent of imidazole is added and further changes are noted in the presence of excess imidazole. Considered together these spectral changes would support the idea that two imidazole groups are bound by $[Fe(VIII)]^+$.

2.3.5 MÖSSBAUER SPECTRA

Mössbauer spectroscopy is the study of recoilless nuclear resonant absorption of fluorescence. An atom in an excited state can decay to the ground state by the emission of a photon. This photon can then be absorbed by a second atom of the same kind of electronic excitation. Subsequent deexcitation re-emits the photon but not necessarily in the initial direction so that scattering or resonant fluorescence occurs. Theoretically one would expect to observe this phenomenon in the gas phase but, because of such effects as nuclear recoil and doppler broadening, it is only found in the solid state.

Mössbauer spectroscopy provides a means of measuring some of the comparatively weak interactions between the nucleus and the surrounding electrons. The isomer shift (δ_{Fe}) can give information on the oxidation state of the metal, a value of +0.5mm/sec is consistent with ionic iron(III) in the high spin state and this decreases with increasing covalency of the bonding. Hence Fe_2Tf, with δ_{Fe} = +0.38mm/sec (129) shows much more covalent character than bicarbonate-free iron-transferrin where δ_{Fe} = +0.47mm/sec (130). The closeness of this latter value to those of ferric hydroxide gels and ferric albumin suggests that this iron is non specifically bound to transferrin.

Complexes of iron with Ib, Ic and II (Table 2.5 and Figure 2.7) have isomer shifts close to +0.5mm/sec indicating the very ionic nature of the ligand-metal bonding in these systems. In contrast complexes of iron

Table 2.5 MÖSSBAUER SPECTRAL DATA OF SMALL MOLECULAR WEIGHT FERRIC ION COMPLEXES

Compound		[a] δ_{Fe} (mm/sec)	ΔEq (mm/sec)
[b] Fe_2Tf		0.38	0.75
[c] HCO_3^- - Free Fe-Tf		0.47	0.72
[c] Ferric Hydroxide Gel		0.46	0.75
[c] Fe^{3+} - Albumin		0.47	0.74
[d] $[Fe(Ia)_3]6H_2O$	(1)	0.411	0.923
	(2)	0.024	-
[d] $[Fe(Ib)_3]4\frac{1}{2}H_2O$		0.499	1.007
[d] $[Fe(Ic)_3]1\frac{1}{2}H_2O$	(1)	0.485	0.685
	(2)	0.017	-
$[Fe(II)_3]$	(1)	0.526	0.565
	(2)	-0.043	-
$[Fe(IIIa)_3]1\frac{1}{2}H_2O$		0.380	0.722
$[Fe(IIIa)_2(MeOH)_2]NO_3.2H_2O$		0.410	1.049
$[Fe(IIIb)_3]4H_2O$		0.392	0.760
$[Fe(IV)_3]1\frac{1}{2}H_2O$		0.335	1.208
$Na[Fe(Va)]4H_2O$		0.371	0.770
$K[Fe(Vb)]2H_2O$		0.383	0.746

a. With respect to soft iron (room temperature spectra).
b. Reference (129).
c. Reference (130).
d. Previously reported in Reference (120).

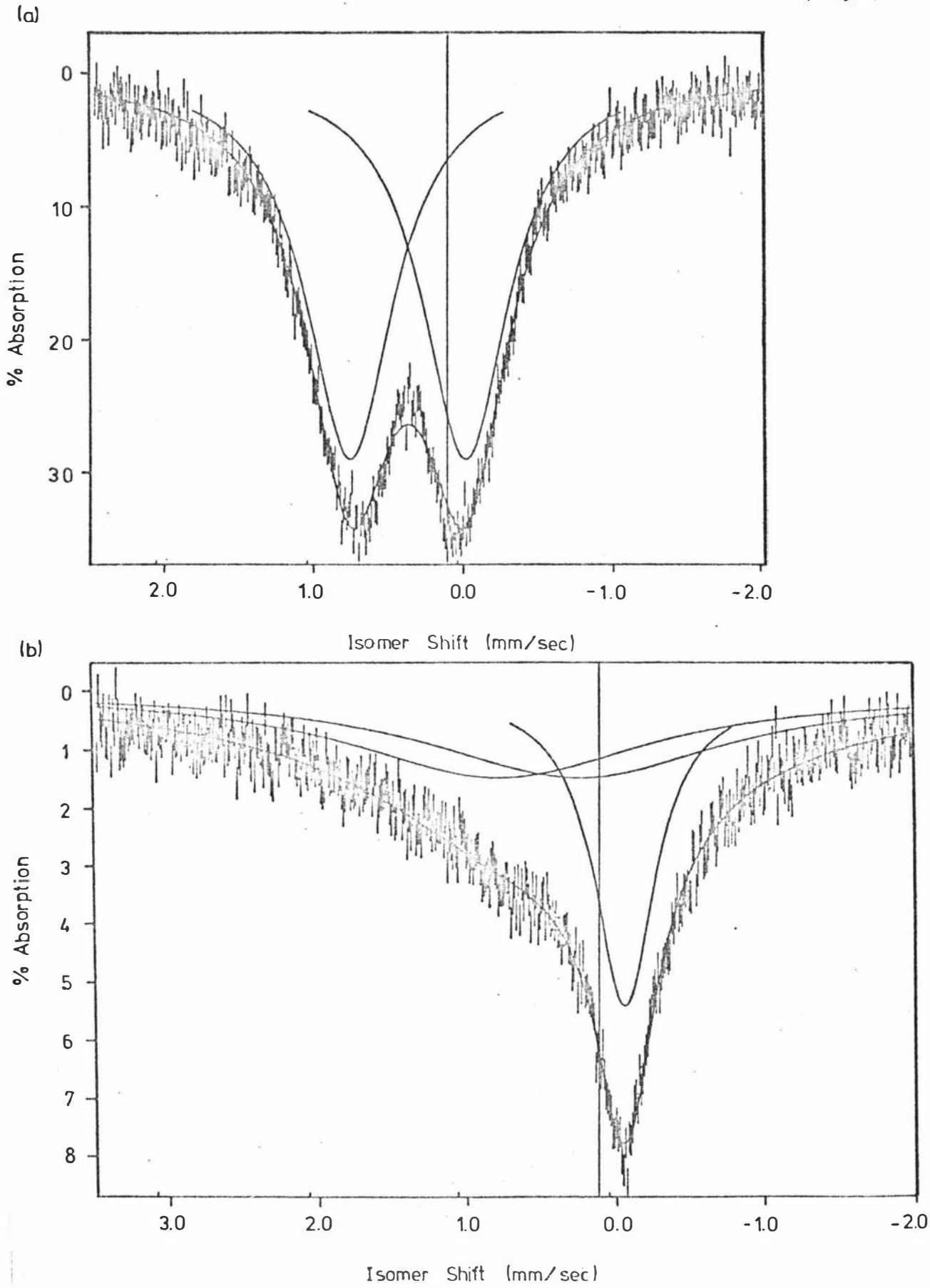

Figure 2.7 Room temperature Mössbauer spectra of (a) $Na[Fe(Va)]4H_2O$ and (b) $[Fe(II)_3]$. The solid line represents the computer fitted spectrum. The actual absorption of the sample across the resonant region at each velocity is represented by an error bar.

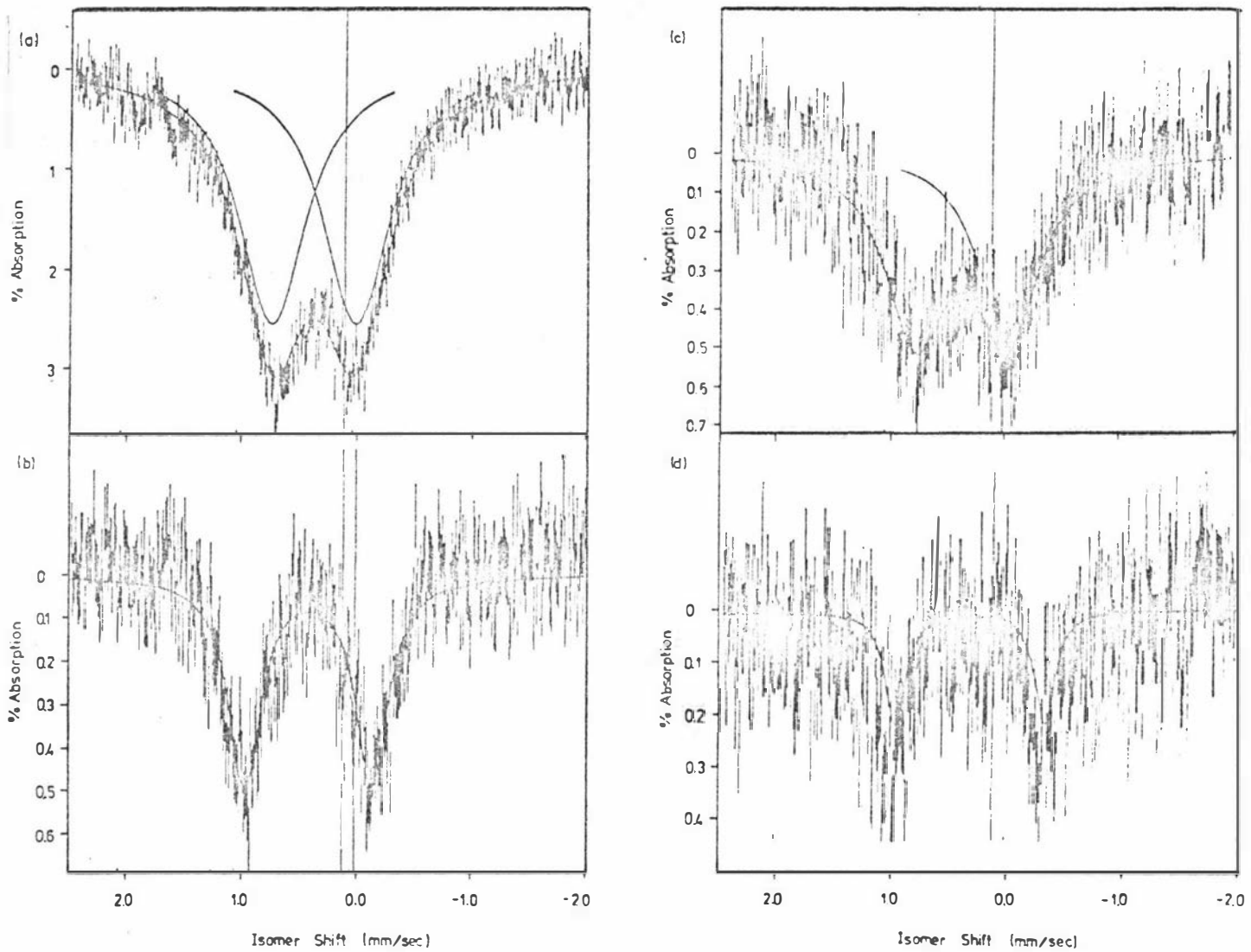

Figure 2.8 Room temperature Mössbauer spectra of (a) $[Fe(IIIa)_3]1\frac{1}{2}H_2O$, (b) $[Fe(IIIa)_2(MeOH)_2]NO_3.2H_2O$, (c) $[Fe(IIIb)_3]4H_2O$ and (d) $[Fe(IV)_3]1\frac{1}{2}H_2O$. The solid line represents the computer fitted spectrum. The actual absorption of the sample across the resonant region at each velocity is represented by an error bar.

with Ia, IIIa, IIIb, Va and Vb all have isomer shifts in the range 0.37 - 0.41 suggesting more covalency in their bonding. There is a significant increase in the isomer shift between $[Fe(IIIa)_3]$ and $[Fe(IIIa)_2(MeOH)_2]NO_3.2H_2O$ (Table 2.5 and Figure 2.8) suggesting a trend towards more ionic character in the bonds with a decrease in the number of bidentate ligands coordinated. The low isomer shift of $[Fe(IV)_3]1\frac{1}{2}H_2O$ coupled with its low magnetic susceptibility would suggest that a mixture of high spin and low spin iron(III) is present in this complex. All of the complexes including those of the protein have large quadrupole splittings, a reflection of the unsymmetric field around the ferric ion. Particularly large quadrupole splittings can be observed with $[Fe(Ib)_3]4\frac{1}{2}H_2O$, $[Fe(IV)_3]1\frac{1}{2}H_2O$ and $[Fe(IIIa)_2(MeOH)_2]NO_3.2H_2O$, in the case of the latter the asymmetry around the ferric ion has been verified by single crystal x-ray structural analysis (Section 2.2.2). The complexes of $[Fe(Ia)_3]6H_2O$, $[Fe(Ic)_3]1\frac{1}{2}H_2O$ and $[Fe(II)_3]$ all show a distinct asymmetry in their absorption peaks which can be attributed to either spin-lattice relaxation effects (120) or to iron-binding in two distinguishable sites in the crystal lattice, where these two sites could be <u>cis</u> or <u>trans</u>, or <u>mer</u> or <u>fac</u> isomers (131).

2.4 Conclusion

The ligands used in this study were selected to cover all types of complexes from FeO_6 to $FeO_2N_2O_2^1$. The study shows the dangers of drawing conclusions from isolated examples and the difficulties in interpretation that arise when a variety of ligand systems such as these are selected. For instance the charge transfer bands of the complexes involving hydroxamic acids are very close in energy to that of Fe_2Lf and Fe_2Tf. However catecholato and hydroxamato ligands do not occur in Fe_2Lf, though they occur in microbial iron-transport compounds. Hence a close fit between the spectral parameters of Fe_2Lf or Fe_2Tf and the model system is not necessarily proof that the type and number of donor atoms is similar.

From the series of complexes prepared from the ligand IIIa it is evident that the energy of the charge transfer

band increases with increasing number of phenolates bound, while binding imidazole also causes a significant increase. Taking the complex $[Fe(4\text{-methylphenolato})(EtOH)_5]^{2+}$ (absorbing at 16400cm^{-1} or 610nm) (126) as a base point it should be possible to calculate the range of values expected for λ_{max} given knowledge of the groups involved in the binding site of transferrin or lactoferrin. Each phenolate bound to the ferric ion causes a shift of about 2000cm^{-1}, towards higher energy, of the charge transfer band, while each imidazole causes a shift of about 1000 - 2000cm^{-1} (depending on whether the phenolates are cis or trans). Thus if the binding site of lactoferrin contains two imidazoles and two phenolates then the charge transfer band would be expected to lie between 19400 - 20400cm^{-1} or 490 - 515nm. If it contains two imidazoles and three phenolates then the charge transfer band would be expected to lie between 21400 - 22400cm^{-1} or 445 - 470nm. Considering that the chelate effect would tend to lower these values by about 10 - 20nm then the absorbance maxima of most of the small molecular weight complexes would fit in with these calculated ranges (Table 2.3). The complexes $Na[Fe(Va)]4H_2O$ and $K[Fe(Vb)]2H_2O$ would appear to be exceptions to this rule, though in this case the carboxylate groups of Va and Vb may have a significant effect on the position of the band. Thus the position of λ_{max} around 470nm for Fe_2Lf and Fe_2Tf would suggest that three, not two, tyrosyl residues and two histidyl residues are likely to be binding to the ferric ion in the specific sites.

From the single crystal x-ray structure of $[Fe(IIIa)_2(MeOH)_2]NO_3.MeOH$ it is evident that the nitrate group is not directly coordinated to the iron atom but interacts with it via a hydrogen bonding system involving the bound and occluded methanol molecules. Nitrate is isoelectronic and isostructural with bicarbonate hence the bicarbonate ion, essential for binding iron in the specific site of lactoferrin, also may not be bound to the metal atom but interacts via the solvent water molecules.

While many complexes have e.s.r. spectra characteristic of Fe^{III} in a rhombic environment the signal at

$g = 4.3$ occupies a very narrow range of values and does not appear to be sensitive to the ligand environment. Mössbauer spectroscopy appears to be more sensitive to the ligand environment than e.s.r. particularly to the degree of covalency of the binding in the complex. Of all of the complexes considered $[Fe(IIIa)_2]1\frac{1}{2}H_2O$ and $Na[Fe(Va)]4H_2O$ have Mössbauer parameters closest to Fe_2Tf. As these two are of the FeO_3N_3 and $FeO_2N_2O_2^1$ types respectively it would appear that Mössbauer spectra are not sensitive to major changes in ligating donor atoms.

In conclusion the evidence presented in this study would favour the ferric ion in lactoferrin and transferrin occupying a site of rhombic symmetry and bound to three tyrosyl and two cis histidyl residues, while the bicarbonate ion is not directly bound but interacts via a solvent (water) molecule.

Chapter 3 SMALL MOLECULE COMPLEXES OF COPPER AND MANGANESE

3.1 Introduction

In addition to binding two ferric ions per protein, apolactoferrin has been shown to bind two copper(II) ions. Ultraviolet difference spectral studies on the related transferrin (55) and ovotransferrin (81) have indicated that one tyrosyl group is bound to copper, while e.s.r. spectral studies on all three proteins have suggested one histidyl residue is involved at physiological pH. Furthermore bicarbonate is required before the typical yellow colour of the complexes develops. Considering that two histidines and two or three tyrosyls are felt to be involved when iron is bound to these proteins it is possible to see the uncertainties that exist about the number and nature of all groups bound to copper as well as its precise stereochemistry.

Whereas iron(III) complexes readily with phenol and substituted phenols to give red or purple solutions copper(II) normally interacts to give oxidatively coupled products in which copper(II)-phenolate is an intermediate. After the completion of this study unsubstituted diphenoxo copper complexes (with ethylenediamine and bipyridyl) were isolated though they are extremely sensitive to moisture (132). In the case of phenol or phenols with activating substituents (such as methyl) two major coupling reactions can occur, depending on the side chain position. When these are located on the para positions ortho-ortho coupling can occur and, conversely, when substituents are located on the ortho position para-para coupling can occur, followed by rearrangement to form diphenoquinones (133). However when the substituents are deactivating (such as $-NO_2$ or -Cl) relatively stable copper phenolates can be isolated (134, 135, 136, 137, 138). In this study new complexes of copper with a variety of nitrogen donor ligands (Figure 3.1) and 2,3,4,5,6-pentachlorophenol or 2,4,6-tribromophenol have been prepared to investigate the copper-phenolate interaction by spectroscopic methods.

Figure 3.1 Nomenclature and structures of the ligands complexed with copper(II)

2,4,6-Tribromophenolato (tbp)

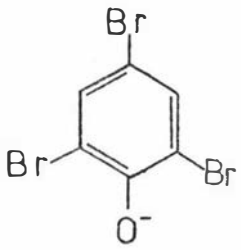

2,3,4,5,6-Pentachlorophenolato (pcp)

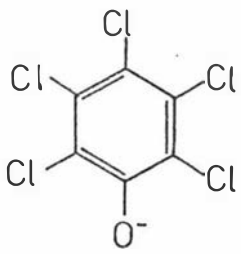

2,4,6-Trichlorophenol (tcp)

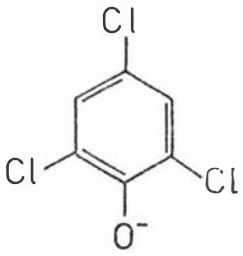

2,4,6-Trimethylpyridine (collidine)

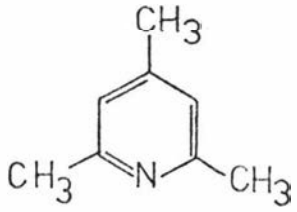

Pyridine (py)

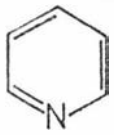

Imidazole (im)

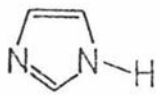

NN'-dimethylformamide (dmf)

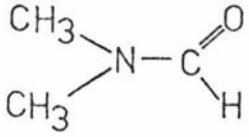

2,9-Dimethyl-1,10-phenanthroline (dmp)

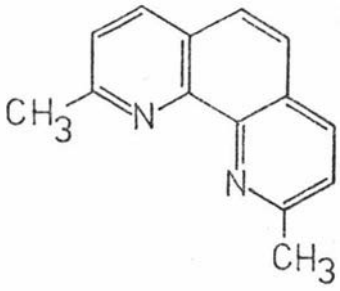

1,4,8,11-Tetraazocyclotetradecane (cyclam)

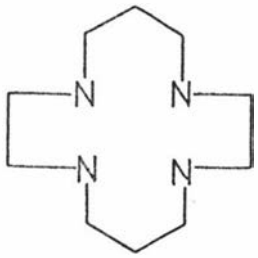

Ethylenediamine (en)

$NH_2CH_2CH_2NH_2$

N,N,N',N'-Tetramethyl-ethylenediamine (TMED)

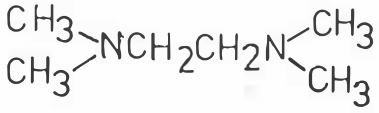

A preliminary investigation was undertaken into the interaction of manganese with tyrosyl-type groups. A complex of manganese with $SALENH_4$ was prepared and its electronic and e.s.r. spectra were examined ($SALENH_4$ is compound VIII in Figure 2.1).

3.2 Experimental

3.2.1 SOURCES OF CHEMICALS AND INSTRUMENTATION

Cupric acetate was obtained from May and Baker Ltd, 2,4,6-tribromophenol and dimethylformamide from Koch-Light laboratories Ltd, 2,3,4,5,6-pentachlorophenol from Fluka A. G. and all the nitrogen bases were obtained from Aldrich, with the exception of imidazole which came from BDH Laboratories and cyclam which came from Strem Chemicals Ltd.

The instrumentation employed in this study has been described in Chapter 2, section 2.2.3.

3.2.2. PREPARATION OF COMPLEXES

A similar method of preparation was followed for all of the complexes considered in this study. Two mmoles of 2,4,6-tribromophenol or 2,3,4,5,6-pentachlorophenol were dissolved by warming in water containing two mmoles of NaOH. To the cooled solution was slowly added an aqueous solution containing two mmoles of cupric acetate and either 1mmole of base (where the base was en, TMED, dmp or cyclam) or 2mmoles of base (where the base was en, py or im). The resulting precipitate was filtered, thoroughly washed with water and air dried. The compounds were re-crystallized by dissolving in EtOH (with the exception of $[Cu(tbp)_2(en)_2]$ and $[Cu(pcp)_2(en)_2]$ which were insoluble in this solvent) and upon reduction in volume on a rotary evaporator were precipitated by water. $[Cu(pcp)_2(collidine)]$ was isolated when either 1 or 2 mmoles of collidine per mole of copper were used and in this case the solvent was methanol. $[Cu(pcp)_2]$ was isolated as a solid from water when no base was added. It was not recrystallized. When it was dissolved in dmf the brown complex $[Cu(pcp)_2(dmf)]$ precipitated shortly afterwards. Yields in all cases were approximately 70%. Conductivities indicated that the

complexes were all non electrolytes in solution with the exception of $[Cu(pcp)_2(Cyclam)]$ which shows signs of partial dissociation (Table 3.2). Analytical data for the compounds is given in Table 3.1.

3.3 Results and Discussion

3.3.1 PREPARATION, STRUCTURE AND STABILITY OF THE COMPLEXES

Complexes of the type $[Cu(pcp)_2]$ and $[Cu\ X_2\ L_n]$ (where X = pcp or tbp, L = en, TMED, cyclam or dmp when n = 1 and L = en, py or im when n = 2) were obtained as described in section 3.2.2 (Table 3.1). In the presence of excess dmf or collidine complexes of the type $[Cu(pcp)_2(dmf)]$ or $[Cu(pcp)_2(collidine)]$ were isolated, presumably the steric requirements of the ligands and metal prevent formation of $[Cu(pcp)_2(base)_2]$. All of the complexes proved to be readily soluble in EtOH or benzene when first prepared, with the exception of $[Cu(tbp)_2(im)_2]$. Over a period of six months most complexes appeared to become less soluble in these solvents, for instance $[Cu(pcp)_2(py)_2]$ was almost completely insoluble in EtOH, suggesting that some dimerisation or polymerisation in these complexes has occurred. $[Cu(tbp)_2(im)_2]$, $[Cu(pcp)_2]$, $[Cu(pcp)_2(dmf)]$ and $[Cu(pcp)_2(collidine)]$ all have magnetic susceptibilities lower than generally found for copper(II) (1.70 - 1.91BM) suggesting structures containing at least binuclear copper(II) with bridging phenolate groups (Table 3.2). The molecular weight of $[Cu(tbp)_2(py)_2]$ was determined to be 794 Daltons (theoretical value of 818 Daltons) while those of $[Cu(tbp)_2(en)]$ and $[Cu(tbp)_2(TMED)]$ were 1068 Daltons (theoretical value of 783 Daltons) and 1188 Daltons (theoretical value of 839 Daltons) respectively. The higher-than-expected molecular weights of the latter two complexes is probably related to the slow decomposition observed to occur while the measurements were made.

The complexes $[Cu(tcp)_2(im)_2]$ (134) and $[Cu(MNOP)_2(py)_2]$ (where MNOP = 2-methoxy-4-nitrophenolato) (135, 136) have been examined crystallographically previously. In both complexes the phenolate and tertiary nitrogen linkages

Table 3.1 COLOURS AND ANALYTICAL DATA FOR THE COPPER PHENOLATE COMPLEXES

Compound	Colour	Found (%)			Calculated (%)		
		C	H	N	C	H	N
$[Cu(tbp)_2(en)]$	Brown	21.9	1.9	3.0	21.5	1.5	3.6
$[Cu(tbp)_2(en)_2]$	Pink	22.3	2.2	6.7	22.8	2.4	6.6
$[Cu(tbp)_2(TMED)]$	Red	26.1	2.5	3.0	25.8	2.4	3.3
$[Cu(tbp)_2(dmp)]\frac{1}{2}H_2O$	Purple	34.5	1.8	2.8	33.1	1.8	3.0
$[Cu(tbp)_2(py)_2]$	Brown	29.4	1.7	3.0	30.0	1.6	3.2
$[Cu(tbp)_2(im)_2]$	Brown	25.6	1.9	5.5	25.2	1.4	6.5
$[Cu(pcp)_2]$	Red-purple	25.2	0.0	-	24.2	0.0	-
$[Cu(pcp)_2(en)]$	Brown	25.6	1.4	4.0	25.6	1.2	4.3
$[Cu(pcp)_2(en)_2]$	Pale orange	27.6	2.1	7.7	26.8	2.2	7.8
$[Cu(pcp)_2(dmp)]$	Purple	40.2	1.7	3.5	39.2	1.5	3.5
$[Cu(pcp)_2(py)_2]$	Brown	35.5	1.4	3.5	35.0	1.3	3.7
$[Cu(cyclam)(pcp)_2]$	Pale purple	33.3	3.2	7.0	33.3	3.0	7.1
$[Cu(pcp)_2(collidine)]$	Brown	35.5	2.0	2.3	35.3	2.0	1.9
$[Cu(pcp)_2(dmf)]$	Brown	27.9	1.1	1.8	26.9	1.1	2.1

Table 3.2 CONDUCTIVITIES AND MAGNETIC MOMENTS FOR THE COPPER PHENOLATE COMPLEXES

Compound	Λ_M (Ω^{-1}mole^{-1}cm^2) Λ_M	Solvent	μeff (BM)
$[Cu(tbp)_2(en)]$	5.27	EtOH	1.76
$[Cu(tbp)_2(en)_2]$	-	-	1.71
$[Cu(tbp)_2(TMED)]$	0.76	Acetone	1.70
$[Cu(tbp)_2(dmp)]\frac{1}{2}H_2O$	-	-	1.65
$[Cu(tbp)_2(py)_2]$	0.85	EtOH	1.80
$[Cu(tbp)_2(im)_2]$	-	-	1.35
$[Cu(pcp)_2]$	1.99	EtOH	1.38
$[Cu(pcp)_2(en)]$	6.11	EtOH	1.71
$[Cu(pcp)_2(en)_2]$	-	-	1.77
$[Cu(pcp)_2(dmp)]$	23	EtOH	1.76
$[Cu(pcp)_2(py)_2]$	1.44	EtOH	1.91
$[Cu(cyclam)(pcp)_2]$	84.6	dmf	1.63
$[Cu(pcp)_2(collidine)]$	3.48	EtOH	1.11
$[Cu(pcp)_2(dmf)]$	-	-	1.30

form an almost regular square plane with a trans con -

$[Cu(tcp)_2(im)_2]$

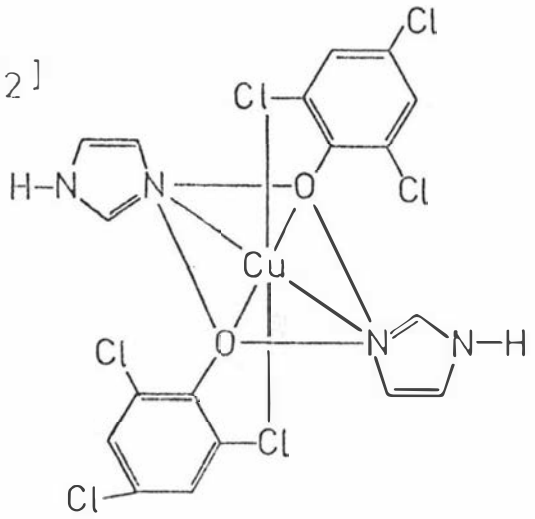

figuration. A tetragonal coordination being completed by the axial chlorines and phenolic-methoxyl oxygens respectively which are in an off Z-axis position and are at a greater distance from the copper than the other coordinating ions. A single crystal x-ray structure determination on $[Cu(MNOP)_2(TMED)]$ (137) shows a cis arranged structure with an almost regular square plane of phenolates and TMED nitrogens, though involvement of the methoxyl oxygens results in a tetragonal structure, somewhat similar to $[Cu(tcp)_2(im)_2]$ and $[Cu(MNOP)_2(py)_2]$. The single crystal x-ray structure of $[Cu(tcp)_2(TMED)]$ (138) shows longer Cu-Cl bonds than observed in $[Cu(tcp)_2(im)_2]$ and appears to have a distorted square-planar stereochemistry, a cis configuration being imposed by the ligand. By comparison then all compounds of the type $[Cu(tbp)_2X_2]$ (X = pyridine,

$[Cu(tcp)_2(TMED)]$

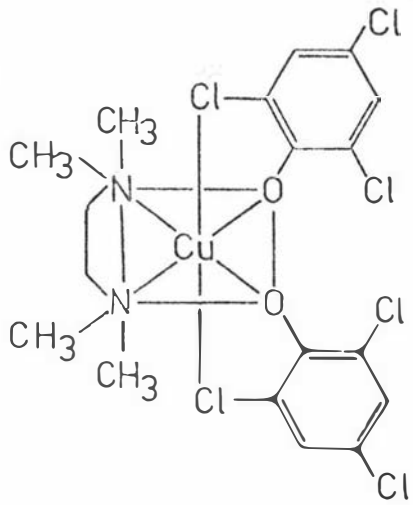

imidazole) are considered to have a trans arrangement while compounds of the type $[Cu(pcp)_2Y]$ (Y = ethylenediamine, dmp,

TMED) are considered to be cis.

An attempt was made to prepare $[Cu(tbp)_2(collidine)]$ following the method for the analogous pcp complex. In the initial stage a white precipitate appeared which had a melting point of 205°C. Mass spectrometry indicated that the highest molecular weight species in this precipitate is tribromophenol (MP = 95°C). Hence it seems likely that this compound is polymeric but it breaks down in the mass spectrometer. Once production of this had ceased it was possible to isolate some brown precipitate which analytical data suggested was impure $[Cu(tbp)_2(collidine)]$. The complex proved to be stable for indefinite periods at high concentration in acetone but on dilution rapidly broke down to give a precipitate which from mass spectrometry was shown to contain collidine hydrobromide. In contrast $[Cu(pcp)_2(collidine)]$ is stable in both polar and non-polar solvents. Similarly $[Cu(tbp)_2(dmp)]\frac{1}{2}H_2O$ is less stable than $[Cu(pcp)_2(dmp)]$; in a range of polar and non-polar solvents the former compound rapidly changed colour from the purple of the crystals to yellow and some white precipitate appeared. $[Cu(pcp)_2(dmp)]$ when dissolved in polar solvents exhibited this colour change only.

While the complexes of in this study are stable, under certain conditions polymerisation reactions of the phenol can occur. When $Cu(ClO_4)_2 6H_2O$ is reacted with tbp in acetonitrile, which raises the redox potential of the copper, an organic compound with a melting point of 214°C results. The compound breaks down when subject to analysis by mass spectrometry the major product being tbp with traces of a pentabromophenol. However, it appears likely that it is a polyether of the type;

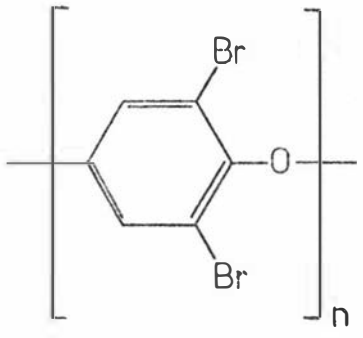

similar to that found when pcp is reacted under the same conditions (139).

3.3.2 INFRARED SPECTRA

Infrared spectra are consistent for the formulations proposed in Table 3.1. In all cases no phenolic -OH stretching frequencies in the region 3300 - 3500cm^{-1} are observed and water appears to be absent in all compounds except $[Cu(tbp)_2(dmp)]\frac{1}{2}H_2O$. Complexes of tbp show absorptions in the region 1240 - 50cm^{-1} while complexes of pcp have absorptions around 1210 - 20cm^{-1}. These can be attributed to the C-O stretching vibration of an oxygen-bonded, coordinated, phenoxide group (132). The complexes involving ethylene diamine all show the symmetric NH_2 stretch at 3360cm^{-1}, the antisymmetric stretch at 3100cm^{-1} and the NH_2 bend at 1585cm^{-1}. Bands due to NH stretching are also exhibited by $[Cu(tbp)_2(im)_2]$ at 3140cm^{-1} and $[Cu(pcp)_2(cyclam)]$ at 3380cm^{-1}. The presence of oxygen coordinated dmf in the complex $[Cu(pcp)_2(dmf)]$ is demonstrated by the C=O stretching frequency at 1640cm^{-1} (cf 1670cm^{-1} for free dmf).

3.3.3 ELECTRONIC SPECTRA

The electronic spectra are characterised by an intense absorption band around 430 - 500nm (Extinction of ~1200l mol^{-1}cm^{-1}) which gives the complexes their characteristic yellow or brown colours. This band is affected by the dielectric constant of the solvent and shifts to lower energy in benzene, which is less polar (i.e. lower dielectric constant) than EtOH. Such a trend has also been observed in some 2,2^1-bipyridyl palladium(II) and platinum(II) complexes (140).

There has been some discussion over the assignment of this band. Gaber et.al. (40) have assigned it to a phenolate-to-copper charge transition but the band was assigned by Harrod (141) to a copper-to-phenolate charge transfer transition. Harrod proposed that the promotion of electrons occurred mainly from the $d\sigma^*$ orbitals though on the basis of overlap considerations Bosnich et.al. (142) maintained that the major source of its intensity is

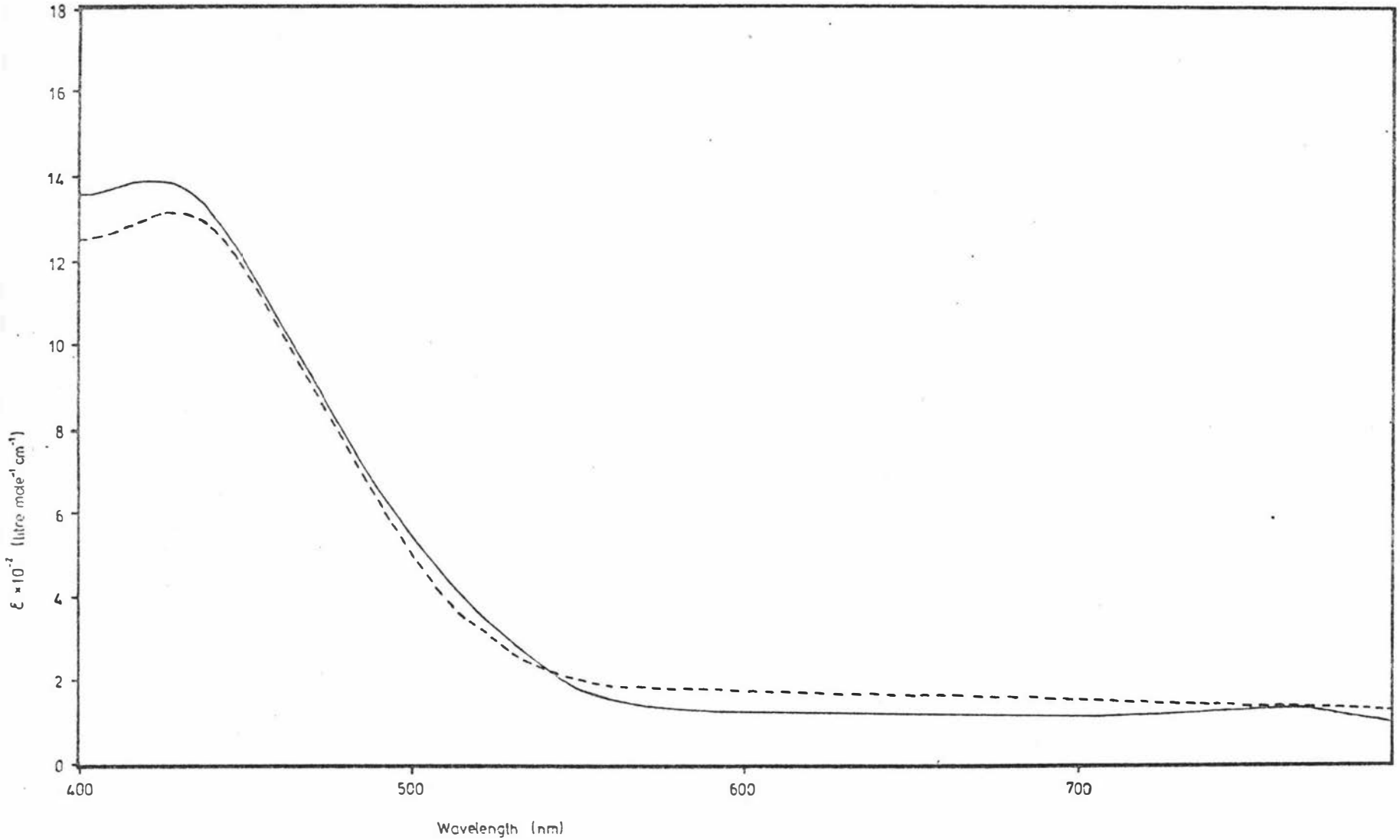

Figure 3.2 Visible absorption spectra of $[Cu(tbp)_2(en)]$ (- -) and $[Cu(tbp)_2(py)_2]$ (——) in ethanol.

Table 3.3 DIFFUSE REFLECTANCE SPECTRA OF THE COPPER PHENOLATE COMPLEXES

Compound	λ_{max} (nm)	Proposed Structure
[a] $[Cu(tcp)_2(im)_2]$	430, ~710	Tetragonal
[b] $[Cu(MMOP)_2(py)_2]$	461, 758	Greater tetragonal distortion along z axis than $[Cu(FOMP)_2(py)_2]$
[b,c] $[Cu(FOMP)_2(py)_2]$	476, 610, 800	Tetragonal
[b] $[Cu(tcp)_2(TMED)]$	487, 735	Small tetragonal interaction (square plane)
[b] $[Cu(MMOP)_2(TMED)]$	472, 541, 719	Tetragonal
$[Cu(tbp)_2(en)]$	475(vb), ~725(sh)	Tetragonal
$[Cu(tbp)_2(en)_2]$	327,480	Planar
$[Cu(tbp)_2(TMED)]$	510(vb), ~ 720(sh)	Tetragonal
$[Cu(tbp)_2(dmp)]\frac{1}{2}H_2O$	567, ≈(800)[d]	Distorted tetrahedral
$[Cu(tbp)_2(py)_2]$	490(vb), 640(sh), 760(sh)	Tetragonal
$[Cu(pcp)_2]$	530(vb)	Tetragonal
$[Cu(pcp)_2(en)]$	470, 705	Tetragonal
$[Cu(pcp)_2(en)_2]$	319, 473	Planar
$[Cu(pcp)_2(dmp)]$	590(vb), ≈800, ≈1000	Distorted tetrahedral
$[Cu(pcp)_2(py)_2]$	457, 790	Tetragonal
$[Cu(cyclam)(pcp)_2]$	326,540	Planar
$[Cu(pcp)_2(collidine)]$	485, 790	Tetragonal
$[Cu(pcp)_2(dmf)]$	485, 820	Tetragonal

Note: sh = shoulder, vb = very broad

a. Reference (64) structure determined by x-ray crystallography

b. Reference (135) structure determined by x-ray crystallography

c. FOMP = 4-formyl-2-methoxyphenolato

d. Band tails into near i.r.

Table 3.4 ELECTRONIC SOLUTION SPECTRA OF THE COPPER PHENOLATE COMPLEXES

Compound	CT and d-d Absorptions	Other Bands	Solvent
$[Cu(tbp)_2(en)]$	428(1290),640(sh)	294(sh), 302(8660), 316(sh)	EtOH
	447, 680(sh)	-	C_6H_6
$[Cu(tbp)_2(TMED)]$	492	296	EtOH
	484(2610), ≈750	-	Acetone
	507	-	C_6H_6
$[Cu(tbp)_2(py)_2]$	423(1370), 755(185)(br)	293(sh), 302(8950), 320(sh)	EtOH
	462, 770(br)	-	C_6H_6
$[Cu(tbp)_2(im)_2]$	447, 743(br)	-	Acetone
$[Cu(tbp)_2(collidine)]$	725	-	Acetone
$[Cu(pcp)_2]$	483	-	CH_3NO_2
	436(1080), 700(sh)	295(sh), 306(7650), 322(sh)	EtOH
$[Cu(pcp)_2(en)]$	442(1270), 640(sh)	309(7610), 321(sh)	EtOH
$[Cu(pcp)_2(dmp)]$	567, 800(sh), 1000(sh)	-	CH_2Cl_2
$[Cu(pcp)_2(py)_2]$	440(1230), 760(130)(br)	296(sh), 306(7765), 322(sh)	EtOH
	467, 765(br)	-	C_6H_6
$[Cu(cyclam)(pcp)_2]$	518	325	MeOH
	526(77.6)	-	DMF
$[Cu(pcp)_2(collidine)]$	434(1210, 725(sh)	300(sh), 307(8010), 322(sh)	EtOH
[a] $[Cu(SALENH_4)]$	392	-	MeOH

Note: sh = shoulder, br = broad, extinction coefficient in brackets in $l mole^{-1} cm^{-1}$)

a. Reference (142)

promotion of an electron from the $d\pi^*$ orbitals (in particular the d_{xz} and d_{yz} orbitals). Depending on the extent of distortion, it is proposed (142) that the $d\pi^* \rightarrow p\pi^*$ phenolate transition could be observed as a weaker band at lower energies, around 1300nm. Results from this study would favour the latter assignment of Bosnich et.al. (142) and Harrod (141) of a copper-to-phenolate charge transfer transition.

In the case of the substituted phenolates under consideration pcp is more electronegative than tbp. Thus copper-to-phenolate transitions would be expected to occur more readily with complexes of pcp (than with the analogous complexes of tbp). Hence they would be expected to absorb at lower energy (143). This has been observed to occur for $[Cu(tbp)_2 L_n]$ and $[Cu(pcp)_2 L_n]$ (where when n = 2, L = py and where n = 1, L = dmp or en)(Table 3.3 & 3.4). Complexes of copper with unsubstituted phenolates would be expected to absorb at higher energy than complexes of pcp or tbp. Such is the case with the complex of $SALENH_4$ where the charge transfer transition is observed at 392nm (142) in methanol. No great change in λ_{max} of $[Cu(SALENH_4)]$ is observed when the solvent is pyridine, suggesting that the axial nitrogens have little effect. Substitution of a nitrogen base, such as en, for one more basic, such as TMED, should increase the electron density on copper. This would promote electron movement from the copper to phenolate and would also lead to a shift of the charge transfer band to lower energy. Such a shift has been observed to occur for $[Cu(tbp)_2(en)]$ and $[Cu(tbp)_2(TMED)]$ (Table 3.3 and 3.4).

Increasing the number of phenolates donating charge to the central metal atom can be expected to destabilise the metal orbitals. Hence the metal-to-phenolate charge transfer band will increase in energy as the coordination number is decreased (143). Studies of potential mono-phenolate copper systems indicate that this is the case. The complex N-n-propyl-5-nitro-salicylaldiminato-copper(II) has been isolated and shown from a single crystal x-ray structure determination to be dimeric with terminal phenolic OH groups (144);

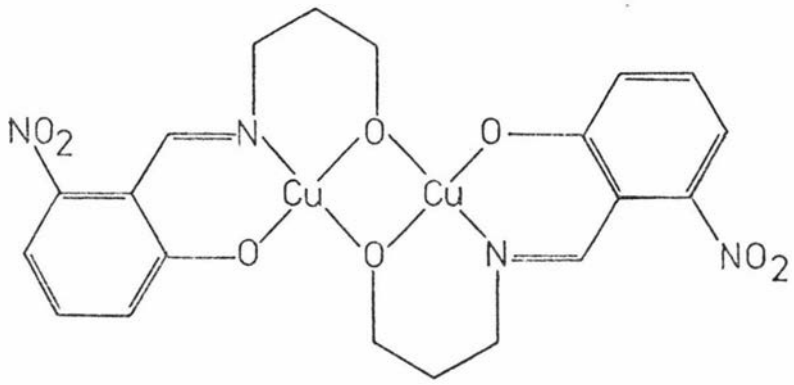

The electronic spectrum of this complex (in which only one phenolic OH group is bound to copper) has a d-d band at 566nm but there is no charge transfer band in the region above 400nm(145). The complex N-salicylidene-glycinato-aquo-copper(II) has also been prepared and is thought to be coordinated in the following manner (146);

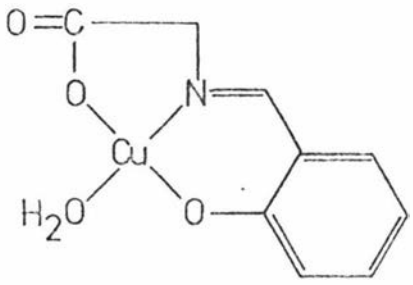

However signals at $g = 4$ as well as $g = 2$ in its e.s.r. spectrum indicate some dimeric character of the complex in solution (147) which, by analogy with the previous compound, would be expected to have terminal phenolic OH groups. This complex has a d-d band at 690nm and an intense band at 357nm the intensity of which could be partly attributed to a copper-to-phenolate charge transfer interaction.

Complexes of known tetragonal symmetry such as $[Cu(tcp)_2(im)_2]$ and $[Cu(MNOP)_2(py)_2]$ (135) have a single d-d band in the diffuse reflectance spectrum near 770nm and sometimes a poorly resolved band can be observed at higher energy. These can often be obscured when the charge transfer band is broad. For some complexes where the mean axial distance is

shorter, as in $[Cu(FOMP)_2(py)_2]$ this shoulder appears as a distinct band. The majority of the complexes and Cu_2Lf show evidence of tetragonal symmetry (having axial positions occupied by Cl or Br) in both the powder and in solution (Table 3.3 and 3.4). For instance $[Cu(tbp)_2(py)_2]$ has two shoulders in its diffuse reflectance spectrum at 640 and 760nm and a discrete band at 770nm in benzene or 755nm in EtOH. The d-d bands of bidentate ligands occur at higher energy than those of monodentate ligands, an indication of the stronger ligand field of the former.

Two bands are present in the diffuse reflectance spectra of $[Cu(cyclam)(pcp)_2]$, $[Cu(pcp)_2(en)_2]$ and $[Cu(tbp)_2(en)_2]$ and in the electronic solution spectrum of the former in MeOH; one around 320nm and one around 500nm (Table 3.3 and 3.4). The band at 320nm can be assigned to a $\pi \longrightarrow \pi^*$ transition of the ionised phenolate group. No such band is observed in the diffuse reflectance spectrum of $[Cu(cyclam)(pcp)_2]$, while a 1:1 mixture of NaOH and pcp absorbs at 322nm. The weak band around 500nm can be assigned to a d-d transition in $[Cu(cyclam)(pcp)_2]$, from the intensity of this band in dmf, and in $[Cu(pcp)_2(en)_2]$ and $[Cu(tbp)_2(en)_2]$, even though the absolute intensities of their bands cannot be determined. Lever and Mantovani (152) found for a series of complexes having an in plane CuN_4 stoichiometry that this band ranged from 476-714nm, the highest energies being observed for the weakly coordinating axial ligands. For instance in the complexes $[Cu(en)_2(X)_2]$ (X = Cl, Br, I, NCS, NO_3, ClO_4, BF_4) λ_{max} ranged from 540nm through 543nm to 553nm when X = Cl, Br, I respectively. The complexes $[Cu(cyclam)(pcp)_2]$, $[Cu(pcp)_2(en)_2]$ and $[Cu(tbp)_2(en)_2]$ all lie at the upper end of this range suggesting only a very weak axial interaction of the phenolate groups.

Out of plane distortions from tetragonal towards tetrahedral symmetry have the effect of shifting the d-d transitions to lower energy. $[Cu(tbp)_2(dmp)]\frac{1}{2}H_2O$ and $[Cu(pcp)_2(dmp)]$ have two d-d bands around 800nm and 1000nm in their reflectance spectra (and in solution in the case of the latter), giving strong evidence for out of plane co-

ordination of the phenolate groups to minimise interaction with the methyls of dmp.

3.3.4 ELECTRON SPIN RESONANCE SPECTROSCOPY

In general e.s.r. spectra of the complexes in this study, with $g_{11} > g_{\perp}$, are consistent with copper(II) in a tetragonal environment, with some complexes showing tetrahedral distortions. Tetrahedral distortions of otherwise tetragonal copper(II) chelates increases g_{11} and decreases $|A_{11}|$. The ratio of $g_{11}:|A_{11}|$ appears to be a convenient empirical index of distortion of the donor set from planar toward tetrahedral distortions (148). This ratio takes a value ranging from about 105 - 135cm for tetragonal structures, values above this indicating distortions towards tetrahedral symmetry. In the copper complexes under consideration (Table 3.5) $[Cu(tbp)_2(dmp)]\frac{1}{2}H_2O$ and $[Cu(pcp)_2(dmp)]$ would appear to have small out of plane distortions tending towards tetrahedral symmetry. The high empirical index $[Cu(pcp)_2]$ in methanol (Figure 3.4) demonstrates a CuO_4 tetrahedral symmetry, changing to a largely tetragonal symmetry in a less polar solvent, nitromethane. The remaining complexes in the series all have e.s.r. spectra consistent with copper(II) in a tetragonal environment. For $[Cu(pcp)_2(en)]$, $[Cu(pcp)_2(collidine)]$ and $[Cu(pcp)_2(dmf)]$ two species are apparent in the spectrum in more polar solvents (EtOH or dmf in the latter case) one of which can be attributed to tetragonal copper(II), while the other shows distortion towards tetrahedral symmetry. Two species are also present in the spectrum of $[Cu(tbp)_2$-(collidine)] though both indicate that only very small distortions from tetragonal symmetry have occurred. The lower than normal magnetic susceptibilities of $[Cu(pcp)_2(collidine)]$ and $[Cu(pcp)_2(dmf)]$ suggest that these complexes exist as either phenoxo bridged dimers in the solid state;

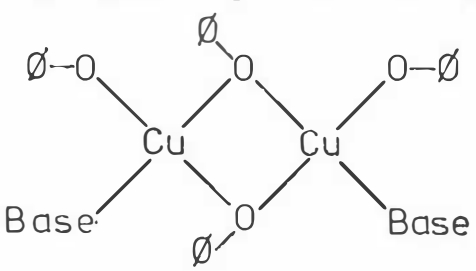

Ø–O = pcp
Base = dmf or collidine

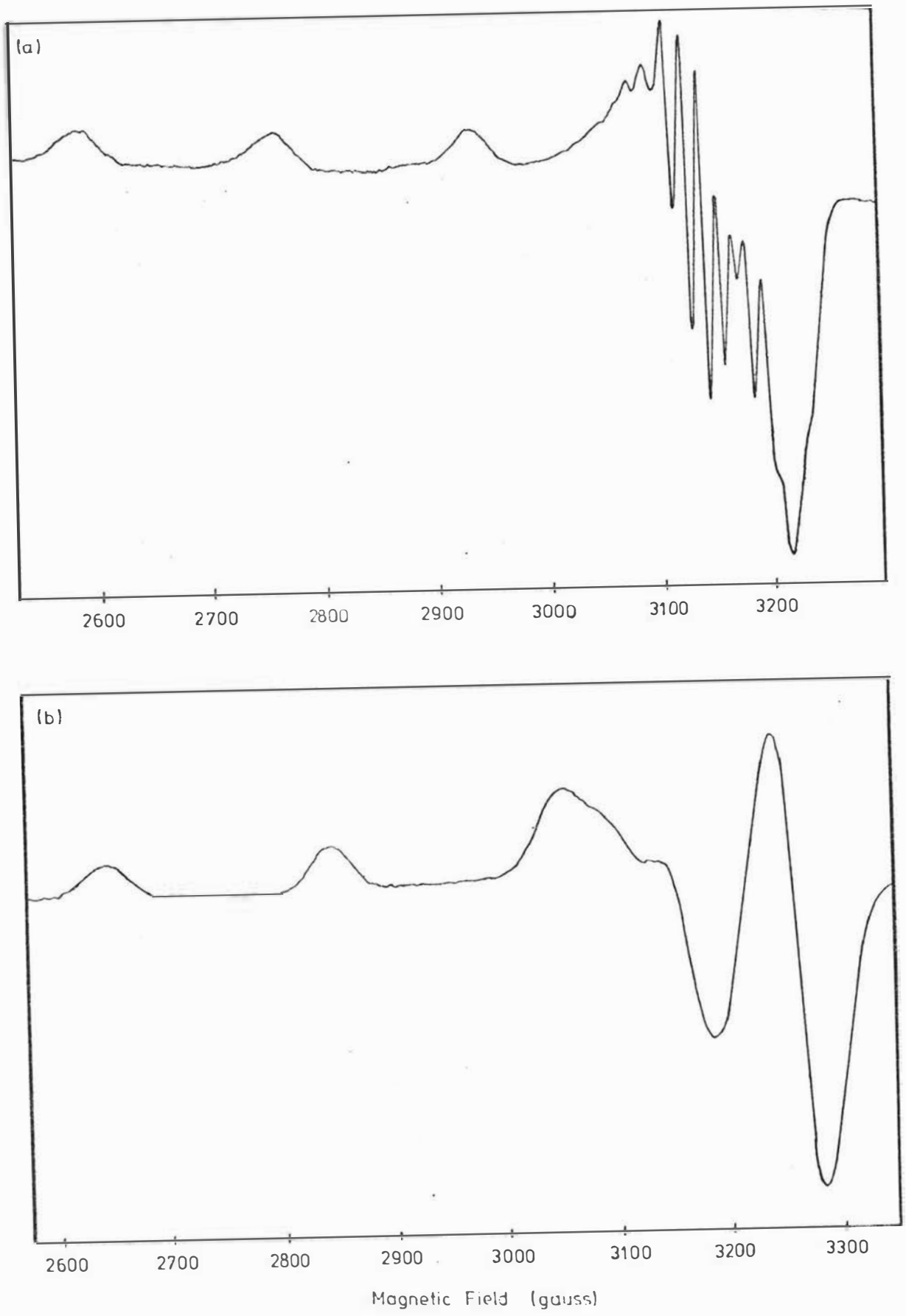

Figure 3.3 E.S.R. spectra at -194°C of (a) $[Cu(tbp)_2(py)_2]$ in ethanol and (b) $[Cu(cyclam)(pcp)_2]$ in dmf.

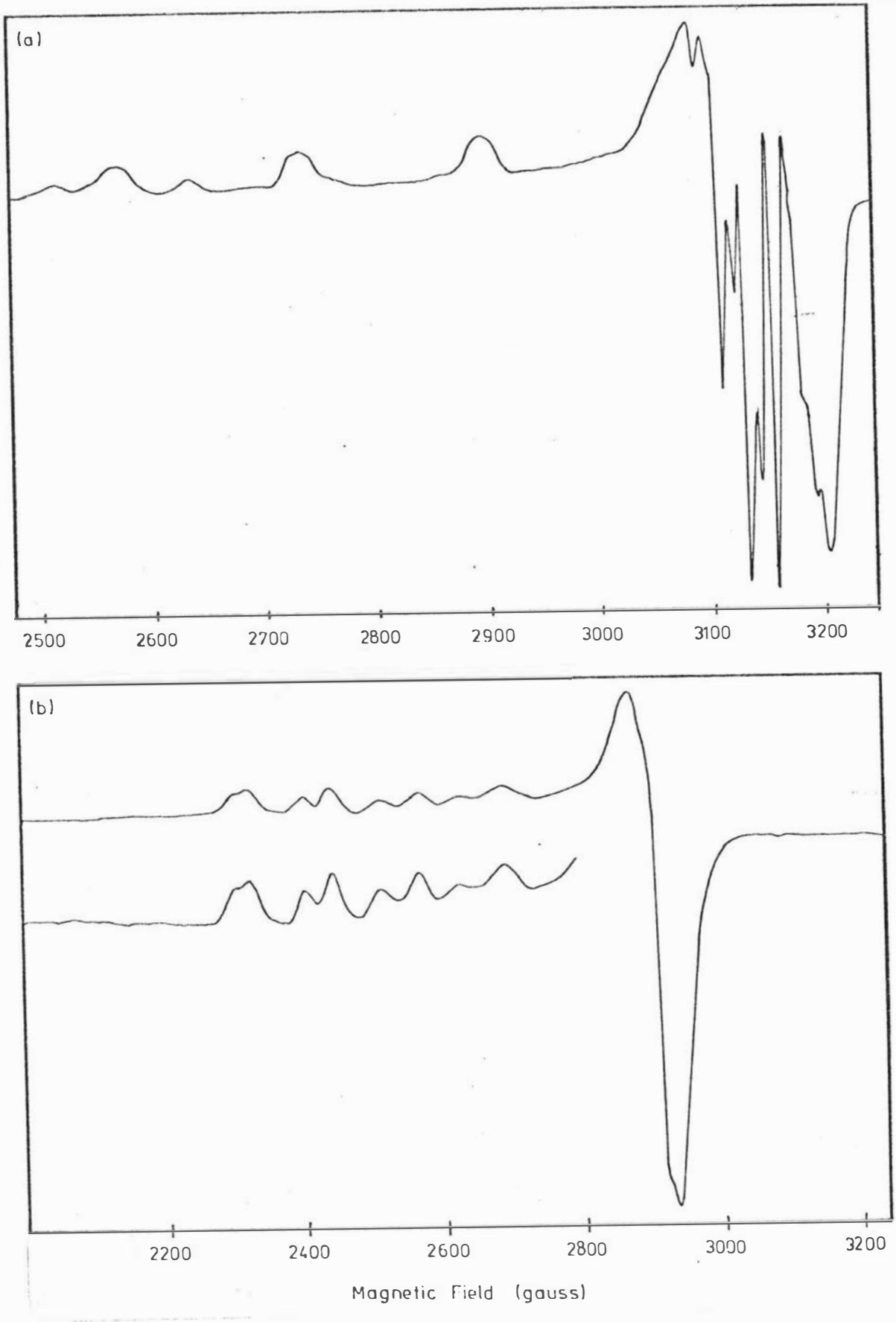

Figure 3.4 E.S.R. spectra at -194°C of (a) $[Cu(pcp)_2(collidine)]$ in acetone and (b) $[Cu(pcp)_2]$ in methanol.

Table 3.5 ELECTRON SPIN RESONANCE SPECTRA OF THE COPPER PHENOLATE COMPLEXES

Compound	g_{11}	[b] A_{11}	$g_{\perp}$	[c] $A_{\perp}$	[d] g_{11}/A_{11}	Colour	Solvent
Cu_2Lf	2.314	151(163)	2.057	11.2	142	Yellow	Phosphate Buffer
$[Cu(tbp)_2(en)]$	2.250	183(192)	2.081	-	117	Yellow	C_6H_6
	2.260	180(190)	2.054	18	119	Yellow	EtOH
$[Cu(tbp)_2(TMED)]$	-	-	2.093	-	-	Red	C_5H_6
	2.240	178(186)	2.083	15	120	Red	EtOH
$[Cu(tbp)_2(dmp)]3H_2O$	[a]2.326	134(145)	2.073	-	160	Brown	Acetone
	2.316	125(135)			172		
$[Cu(tbp)_2(py)_2]$	2.265	174(184)	2.063	-	123	Yellow	C_6H_6
	2.266	175(185)	2.062	16	122	Yellow	EtOH
$[Cu(tbp)_2(1m)_2]$	2.267	176(186)	2.044	15	122	Yellow	EtOH
$[Cu(tbp)_2(collidine)]$	[a]2.331	148(161)	2.075	24	145	Brown	Acetone
	2.303	177(165)			130		
$[Cu(pcp)_2]$	2.437	106(121)	2.082	-	201	Yellow	MeOH
	[a]2.393	121(130)			184		
	2.267	155(164)	2.069	14	138	Red	CH_3NO_2
$[Cu(pcp)_2(en)]$	2.239	188(197)	2.082	-	113	Yellow	C_6H_6
	[a]2.280	159(169)	2.066	15	135	Yellow	EtOH
	2.276	100(106)			214		
$[Cu(pcp)_2(dmp)]$	2.304	138(148)	2.117	-	156	Purple	CH_2Cl_2
$[Cu(pcp)_2(py)_2]$	2.239	182(190)	2.058	-	118	Yellow	C_6H_6
	2.301	158(170)	2.056	13	135	Yellow	EtOH
$[Cu(cyclam)(pcp)_2]$	2.193	200(205)	2.049	-	107	Pink	dmf
$[Cu(pcp)_2(collidine)]$	2.295	166(178)	2.067	-	129	Yellow	CH_3NO_2
	[a]2.292	165(177)	2.080	12	129	Yellow	EtOH
	2.394	136(122)			176		
$[Cu(pcp)_2(dmf)]$	2.374	125(138)	2.074	-	172	Yellow	dmf
	2.311	159(177)			135		

$[Cu(tbp)_2(en)_2]$	g = 2.148, 2.029 in the solid state
$[Cu(pcp)_2(en)_2]$	g = 2.144, 2.026 in the solid state

a. Major species

b. A_{11} in gauss and in $10^{-4}cm^{-1}$ in the brackets

c. $A_{\perp}$ in gauss

d. g_{11}/A_{11} in cm

or as a polymeric structure with more extensive phenolate bridging. Partial or full solvolysis of this dimer by the solvent may account for the two species observed in the spectrum.

In complexes of tetragonal symmetry there is a trend of decreasing g_{11} and increasing A_{11} values with increasing numbers of nitrogens coordinating and when σ bonding is really significant these g_{11} values fall into a narrow range (149, 150). In some of the tetragonal copper(II) complexes in this study such a trend is apparent. The complexes of $[Cu(tbp)_2(collidine)]$ and $[Cu(pcp)_2(collidine)]$ (Figure 3.4), both with only one nitrogen coordinated, have values of g_{11} around 2.30 and A_{11} around 177 x $10^{-4}cm^{-1}$, when acetone and ethanol respectively are the solvents. When two nitrogens are coordinated to the metal, as with complexes of $[Cu(tbp)_2L_n]$ (L = en, TMED when n = 1 and L = py, im when n = 2) when ethanol or benzene is the solvent, g_{11} drops to 2.240 - 2.267 and A_{11} rises to 185 - 190 x $10^{-4}cm^{-1}$. The g_{11} and A_{11} values of $[Cu(pcp)_2(en)]$ and $[Cu(pcp)_2(py)_2]$ in benzene are also consistent with this scheme. When four nitrogens are coordinated, as in $[Cu(cyclam)(pcp)_2]$ in dmf, g_{11} drops to 2.193 and A_{11} rises to 2.05 x $10^{-4}cm^{-1}$. However values of g_{11} and A_{11} when $[Cu(pcp)_2(en)]$ and $[Cu(pcp)_2(py)_2]$ in ethanol lie outside the ranges proposed (Table 3.5).

3.3.5 TRIVALENT MANGANESE PHENOLATE COMPLEXES

(a) Preparation of $[Mn(SALENH_4)(Acetato)](Acetone)1\frac{1}{2}H_2O$

A slurry of $Mn(Acetate)_3 2H_2O$ (0.26g, 1mmole) in acetone was added to a solution of $SALENH_4$ (0.29g, 1mmole) in acetone. As the $Mn(Acetate)_3 2H_2O$ dissolved with stirring a brown solution resulted from which a precipitate was obtained. This was recrystallized by dissolving in acetone and precipitating with diethyl ether. The conductivity of the complex of 1.35 $\Omega^{-1}mole^{-1}cm^2$ in ethanol, is consistent with a non-electrolyte.

The presence of a band at $1700cm^{-1}$ in the i.r. spectrum which disappeared on heating for 12 hours at 105°C suggested that acetone was present in the complex.

Analytical figures calculated for $[Mn(SALENH_4)(Acetato)]$ $(Acetone)H_2O$ were C; 54.7%, H; 6.7%, N; 5.8% and for the complex were found to be C; 55.0%, H; 6.0%, N; 6.1%.

(b) Characterisation of $[Mn(SALENH_4)(Acetato)]$ $(Acetone)1\frac{1}{2}H_2O$

The complex exhibits a signal in its e.s.r. spectrum of $g = 2.017$, $A = 95$gauss and this is strongly characteristic of manganese(II) rather than manganese(IV), which exhibits stronger signals at $g = 4$ (151). The magnetic susceptibility of the complex of 5.43 BM would suggest that a mixture of manganese(II) ($\mu eff = 5.65 - 8.10$ BM) and manganese(III) ($\mu eff = 4.9 - 5.0$ BM) is present in the preparation.

The electronic spectrum of the complex in EtOH is characterised by an intense band at 398nm which from its intensity of $\varepsilon = 46601 mole^{-1}cm^{-1}$ is likely to be a metal-to-phenolate or phenolate-to-metal charge transfer interaction. The spectrum also exhibits shoulders at lower energy, of which one is found near 480nm. This electronic spectrum is very similar to Mn_2Lf (Figure 1.7) and is probably mainly due to the Mn(III) species present.

3.4 Conclusion

Cu_2Lf has a charge transfer band at 438nm which is similar in energy to many of the compounds listed in Table 3.4, but this band is at much lower energy than in those complexes thought to have only one phenolate coordinated to the metal. Fluctuations in charge transfer energy of these compounds arise from the nature of the base and the phenolate as well as the stereochemistry about copper. Given the same co-ligands and arrangement of them about copper as the small molecular weight complexes, it would be expected that the charge transfer energy of Cu_2Lf would be greater than these complexes because in the former the phenolate component of tyrosine is not halo substituted. The best example of a CuO_2N_2 system containing unsubstituted phenolates is $[Cu(SALENH_4)]$ where λ_{max} is 392nm, though in this case the chelate effect would have shifted this

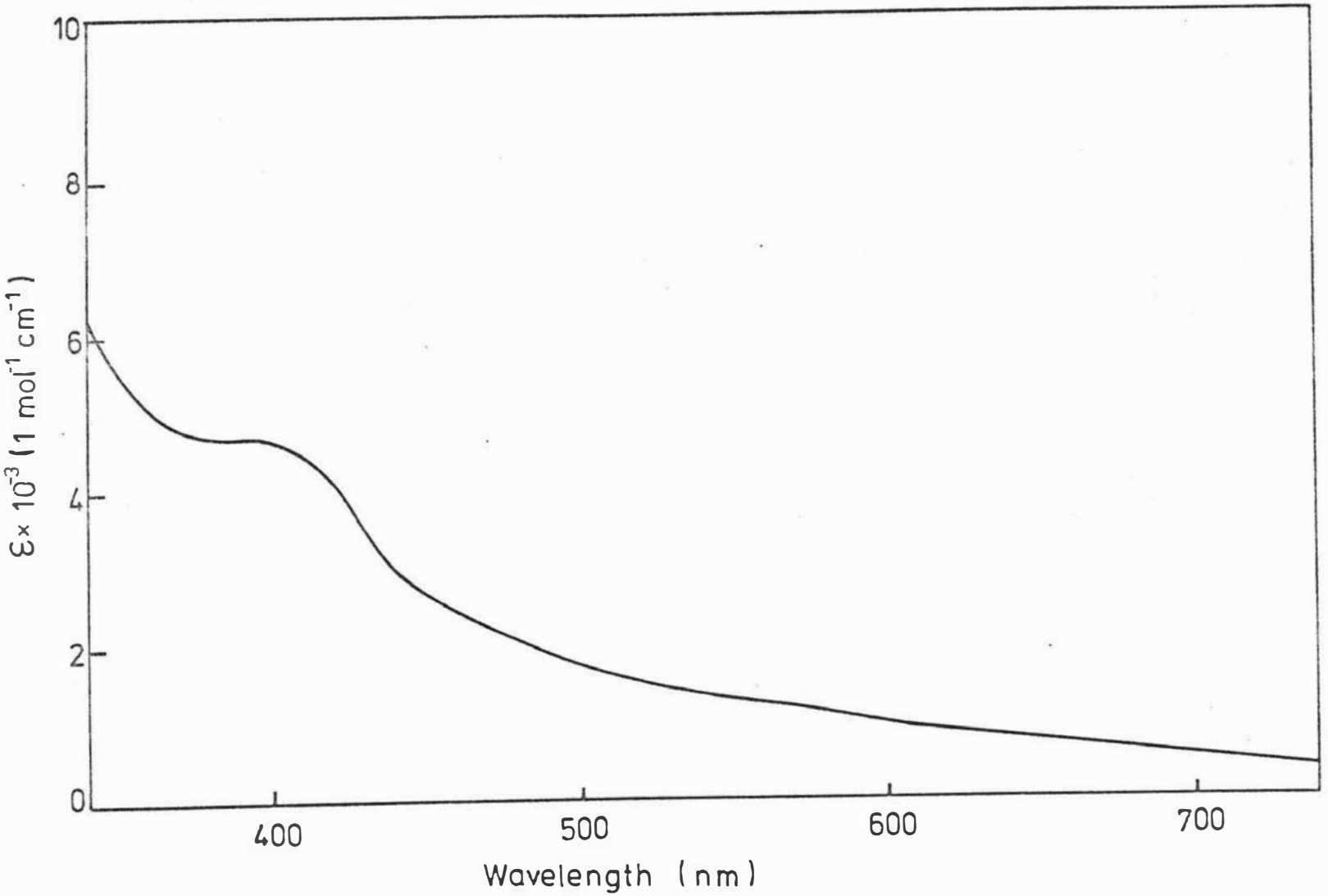

Figure 3.5 Visible absorption spectrum of $[Mn(SALENH_4)(acetato)](Acetone)1\frac{1}{2}H_2O$ in EtOH.

band to lower energy. Replacing the ethylenediamine component of $SALENH_4$ by two imidazoles would be expected to shift λ_{max} by at least 20nm to lower energy (Table 3.4). On the basis of these values then, a monodentate CuO_2N_2 would be expected to absorb between 400 - 410nm. While a third phenolate group binding to copper would be expected to cause a shift of the charge transfer band to lower energy, precisely how great a shift is difficult to determine, though it would be expected to be small for an axial phenolate. Thus while the position of the charge transfer band in Cu_2Lf, at 438nm, would be more consistent with two (as opposed to one) tyrosyl residues binding to copper the involvement of a third tyrosyl residue cannot be discounted. In addition to indicating the number of tyrosyls involved in the binding site of Cu_2Lf the electronic spectrum, in conjunction with the e.s.r. spectrum, points to copper(II) in a distorted tetragonal environment.

Studies on transferrin (see Introduction) have indicated that there are two histidyl groups and, at the most, three tyrosyl groups in the binding sites. From results presented in this study the electronic spectra would suggest that when copper is bound at least two tyrosyl residues are bound equatorially and do not discount the possibility that a third may be interacting axially, even if unionised. The e.s.r. spectra of Cu_2Lf and Cu_2Tf point to the presence of one equatorial histidyl group. However electronic spectra would not be incompatible with one or two equatorial imidazole-type groups, while axial nitrogens appear to have little effect on the absorbance maximum. Hence this would point to an axial coordination of the second histidyl in Cu_2Lf and Cu_2Tf. A possible arrangement of the groups in the specific sites of lactoferrin, transferrin and ovotransferrin, based on the evidence presented in this thesis, is illustrated in Figure 3.6.

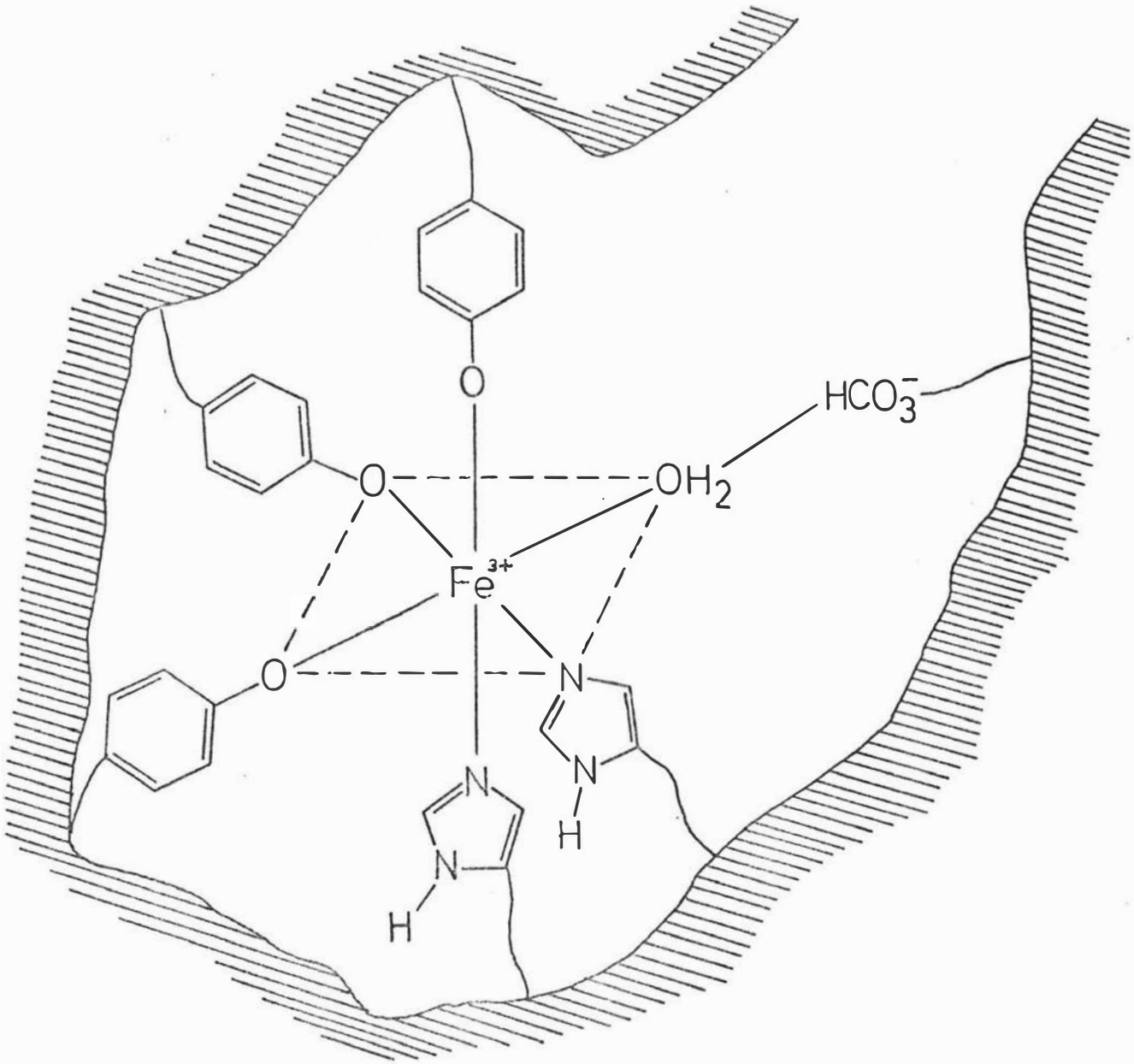

Figure 3.6 Proposed coordination sphere of iron(III) in the binding site of lactoferrin, transferrin and ovotransferrin based on the evidence presented in this thesis.

Appendix PUBLICATIONS ARISING FROM THIS THESIS

REFERENCES

1. Schafer, K. H., Monatsschr Kinderheilk 99, 69 (1951)
2. Sörenson, M. and Sörenson, P. L., Compt. Rend., Trav. Lab. Carlsberg 23, 55 (1939)
3. Laurell, C. B. and Ingleman, B., Acta. Chem. Scand. 1, 770 (1947)
4. Holmberg, C. G. and Laurell, C. B., Acta. Physiol. Scand. 10, 307 (1945)
5. Holmberg, C. G. and Laurell, C. B., Acta. Chem. Scand. 1, 944 (1947)
6. Schade, A. L. and Caroline, L., Science 100, 14 (1944)
7. Aisen, P. and Leibman, A., Biochim. Biophys. Acta 257, 314 (1972)
8. Bullen, J. J., Rogers, M. J. and Griffiths, E., Chapter 20 In Neilands, J. B. ed. Microbial Iron Metabolism. Academic Press (1972)
9. Mason, S., Arch. Diseases. Children 37, 387 (1962)
10. Feeney, R. E. and Komatsu, S. S., Structure and Bonding 1, 149 (1966)
11. Aisen, P., p280 In Eichhorn, G. I. ed. Inorganic Biochemistry. Elsevier (1973)
12. Bezkorovainy, A., J. Dairy Science 60, 1023 (1977)
13. Schade, A.L. and Caroline, L., Science 104, 3420 (1946)
14. Schade, A. L., Reinhart, R. W. and Levy, H., Arch. Biochem. 20, 170 (1949)
15. McMillan, J. A., Landaw, S. A. and Oski, F. A. Pediatrics 58, 686 (1976)
16. Feeney, R. E. and Allison, R. G., p149 In Evolutionary Biochemistry of Proteins. Wiley - Interscience (1969)
17. Greene, F. C. and Feeney, R. E., Biochemistry 7, 1366 (1968)
18. Querinjean, P., Masson, P. L. and Heremans, J. F., Eur, J. Biochem. 20, 420 (1971)
19. Jollēs, J., Mazurier, J., Boutigue, H. H., Spik, G., Montrieul, J. and Jollēs, P., F.E.B.S. Letters 69, 27 (1976)
20. Bluard-Deconinck, J. M., Williams, J., Evans, R. W., Van Snick, J., Osïnski, P.A. and Masson, P. L., Biochem. J. 171, 321 (1978)

21. Evans, R. W. and Williams, J., Biochem. J. 173, 543 (1978)
22. Karlsson, K. A., Pascher, I., Samuelsson, B. E., Finne, J., Krusius, T. and Rauvala, H., F.E.B.S. Letters 94, 413 (1978)
23. Dorland, L., Haverkamp, J., Schut, B. L., Vliegenthart, J.F.G., Spik, G., Strecker, G., Fournet, B. and Montrieul, J., F.E.B.S. Letters 77, 15 (1977)
24. Van Bockxmeer, F. M. and Morgan, E. H., Biochim. Biophys. Acta. 468, 437 (1977)
25. Kornfield, S., Biochemistry 7, 945 (1968)
26. Morgan, E. H., Chapter 2 In Jacobs, A. and Worwood, M. ed. Iron in Biochemistry and Medicine. London Academic Press (1974)
27. MacGillivray, R.J.A. and Brew, K., Science 190, 1306 (1975)
28. Surgenor, D. M., Koechlin, B. A. and Strong, L. E., J. Clin. Invest. 28, 73 (1949)
29. Aasa, R., Malmstrom, B. G., Saltman, P. and Vannegärd, T., Biochim. Biophys. Acta. 75, 203 (1963)
30. Aisen, P., Leibman, A. and Reich, H. A., J. Biol. Chem. 241, 1666 (1966)
31. Ross, J., Kochwa, S. and Wasserman, L. R., Biochim. Biophys. Acta. 154, 70 (1968)
32. Groves, M. L., J. Amer. Chem. Soc. 82, 3345 (1960)
33. Warner, R. G. and Weber, I., J. Amer. Chem. Soc. 75, 5094 (1953)
34. Bezkorovainy, A., Biochim. Biophys. Acta 127, 535 (1966)
35. Fuller, R. A. and Briggs, D. R., J. Amer. Chem. Soc. 78, 5253 (1956)
36. Teuwissen, B., Masson, P. L., Osinski, P. and Heremans, J. F., Eur. J. Biochem. 31, 239 (1972)
37. Wishnia, A., Weber, I. and Warner, R. G., J. Amer. Chem. Soc. 83, 2071 (1961)
38. Bezkorovainy, A. and Grohlich, D., Biochim. Biophys. Acta. 263, 645 (1972)
39. Phillips, J. L. and Azari, P., Arch. Biochem and Biophys. 151, 445 (1972)
40. Gaber, B. P., Miskowski, V. and Spiro, T. G., J. Amer. Chem. Soc. 96, 6868 (1974)

41. Rogers, T. B., Gold, A. and Feeney, R. E., Biochemistry 16, 2299 (1977)
42. Koenig, S. H. and Schillinger, W. E., J. Biol. Chem. 244, 6520 (1969)
43. Lehrer, S. S., J. Biol. Chem. 244, 3613 (1969)
44. Price, E. M. and Gibson, J. F., Biochem. Biophys. Res. Com. 46, 646 (1972)
45. Rogers, T. B., Børresen, T. and Feeney, R. E., Biochemistry 17, 1105 (1978)
46. Aisen, P., Aasa, R., Malmstrom, B. G. and Vannegärd, T., Biol. Chem. 242, 2484 (1967)
47. Young, J. W. and Perkins, D. J., Eur. J. Biochem. 4, 385 (1968)
48. Schlabach, M. R. and Bates, G. W., J. Biol. Chem. 250, 2182 (1975)
49. Aisen, P., Pinkowitz, R. A. and Leibman, A., Ann. N. Y. Acad. Sciences 222, 337 (1973)
50. Egyed, A., Biochim. Biophys. Acta. 304, 805 (1973)
51. Aisen, P. and Leibman, A., Biochim. Biophys. Acta. 304, 797 (1973)
52. Harris, D. C. and Aisen, P., Fed. Proc. 33, 1503 (1974)
53. Najaran, R. C., Harris, D. C. and Aisen, P., J. Biol. Chem. 253, 38 (1978)
54. Aisen, P., Aasa, R. and Redfield, A. G., J. Biol. Chem. 244, 4628 (1969)
55. Aisen, P. and Aasa, R., J. Biol. Chem. 243, 2399 (1968)
56. Zweier, J. L. and Aisen, P., J. Biol. Chem. 252, 6090 (1977)
57. Aisen, P., Leibman, A. and Zweier, J., J. Biol. Chem. 253, 1930 (1978)
58. Warner, R. G. and Weber, I., J. Biol. Chem. 191, 173 (1951)
59. Stratil, A., Comp. Biochem. Physiol. 22, 227 (1967)
60. Williams, J., Phelps, C. F. and Lowe, J. M., Nature London 226, 858 (1970)
61. Wenn, R. V. and Williams, J., Biochem. J. 108, 69 (1968)
62. Van Eyk, H. G., Vermaat, R. J. and Leijnse, B., F.E.B.S. Letters 3, 193 (1969)
63. Windle, J. J., Wiersman, A. K., Clarke, J. R. and Feeney, R. E., Biochemistry 2, 1341 (1963)

64. Tsang, C. P., Boyle, A.J.F. and Morgan, E. H., Biochim, Biophys. Acta. 328, 89 (1973)
65. Luk, C. K., Biochemistry 10, 2838 (1971)
66. Williams, S. C. and Woodworth, R. C., J. Biol. Chem. 248, 5848 (1973)
67. Aisen, P., Lang, G. and Woodworth, R. C., J. Biol. Chem. 248, 649 (1973)
68. Aasa, R., Biochem. Biophys Res. Comm. 49, 806 (1972)
69. Fletcher, J. and Huehns, E. R., Nature 215, 548 (1967) and 218, 1211 (1968)
70. Cannon, J. C. and Chasteen, N. D., Biochemistry 14, 4573 (1975)
71. Campbell, R. F. and Chasteen, N. D., J. Biol. Chem. 252, 5996 (1977)
72. Harris, D. C., Biochemistry 16, 560 (1977)
73. Masson, P. L. and Heremans, J. F., Comp. Biochem. Physiol. 39B, 119 (1971)
74. Masson, P.L., Heremans, J. F. and Dive, C. H., Clin. Chim. Acta. 14, 735 (1966)
75. Gray, I.K., Newstead, D.F. and Mickleson, K.N.P., 20th Int. Dairy Congress - Brief Communications, p1062
76. Bloor, S.J., Honours Report (1979)
77. Masson, P.L. and Heremans, J.F., Eur. J. Biochem. 6, 579 (1968)
78. Bates, G.W. and Schlabach, M.R., J. Biol. Chem. 248, 3228 (1973)
79. Bates, G.W., Billups, C. and Saltman, P., J. Biol. Chem. 242, 2810 and 2816 (1967)
80. Peaker, M. and Linzell, J.L., Nature 253, 464 (1975)
81. Tan, A.T. and Woodworth, R.C., J. Polymer Science 30, 599 (1970)
82. Tan, A.T. and Woodworth, R.C., Biochemistry 8, 3711 (1969)
83. Tominatsu, Y., Kint, S. and Scherer, J.R., Biochemistry 15, 4918 (1974)
84. Cotton, F.A. and Wilkinson, G., Advanced Inorganic Chemistry 3rd Edition, Wiley Interscience (1972), p851
85. Davies, T.S., Fackler, J.P. and Weeks, M.J., Inorg. Chem. 7, 1994 (1968)
86. Bullock, J.I., Patel, M.M. and Salmon, J.E., J. Inorg. Nuclear Chem. 31, 415 (1969)

87. Mazurier, J., Lhoste, J.M., Spik, G. and Montrieul, J., F.E.B.S. Letters 81, 371 (1977)
88. Reference 84, p914
89. Billo, E.J., Inorg. Nucl. Chem. Letters 10, 613 (1974)
90. Reference 84, p838
91. Thorneley, R.N.F. and Sykes, A.G., J. Chem. Soc. (A), 742 (1969)
92. Moore, P. and Basolo, F., Inorg. Chem. 4, 1670 (1965)
93. Isied, S.S., Kuo, G. and Raymond, K.N., J. Amer. Chem. Soc. 98, 1763 (1976)
94. Childers, R.F., Vauder Zyl, K.G., House, D.A., Hughes, R.G. and Garner, C.S., Inorg. Chem. 7, 749 (1968)
95. Weyh, J.A. and Hamm, R.E., Inorg. Chem. 7, 2431 (1968)
96. Reference 84, p836
97. Price, E.M. and Gibson, J.F., J. Biol. Chem. 247, 8031 (1972)
98. Knowles, P.F., Marsh, D. and Rattle, H.W.E., Magnetic Resonance of Biomolecules, John Wiley and Sons (1976), Chapter 6
99. Tennant, W.C., Private Communication
100. Stability of Metal-Ion Complexes, Suppliment No. 1, The Chemical Society (1971) p634
101. Alywood, G.H. and Findlay, T.J.V., S.I. Chemical Data Book, Wiley Interscience
102. Folting, K., Cox, M.M., Moore, J.W. and Merrit, L.L., Chem. Comm. 1170 (1968)
103. Bailey, N.A., Cummins, D., McKenzie, D.E. and Worthington, J.M., Inorg. Chim. Acta 18, L13 (1976)
104. Raston, C.L., White, A.H., Willis, A.C. and Murray, K.S., J. Chem. Soc. Dalton 1793 (1974)
105. Hems, R., Cardwell, T.J. and MacKay, M.F., Aust. J. Chem. 28, 443 (1975)
106. Figgis, B.N., Raston, C.L., Sharma, R.P. and White, A.H., Aust. J. Chem. 31, 2545 (1978)
107. Brown, K.L., Private Communication
108. Loehr, T.M., Loehr, J. and Keyes, W.E., Private Communication
109. Albrecht, A.C. and Hatley, M.C., J. Chem. Phys. 55, 4438 (1971)
110. Tatsuno, Y., Saeki, Y., Iwaki, M., Nozaki, M., Kitagawa, T. and Otsuka, S., J. Amer. Chem. Soc. 100 4614 (1978)

111. Keyes, W.E., Loehr, T.M. and Taylor, M.L., Biochem. Biophys. Res. Comm. 83, 941 (1978)
112. Que, L. Jr. and Heistand, R.H.II, J. Amer. Chem. Soc. 101, in press (1979)
113. Aisen, P. and Leibman, A., Biochem. Biophys. Res. Comm. 30, 407 (1968)
114. Spik, G., Ann. Nutr. Alim. 25, A81 (1971)
115. Spik, G., Private Communication
116. Frushour, B.G. and Koenig, J.L., Chapter 2 In Clarke, R.J.H. and Hester, R.E. eds, Advances in Infrared and Raman Spectroscopy Vol. 1, Heyden, London (1975)
117. Cook, J.W., Gibb, A.R., Raphiel, R.A. and Sommerville, A.R., J. Chem. Soc. 503 (1951)
118. Tweedle, M.F. and Wilson, L.J., J. Amer. Chem. Soc. 98, 4824 (1976)
119. Anderson, B.F., Buckingham, D.A., Robertson, G.B., Webb, J., Murray K.S. and Clark, P.E., Nature 262, 722 (1976)
120. Epstein, L.M. and Straub, D.K., Inorg. Chem. 8, 453 (1969)
121. Einstein, F.W.B. and Willis, A.C., Inorg. Chem. 17, 3040 (1978)
122. Adams, D.M., p202 In Inorganic Solids, Wiley-Interscience (1974)
123. Gans, P., Buisson, G., Duee, E., Regnard, J.-R. and Marchon, J.-C., J.C.S. Chem. Comm. 393 (1979)
124. Schurgar, H.J., Walling, C., Jones, R.B. and Gray, H.B., J. Amer. Chem. Soc. 89, 3712 (1967)
125. Hamar, T.A. and Watkin, D.J., Chem. Comm. 441 (1969)
126. Ackermann, G.A. and Hesse, D., Z. Anorg. Allg. Chem. 375, 77 (1970)
127. L'Eplattenier, F., Murase, I. and Martell, A.E., J. Amer. Chem. Soc. 89, 837 (1967)
128. Linder, H.J. and Gottlicher, S., Acta Crystallogr. B25, 832 (1969)
129. Spartalian, K. and Oosterhuis, W.T., J. Chem. Phys. 59, 617 (1973)
130. Tsang, C.P., Boyle, A.J.F. and Morgan, E.H., Biochim. Biophys. Acta 386, 32 (1975)
131. Gainsford, A.R., Private Communication
132. Calderazzo, F. and Dell'Amico, D., J. Chem. Soc. Dalton 1238 (1979)

133. Anderson, R.A., Dalgleish, D.T., Nonhebel, D.C. and Paulson, P.L., J. Chem. Res. (M), 0210 (1978)
134. Wong, R.Y., Palmer, K.J. and Tominatsu, Y., Acta. Crystallogr. B32, 567 (1976)
135. Bullock, J.I., Hobson, R.J. and Povey, D.C., J. Chem. Soc. Dalton 2037 (1974)
136. Hobson, R.J., Ladd, M.F.C. and Povey, D.C., J. Cryst. Mol. Struct. 3, 377 (1973)
137. Ladd, M.F.C. and Povey, D.C., J. Cryst. Mol. Struct. 6, 205 (1976)
138. Vogt, L.H., La Placa, S. and Bednowitz, A., Amer. Chem. Soc. Meeting, Inorg. Div., San Francisco, March 1968
139. Ainscough, E.W. and Addison, A.W., Unpublished Results
140. Gidney, P.M., Gillard, R.D. and Heaton, B.T., J. Chem. Soc. Dalton 132 (1973)
141. Harrod, J.F., Canadian J. Chem. 47, 637 (1969)
142. Amundsen, A.R., Whelan, J. and Bosnich, B., J. Amer. Chem. Soc. 99, 6730 (1977)
143. Lever, A.P.B., J. Chem. Ed. 51, 612 (1974)
144. Davis, J.A. and Sinn, E., J. Chem. Soc. Dalton 165 (1976)
145. Kato, M., Muto, Y., Jonassen, H.B., Imai, K., and Harano, A., Bull. Chem. Soc. Jap. 41, 1864 (1968)
146. Nakahara, A., Bull. Chem. Soc. Jap. 32, 1195 (1959)
147. Ainscough, E.W. and Brodie, A.M., This Laboratory
148. Sakaguchi, U., and Addison, A.W., J. Chem. Soc. Dalton 600 (1979)
149. Alei Jr., M., Lewis, W.B., Dennison, A.B. and Morgan, L.O., J. Chem. Phys. 47, 1062 (1967)
150. Barbucci, R. and Campbell, M.J.M., Inorg. Chim. Acta. 16, 113 (1976)
151. Richens, D.T. and Sawyer, D.T., J. Amer. Chem. Soc. 101, 3681 (1979)
152. Lever, A.P.B. and Mantovani, E., Inorg. Chem. 10, 817 (1971)

Table 4a Spectral Characteristics of Metal-lactoferrin complexes

	Electronic and Fluorescence Spectra	E.S.R. Spectra	Resonance Raman Spectra
Fe_2Lf	CT band suggests tyrosines (p29).	Fe(III) in a rhombic site (p37) some suggestion of site heterogeneity (p46).	The CT band is due to tyrosines and not histidine or HCO_3^- (p50-7).
Cu_2Lf	CT band suggests tyrosines and d-d band suggests 1 or 2 equatorial nitrogens in a site of tetragonal symmetry (p30,35). Fluorescence suggests specific site binding (p25-9).	Cu(II) in a tetragonal site, 1 equatorial nitrogen present (p41). No specific binding in absence of HCO_3^- (p47).	Ditto
Co_2Lf	CT band suggests tyrosines (p29). Fluorescence suggests specific site binding (p25-9).	E.s.r. inactive-consistent with Co(III) (p20).	Ditto
Mn_2Lf	CT band suggests tyrosines, presence of d-d bands consistent with distorted octahedral Mn(III) (p29). Fluorescence suggests specific site binding (p25-9).	E.s.r. inactive - consistent with Mn(III) (p20). Protein possibly adopts a different conformation (p49).	Ditto
Cr_2Lf	No CT band, d-d bands suggest Cr(III) bound to Cl as well as 1 or 2 nitrogens and oxygens in a distorted octahedral site (p35-6).	Cr(III) in a distorted octahedral site. Distinctive site heterogeneity (p45-7).	Ditto

Conclusions

(1) The electronic and resonance Raman spectra both support the involvement of tyrosines in the binding site of Fe_2Lf.

(2) Electronic and e.s.r. spectra of Cu_2Lf and electronic spectra of Cr_2Lf support the involvement of 1 or 2 nitrogen ligands on the metal and hence these ligands are expected to be bound to iron.

(3) The absence of specific Cu_2Lf e.s.r. signals in HCO_3^- free conditions supports the involvement of this ion.

(4) From spectroscopic and chemical modifications of Fe_2Tf (and ovotf) it has been suggested that the sites in both proteins are similar and that these include 2-3 tyrosines, 2 histidines, 1 water and 1 bicarbonate molecule. A similar situation appears to hold for Fe_2Lf because it is spectroscopically similar.

(5) The protein appears to be able to adopt a conformation to suit the stereochemical requirements of each metal ion. For instance high spin $Mn^{3+}(3d^4)$ and $Cu^{2+}(3d^9)$ are likely to be subject to Jahn Teller distortions hence adopt a tetragonal coordination, while $Cr^{3+}(3d^3)$, high spin $Fe^{3+}(3d^5)$ and low spin $Co^{3+}(3d^6)$ have spherically symmetric electronic configurations and would adopt a more regular octahedral coordination (possibly with some rhombic distortion).

Table 4b Comparison of Small Molecular weight complexes with the metal-lactoferrin complexes

	Electronic Spectra	E.S.R. Spectra	Other Data
FeO_6	CT band in right range, but complexes not suitable (p73).	Most complexes have g=4.3 signals consistent with rhombic symmetry. As symmetry becomes more tetragonal, signal at g=6 becomes prominent. E.s.r. is not sensitive to numbers of oxygen and nitrogen ligands (p78-83).	Mossbauer Sensitive to degree of covalency in molecule, but not to number of oxygens or nitrogens coordinated (p83-7) X-Ray Structure Structure determination of $[Fe(IIIa)_2(MeOH_2]NO_3.MeOH$ shows interaction of nitrate (a bicarbonate analogue) via solvent molecules (MeOH) (p70-2).
$FeONO_4^1$	CT band of $[Fe(IIIa)\ (MeOH)_4]^{2+}$ too low in energy (p75).		
FeO_4N_2	CT band too high in energy (p.75).		
$FeO_2N_2O_2^1$	CT band too low in energy but in the case of IIIa and VIII addition of 2 imidazoles shifts band to higher energy (p75,77).		
FeO_3N_3	CT band in right range (p75).		
FeO_2N_4	CT band for complex of VId (tridentate) of similar energy but too low for complexes of VIIb and VIId (hexadentate) (p77).		
General	Intensity of CT band of all complexes is around 4000 $lmol^{-1}cm^{-1}$ (p74).		
$CuONO_2^1X_2$	CT band is too high in energy (p102-3).	Compound is a dimer	
$CuO_3N\ Y_2$	CT band is similar in energy (p101).	$g_{//}$ and $A_{//}$ same as Cu_2Lf	
$CuO_2N_2Y_2$	CT band is similar in energy. Addition of axial N ligands has no effect on band position (p101.2)	$g_{//}$ lower and $A_{//}$ higher	
$CuN_4(O_2)$	No CT band-axial phenolates are weakly interacting with copper (p104).	$g_{//}$ much lower and $A_{//}$ much higher	
General	d-d band suggests tetragonal symmetry (p103-4)	Indicates tetragonal not tetrahedral symmetry (p105 & 108).	
Manganese	Indicates phenolate in specific site (p110).	Mixture of Mn(III)/Mn(II) (p110).	

Note O = phenolate oxygen, (O) = axial phenolate oxygen, O^1 = carboxylate and other oxygen, N = nitrogen, X = axial solvent, Y = axial halide.

Conclusions

(1) CT band of Fe(III) complexes increases in energy as number of phenolates and nitrogens bound to iron increases; approximately by $2000cm^{-1}$ per phenolate and $1\text{-}2000cm^{-1}$ per imidazole.

(2) E.s.r. spectra of Fe(III) complexes show iron in Fe_2Lf is in a site of rhombic (rather than tetragonal symmetry)

(3) Structure of $[Fe(IIIa)_2(MeOH)_2]NO_3.MeOH$ suggests interaction of bicarbonate with iron via a solvent molecule.

(4) Electronic spectra of Cu(II) complexes suggest two equatorial phenolates and one or two equatorial nitrogens bound to copper in a site of tetragonal symmetry; also that axial phenolates and nitrogens have little influence on the position of the CT band.

(5) E.s.r. spectra of Cu(II) complexes favour an equatorial CuO_3N system in a site of tetragonal symmetry.

Conclusion (see Figure 3.6)

Studies on metal-lactoferrin complexes have revealed that tyrosyl and histidyl residues are involved in binding to iron(III) in a site of rhombic symmetry and that bicarbonate is essential for this binding to occur. Studies of small molecular weight iron(III) complexes have shown that the charge transfer band shifts to higher energy as the number of phenolates and imidazoles bound increases. Using the complex $[Fe(4\text{-Me-phenolato})(EtOH)_5]^{2+}$ as a basepoint, in section 2-4 it has been argued that three phenolates and 2 imidazoles are likely to be found in the specific site. The single crystal X-ray structure of $[Fe(IIIa)_2(MeOH)_2]NO_3.MeOH$ would support the proposal for the interaction of bicarbonate via a solvent (water) molecule. Studies of small molecular weight complexes of copper would suggest that in Cu_2Lf there are likely to be two phenolates and one or two imidazoles equatorially bound. Furthermore they would suggest that one phenolate(or its unionised equivalent) and one imidazole are interacting axially. The tetragonal symmetry favoured by copper(II) would suggest that this axial interaction would be very weak. Hence for iron(III), which favours rhombic symmetry these axial ligands would be more strongly bound.